UNIVERZITA KARLOVA V PRAZE

Přírodovědecká fakulta

Katedra genetiky a mikrobiologie

Studijní program: Biologie

Studijní obor: Navazující genetika, molekulární biologie a virologie

Bc. Rebeka Göblová

Význam exosomů a ektosomů pro virulenci *Trichomonas vaginalis*

Role of exosomes and ectosomes in *Trichomonas vaginalis* virulence

Diplomová práce

Školitel: prof. RNDr. Jan Tachezy, Ph.D.

Konzultant: RNDr. Petr Rada, Ph.D.

Praha, 2020

Prohlášení:

Prohlašuji, že jsem závěrečnou práci zpracoval/a samostatně a že jsem uvedl/a všechny použité informační zdroje a literaturu. Tato práce ani její podstatná část nebyla předložena k získání jiného nebo stejného akademického titulu.

V Praze, 03.08.2020

Podpis: .....

Poďakovanie:

Moje poďakovanie patrí predovšetkým môjmu školiteľovi, prof. RNDr. Janovi Tachezymu, Ph.D za pomoc, vedenie a odborné rady počas písania tejto práce. Ďalej chcem poďakovať môjmu konzultantovi RNDr. Petrovi Radovi, Ph.D za pomoc pri experimentálnej časti. Veľké ďakujem patrí mojím kolegom z laboratória molekulárnej biológie a biochémie parazitických prvokov, hlavne našej laborantke, Michaele Marcinčíkovej, bez ktorej by som to nezvládla, pánom Dr. Ravi Kumar Narayanasamymu, Ph.D a RNDr. Zdeňkovi Vernerovi za konzultácie a Mgr. Jitke Kučerovej za trpezlivosť pri odpovedaní na moje dotazy. Nakoniec chcem poďakovať mojím priateľom a hlavne mojím rodičom za lásku, čas a neustálu podporu.

Abstract

Trichomonas vaginalis is a causative agent of the most common non-viral sexually transmitted disease with approximately 275 mil new cases annually. Virulence of this parasitic depends on at least four factors: cell shape transformation, cytoadherence, secretion of cysteine proteases, and presence of endosymbionts. Over the past decades, extracellular vesicles appeared being another important player in the host-parasite interaction. It was discovered that *T. vaginalis* is one of the protists that can shed the extracellular vesicles such as exosomes and ectosomes. These vesicles are possibly involved in host-parasite communications, however limited information is available about their function. To investigate a possible role of exosomes in *T. vaginalis* virulence, we first selected suitable strain, which is free of endosymbionts (TV 17-2MI). Next we prepared six clones of TV 17-2MI strain to test whether the strain is homogenous concerning the virulence, or there are differences in virulence among individual cells. Mouse intraperitoneal virulence tests revealed that the clones displayed significant differences in virulence level, particularly in abscess formation and mortality of infected animals. Thus, for the first time we demonstrated heterogeneity of cells derived from a single *T. vaginalis* strain in their virulence. Observed heterogeneity is not based on endosymbiont presence or absence.

Next, we established a protocol for exosome isolation. First step was to select suitable exosomal protein marker. We selected three candidates (tetraspanin 1, SNARE protein and multivesicular body protein - MBP) that were expressed with hemagglutinin tag in *T. vaginalis*. Immunofluorescence microscopy shown the localization of all three proteins inside of the cell, however only tetraspanin 1 (TSP1) was detected on the membrane of vesicles inside of the cell that could be multivesicular bodies. In the preliminary isolation of exosomes, we verified presence of exosomes in the microvesicular fraction using immunoblotting. To determine the protein composition of exosomes, we isolated exosomes from two *T. vaginalis* strains (TV T1 that expressed tagged-TSP1, and TV 17-2MI) and analyzed them using mass spectrometry. Our proteomic analyses showed significantly higher number of identified proteins (for TV T1 exosomes 2305 and for TV 17-2MI 1335 proteins) than in previous study (215 protein, Twu et al., 2013). Most of proteins from all studies significantly overlapped and all three marker proteins (TSP1, SNARE and MBP) were detected. The possible reasons for higher number of identified proteins in our experiments are discussed.

Key words: parasite, organelle, exosome, ectosome, pathogeny, virulence, protist, cell, virus.

Abstrakt

Trichomonas vaginalis je s přibližně 275 miliony případů ročně původcem nejčastějšího nevirového sexuálně přenosného onemocnění. Virulence tohoto parazita závisí nejméně na čtyřech faktorech: transformaci tvaru buněk, cytoadherenci, sekreci cysteinových proteáz a přítomnosti endosymbiontů. V posledních desetiletích se při interakci parasita s hostitelem ukázaly jako důležité také extracelulární vezikuly. Bylo zjištěno, že *T. vaginalis* je jedním z protistů, který má schopnost tyto extracelulární vezikuly v podobě exosomů a ektozomů tvořit. Tyto vezikuly jsou pravděpodobně zapojeny do komunikace mezi hostitelem a parazity, o jejich funkci je však k dispozici jen omezené množství informací. Pro zkoumání možné role exosomů ve virulenci *T. vaginalis* jsme nejprve vybrali vhodný kmen, který je bez endosymbiontů (TV 17-2MI). Dále jsme připravili šestklonů kmene TV 17-2MI, abychom otestovali, zda je kmen, co se týče virulence homogenní nebo zda existují mezi jednotlivými buňkami rozdíly. Myší intraperitoneální virulenční testy odhalily, že klony vykazovaly významné rozdíly v úrovni virulence. Zejména ve tvorbě abscesu a úmrtnosti infikovaných zvířat. Prokázali jsme virulentní heterogenitu buněk získaných z jediného kmene *T. vaginalis*. Pozorovaná heterogenita není založena na přítomnosti nebo nepřítomnosti endosymbiontů.

Dále jsme zavedli protokol pro izolaci exosomů. Prvním krokem bylo vybrat vhodný exozomální proteinový marker. Vybrali jsme tři kandidáty (tetraspanin 1, SNARE protein a multivesicular body protein - MBP). Tyto proteiny byly exprimovány s hemaglutininovou značkou v *T. vaginalis*. Imunofluorescenční mikroskopie ukázala lokalizaci všech tří proteinů uvnitř buňky, avšak na membráně vezikulů uvnitř buňky byl detekován pouze tetraspanin 1 (TSP1), což by mohla být multivesikulární tělíska. V předběžné izolaci exosomů jsme pomocí imunoblottingu ověřili přítomnost exosomů v mikrovezikulární frakci. Abychom určili proteinové složení exosomů, izolovali jsme exosomy ze dvou kmenů *T. vaginalis* (TV T1, který exprimoval značený TSP1 a TV 17-2MI) a analyzovali je pomocí hmotnostní spektrometrie. Naše proteomické analýzy ukázaly výrazně vyšší počet identifikovaných proteinů (pro TV T1 exosomy 2305 a pro TV 17-2MI 1335 proteiny) než v předchozí studii (215 protein, Twu et al., 2013). Většina proteinů ze všech studií se významně překrývala a byly detekovány všechny tři markerové proteiny (TSP1, SNARE a MBP). V diskuzi jsou pak shrnuty možné důvody pro vyšší počet identifikovaných proteinů v našich experimentech.

Klíčová slova: parazit, organela, exosom, ektosom, patogenita, virulence, prvok, buňka, viry.

1. Introduction

Trichomonas vaginalis is a flagellated protozoan that is responsible for human trichomoniasis, the most common non-viral sexually transmitted infection (Johnston and Mabey, 2008). According to the World health organization, the number of new cases of trichomoniasis was 173 mil. in 1999 (WHO, 2001), and this number increased to 275 mil cases in 2008 (WHO, 2012). However, these numbers are likely underestimated because up to 1/3 of cases in females and majority of infections in men are asymptomatic (Johnston and Mabey, 2008). Symptomatic cases are often manifested with various indications such as vaginitis, cervicitis, urethritis, pelvic inflammatory disease and in addition, trichomoniasis was associated with adverse birth outcomes (Swygard et al., 2004). Moreover, trichomoniasis increases the risk of HIV transmission and occurrence of prostate and cervical cancer (McClelland et al., 2007; Stark et al., 2009; Zhang and Begg, 1994). The risk of development of malignant changes and the higher risk of HIV transmission is mostly associated with non-treated asymptomatic cases. Increase prevalence of trichomoniasis occur in certain high-risk group such as prison inmates, drug users and sex workers (Garcia et al., 2004; Flom et al., 2001; Ward et al., 2000). While sex workers are primarily infected by direct exposure to the infection (Ward et al., 2004), drug users are often affected due to change in sexual behaviors (Tyndall et al., 2002). Prison inmates with trichomoniasis, are often imprisoned sex workers and drug users, which represent the high-risk category (Garcia et al., 2004; Shuter et al., 1998).

2. Review of literature

2.1. Morphology of *Trichomonas vaginalis*

T. vaginalis is a parasitic protist that belong to phylum Parabasalia, class Trichomonadea, order Trichomonadida, family Trichomonadidae (Čepička, Hampl and Kulda, 2010). Genus *Trichomonas* was described in 1836 by Donné. *T. vaginalis* cells have variable shape and size. According to the biometric measurements of flagellates from women with asymptomatic, acute and chronic infection, there is a significant difference in length, nucleus shape/size, breadth, cell shape etc. Cells appeared to be of smaller size in women with acute

trichomoniasis and larger in those with chronic infection (Kurnatowska, 1964; Kurnatowska, 1966).

T. vaginalis trophozoites (free-swimming form) are ovoid shaped cells with 4 anterior unequally long flagella (Fig. 1). *T. vaginalis* cytoskeleton includes specific structures such as parabasal apparatus, costa and microtubular structure called pelta-axostylar system (Honigberg et al., 1971). Axostyle consists of single ribbon of microtubules in a linear array. The pelta supports the wall of periflagellar canal, the part from where flagella emerge (Fig. 1). The pelta-axostylar system consists of two microtubular sheets that overlap forming pelta-axostylar junction (Benchimol et al., 2000).

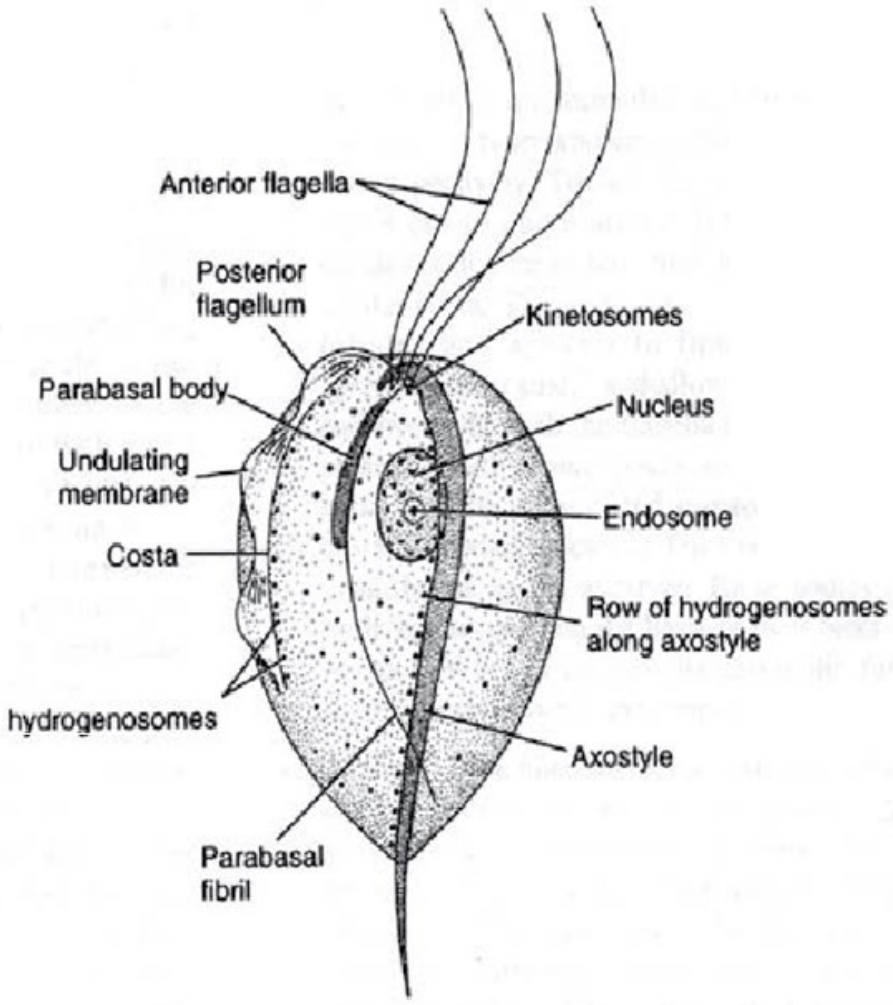

Fig. 1 *T. vaginalis* trophozoite scheme (based on Wenrich and Emmerson, 1933)

A specific organelle of this parasite is the hydrogenosome, an anaerobic form of mitochondria (Čerkasov et al., 1978; Lindmark and Müller, 1973). Hydrogenosomes are

adapted to the environment with low content of oxygen (urogenital tract) and produce ATP on substrate level phosphorylation with the hydrogen as a metabolic end product (Müller et al., 1988). Hydrogenosomes are organized along axostyl and costa (Fig. 1).

Two parabasal filaments support dictyosomes of Golgi apparatus forming parabasal apparatus (Brugerolle and Viscogliosi, 1994). There is also a structural filamentous bridge between parabasal filaments and the first cisternae on *cis*-side of Golgi. On the same site a proximal connection between Golgi apparatus and endoplasmic reticulum is located (Benchimol et al., 2001). In higher eukaryotes, the Golgi apparatus undergoes fragmentation during the mitosis, the secretion activity alters, and the trafficking from endoplasmic reticulum to Golgi apparatus and exocytosis stops (Alberts et al., 1994). In trichomonads, Golgi apparatus is preserved during mitosis, so it seems that exocytosis and secretion continues (Benchimol et al., 2001). The presence of thin filaments shed a light on understanding why the Golgi migration follows migration of basal basal bodies and flagella during mitosis (Zuo et al., 1999; Riberio et al., 2000).

2.2. Division of *T. vaginalis*

The centrosome is the major microtubule organizing centers (MTOC) in the metazoan eukaryotic cell. The duplication of MTOC ensures that during mitosis the mitotic spindle is bipolar providing each daughter cell with one centrosome and set of microtubules that form the mitotic spindle and attach to the kinetochore of chromosomes. The nuclear envelope breaks down during prometaphase and is reformed in telophase. Mitosis of *T. vaginalis* is very different. The nuclear envelope remains intact, the microtubular spindle is formed extranuclearly and kinetochoral microtubules contact the chromosomes at the nuclear envelope. This type of mitosis is called closed extranuclear pluromitosis (Heath, 1980). The role of MTOCs in this case play specialized structures called atractophores that are associated by one end to the kinetosomes and by the other end to the spindle.

According to the study by Ribeiro (2000), *T. vaginalis* and related bovine parasite *Tritrichomonas foetus* both share the same type of mitosis. The process of cell division is characterized by six distinct phases. The cell initiates mitosis once the extra set of flagella appears. At this point cell shape seems more rounded with some structures, such as pelta-axostyle, costa and flagella already duplicated. The mitotic phase of cell division starts with migration of basal bodies. As the reaction, axostyle and flagella move together with

kinetosomes and centrosomes changing the shape of the cell to triangle or heart shape (metaphase). As the division progresses, nucleus elongates and axostyles cross on posterior end. Both press elongated nucleus until karyokinesis is achieved (anaphase). In telophase, two small teardrop shaped cells with straight connection are observed. The movement of the daughter cells is limited by their connection, thus they tend to rotate along the axostyle. Once the cytokinesis is finished, the normal movement is recovered. (Ribeiro et al., 2000).

2.3. Virulence of *T. vaginalis*

T. vaginalis is a flagellated eukaryote known to exist in several forms (Fig. 2). Two of them are well-characterized: trophozoite, free-swimming, pear-like, and amoeboid, pancake-like form characterized by a significant increase in surface (Hirt, 2013). The cell shape transformation, cytoadherence, secretion of cysteine proteases, and presence of endosymbionts are key virulence factors of this parasite.

2.3.1. Transformation of *T. vaginalis* to amoeboid stage and cytoadherence

Transformation to amoeboid form is an important step in establishing the infection. When the ovoid, free-swimming flagellated trichomnads come to contact with the host cells, then they change to the flat form with pseudopodia and flagella on the dorsal site (Fig. 2). The transition to amoeboid form together with expression of specific proteins contribute to the adherence of *T. vaginalis* to the host cells. Transformation and cytoadherence are both rapid mechanisms taking only a few minutes after the contact of *T. vaginalis* with the host tissue (Lal et al., 2016). Studies of *T. vaginalis* surface proteins uncovered three classes of proteins that mediate the parasite cell adherence (Hirt et al., 2011; Ryan et al., 2011).

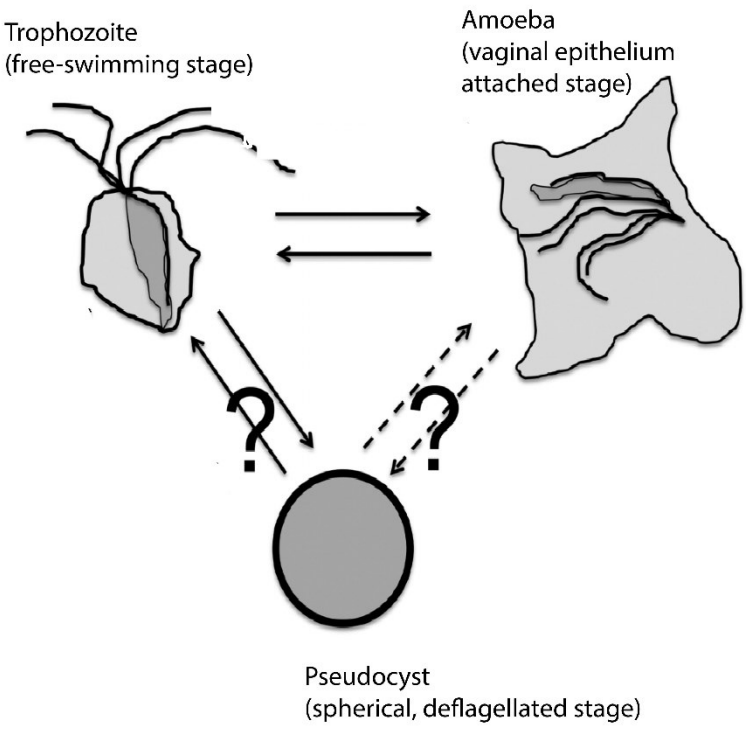

Fig. 2 Cellular forms of *T. vaginalis* (based on Hirt, 2013)

First, the members of large *Bacteroides forsythus* surface protein A (BspA) family have been localized on the parasite's surface. BspAs serves as adhesines in bacteria and similar function is expected for trichomonads. The genome of *T. vaginalis* encodes exceptionally large number of BspA-like proteins. There are over 911 genes coding BspAs, but only few of them have been detected on the trichomonad surface and in secretome. (Noël et al., 2010; Štáfková et al., 2018). The second class consist of the proteins of thick glycocalyx that also interact directly with host extracellular matrix. The study by Okumura et al., (2008) focuses on lipophosphoglycan (LPG) for its evidence for a role in attachment to host cells (Bastida-Corcuera et al., 2005; Fichorova et al., 2006). The third group of proteins is controversial, as they are thought to have dual functions: as an adhesion proteins on the cell surface and as an enzymes in hydrogenosomes, malic enzyme (ME), pyruvate:ferredoxin oxidoreductase (PFO), and subunits of succinyl-CoA synthetase (SCS) (Garcia and Alderete, 2007; Meza-Cervantez et al., 2011). Role of these proteins in adhesion has been challenged in several reports (Hirt et al., 2007; Ryan et al., 2011; Tachezy, 1999). It is unlikely that they represent truly adhesins as they are not targeted to and passing through the secretory pathways (Rada et al., 2019).

During the life cycle, trichomonads are not forming resistant cysts, however, there's an evidence of spherical forms with internalised flagella – called pseudocysts or endoflagellar forms (Lipman et al. 1999; Granger et al. 2000; Pereira-Neves et al. 2003, 2011, 2012; da Costa and Benchimol 2004; Ribeiro et al. 2015; Castro et al. 2016). The pseudocysts are often observed under destitute growth conditions and under suboptimal conditions in *in vitro* axenic cultures (Pereira-Neves et al. 2003). Among any other vital functions in trichomonads, iron is also responsible for maintenance the trophozoite morphology in this species (de Jesus et al., 2007). In media without iron, *T. vaginalis* cell culture lost not only the proliferation ability, but also the cells couldn't maintain the trophozoite morphology and morphed to immotile pseudocyst stage (Dias-Lopes et al., 2017). Pseudocysts in *T. vaginalis* were observed e.g. in patients with cervical neoplasia (Afzan and Suresh, 2012).

2.3.2. *T. vaginalis* symbionts and virulence

The host-parasite interaction is very complex, and the variety of symptoms is unlikely due to only a single pathogenic mechanism. The pathogenicity that leads into wide variation of virulence have not been clearly understood yet (Petrin et al., 1998). Moreover, there are two known endosymbionts of *Trichomonas vaginalis – Mycoplasma hominis* and *Trichomonas vaginalis* virus = *trichomonasvirus* (*TVV*), presence of which also contribute to *T. vaginalis* properties related to virulence

Mycoplasma hominis

In 1975, the transmission electron microscopy revealed the presence of bacteria class without defined cell wall – *Mollicutes* in the *T. vaginalis* cell culture (Nielsen, 1975). Few years later, another study identified *Mycoplasma fermentans* in *T. vaginalis* culture (Scholtyseck et al., 1985). In 1997, Koch found the association between *T. vaginalis* and *M. hominis* (Koch et al., 1997). Year after, PCR detection of viable *M. hominis* in *T. vaginalis* culture was established (Rappelli et al., 1998). The cooperative relationship between mycoplasma and trichomonas was the first described symbiosis between two obligatory human mucosal pathogens that are capable to invade the same host niche. They cause the separate infections, but these infections result in similar syndromes (Dessi et al., 2006).

M. hominis is the smallest organism to be known for independent replication. The size is 0.2 - 0.3 μm, it is without a cell wall and lives in human urogenital tract. With genome size of only 650 kb, its metabolic capacity is rather limited and consequently dependent on the

host cell metabolism. *Mycoplasma* is able to enter trichomonads via endocytosis, where it multiplies in coordination with the host cell or it is attached to the cell surface (Fichorova et al., 2017). *Mycoplasma* infection of trichomonads has interesting associations with the biochemistry and physiology of *T. vaginalis*. Both endosymbionts share arginine dihydrolase (ADH) pathway that led to ATP synthesis using arginine as substrate (Yarlett et al., 1996). This pathway represents an important source of energy for *Mycoplasma* as well as *T. vaginalis* (Pereyre et al., 2009). For *Trichomonas*, under the anaerobic conditions, parasite can gain up to 10% of a cell energy requirements (Yarlett et al., 1996). Because arginine is required for production of toxic NO by macrophages, decreased level of arginine might be beneficial for trichomonads during infection (Margarita et al., 2016). Presence of *Mycoplasma* in the *T. vaginalis* cells is connected with ~20% faster cell growth compared to mycoplasma-free culture and with ~40% higher cell density during stationary phase of growth (Margarita et al., 2016). All the biochemical aspects of symbiotic relationship between the two organisms can be an important factor of host physiopathology and definition of the microbe-host dynamics.

In vitro, *M. hominis* can be transferred from *T. vaginalis* infected culture to the mycoplasma-free cultures and also to human host cells. These experiments suggest that trichomonads may pass the mycoplasma infection to the human host cells *in vivo* (Rappelli et al., 2001). The *in vitro* data were supported by clinical findings from Italy and Netherlands showing that there were almost 80% coinfections of mycoplasma and *T. vaginalis*. The mycoplasma without trichomonad coinfection was detected in both studies in less than 6% of cases (Rappelli et al., 2001; van Belkum et al., 2001).

Endosymbiosis of mycoplasma in *T. vaginalis* increases *in vitro* cytopathogenicity of the protist, such as hemolytic property by almost twice, compared to the mycoplasma-free isolates (Margarita et al., 2016). Regarding immunomodulation, surface proteins of *M. hominis* are able to trigger massive immune response by proinflammatory cytokine production. Symbiotic presence of mycoplasma in trichomonads increases IL-1β, IL-6 and IL-8 production by peripheral host's macrophages (Mercer et al., 2016). There is also possible association with presence of mycoplasma and the malignant transformation as well as genomic instability of human prostate cells (Namiki et al., 2009).

Trichomonas vaginalis virus (TVV)

It's estimated that around 45–95% of *T. vaginalis* isolates shown the presence of small double stranded RNAs virus (dsRNA), named *Trichomonas vaginalis* virus (TVV) (Wang A and Wang C, 1986; Flegr et al. 1987). TVV has been found in the cytoplasm, often closely associated with Golgi apparatus or adjacent to plasma membrane. The virus population varies in size (33 – 200 nm) and shape (filamentous, cylindrical and spherical particles) (Benchimol et al., 2002). TVV virus was placed in family *Totiviridae*, genus *Trichomonasvirus* by phylogenetic and genomic sequence (Tai et al., 1993; Goodman et al., 2011). *Totiviridae* family includes wide range of viruses characterized by isomeric virions. 30 – 40 nm in diameter, containing no segmented genomes with overlapping open reading frames encoding enzyme RNA-dependent RNA polymerase and a capsid protein. The members of *Totiviridae* are known to cause noncytopathic, persistent infections in various range of fungi and protists (Ghabrial, 2008). There are four species of TVVs called TVV1, 2, 3 and 4 identified by comparison of genome sequencing and phylogenic study (Goodman et al., 2011). A single clinical isolate can be infected with more than one TVV species simultaneously (Bessarab et al., 2000; Goodman et al., 2011, Fraga et al., 2012).

TVV infection of *T. vaginalis* culture can modulate the host expression of immunogenic proteins, such as cysteine proteinases and protein P270 (Khoshnan et al., 1994; He et al., 2017). Thus, TVV infections can modulate the virulence of trichomoniasis, cause the difference in symptoms, transmissibility, affect the drug sensitivity etc. (Goodman et al., 2011). The presence of symptoms such as vaginal discharge, dysuria and cervical erythema was significantly associated with TVV infection of the parasite (Fraga et al., 2007). The study performed on *T. vaginalis* strains isolated in Cuba showed difference in number and severity of symptoms caused by TVV+ vs TVV- trichomonads and the unequal level of symptoms depend on the type of virus in the TVV+ trichomonads (TVV1 or TVV2). While parasites isolated from patients with mild symptoms shown the presence of only TVV1, the isolates taken from patients with moderate to severe symptoms displayed presence of TVV2 in the culture (Fraga et al., 2012).

One of the critical steps in *T. vaginalis* pathogenesis is cytoadherence of the parasite to the vaginal epithelium (Singh et al., 2009). Virus-infected trichomonads displayed substantially higher level of cytoadherence in comparison with virus-free strains. Moreover, parasites infected with TVV 2 showed higher adhesion level in comparison to strain with TVV 1. (Fraga et al., 2012). To study pathogenesis of *T. vaginalis* on cellular and molecular level, *in vitro* experimental model of vaginal mucosa was established reference. There was a

clear evidence that presence of TVV endosymbiont in the *T. vaginalis* dramatically upregulates the host pro-inflammatory response mediated by toll-like receptor (TLR-3) and interferon regulatory factor (IRF-3) signaling (Fichorova et al., 2012). Furthermore, the study shown that the conventionally used anti-parasitic drugs (e.g. metronidazole) caused an increase in the inflammatory pathology, connected with trichomoniasis due to release of virions from dead or stressed parasitic cells. (Fichorova et al., 2012).

The impact of TVV presence in *T. vaginalis* on virulence is controversial topic. While studies mentioned above showed causative connection of TVV infection to the host immunity and course of infection, there are studies that disapprove the association. In the latest study by Graves et al. (2019) 355 *T. vaginalis* strains were tested of which 40% was infected with TVV. The results haven't shown association between TVV positivity of isolate and genital symptoms. Surprisingly, correlation between smoking and TVV positivity occurred as a result of reduction of vaginal lactobacilli (*Lactobacillus crispatus*). The study also revealed that women with TVV negative isolates of *T. vaginalis* were significantly more likely to report the history of gonorrhea. It's interesting finding, however self-reported cases of previous STIs have to be interpreted with caution. Possible connections between *Trichomonasvirus* and prostate and cervical cancer or oncogenic HPV infection are yet to be evaluated.

2.3.3. Extracellular vesicles

Extracellular vesicles (EVs) are described as the "generic term for particles naturally released from the cell that are delimited by a lipid bilayer and cannot replicate" and the EV concept can be modified based on clear, measurable characteristics such as cell of origin, molecular markers, size, density, function, etc. (Théry et al., 2018). Communication via EVs represents a new approach when it comes to parasite-host interactions. EVs are known from wide range of host cell types, such as immune cells, tumor cells, epithelial cells or embryotic stem cells and also parasites (Evans-Osses et al., 2015).

2.3.4. Biogenesis of extracellular vesicles

Many authors tend to use term "exosomes" as a synonym of "EVs". In fact, International Society for Extracellular Vesicles (ISEV) recommended to use EVs as a generic term for various vesicles with further defining characteristics (Witwer and Théry, 2019). The

classification of EVs typically defines three categories of vesicles according to the size and origin:

1) exosomes – the smallest of all three categories with size from 40 to 100 nm
2) microvesicles (also called micropatricles or ectosomes) – size range 100 to 1000 nm
3) apoptotic bodies – the largest type of extracellular vesicles with size from 2 to 4 μm (Tetta et al., 2012).

The studies on parasitic protist revealed two other groups of extracellular vesicles (de Souza and Barias, 2020):

4) vesicles released from the cell surface following a process of patching and capping of ligand-receptor complexes
5) exosome-like structures that originate from extracellular tubule-like structures.

The best characterized category are apoptotic bodies. Large vesicles that originate from the cell in process of programmed death – apoptosis (Fig. 2).

Microvesicles, are generated at the plasma membrane, and their release is dependent on rising intracellular calcium level (Fig. 2) (Silvermann et al., 2010). Term ectocytosis was established in early 1990's by Stein and Luzio (1991) to describe component-produced shedding of right-side-out membrane vesicles derived from the surface of polymorphonuclear leucocytes. Surprisingly, the vesicular formation looked somehow similar to the process reported in Gram-negative bacteria. The process can be involved in the mechanism that can release and transmit the virulence factors to other bacteria (Vidakovics et al., 2010). Ectosomal formation may include participation of cytoskeletal units associated with target part of plasma membrane facing cytoplasm (Sadallah et al., 2011). Just like exosomes, microvesicles can mediate horizontal transfer of different molecules such as soluble proteins, membrane proteins, lipids and nucleic acids (miRNA, DNA, mRNA) (Choi et al., 2015). Thus, ectosomes may contain physiologically active effectors playing important roles in different biological processes such as inflammation, cancer, vascular reactivity etc. (Sadallah et al., 2011).

Particles of our main interest, exosomes, are derived from the endosomal cell compartment via exocytosis of multivesicular bodies and are released to the extracellular space by fusion with the plasma membrane in a cytoskeleton-dependent activation. Unlike microvesicles, their release is nor dependent on calcium (Fig. 2) (Schara et al., 2009).

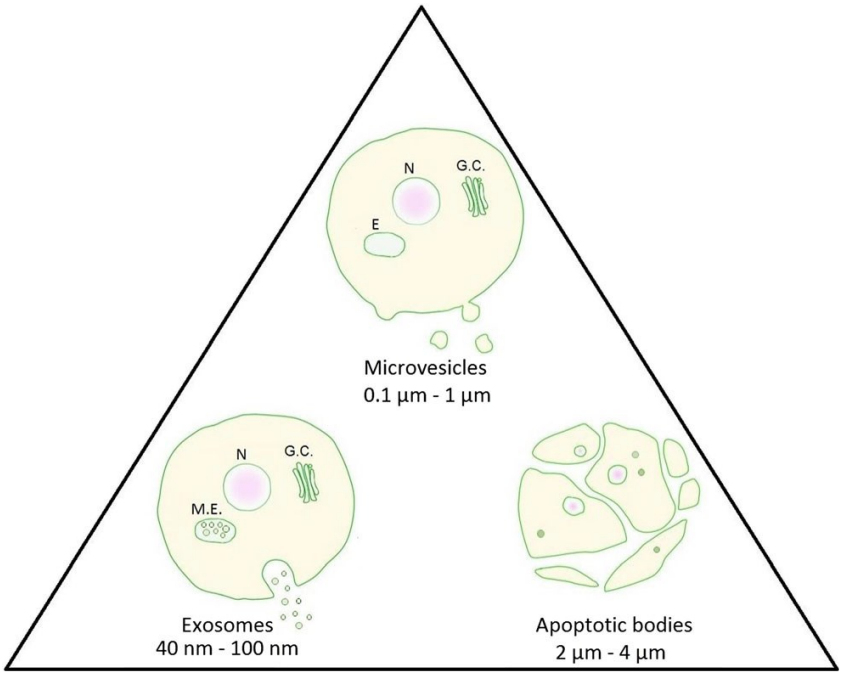

Fig. 3 Extracellular vesicles. Three categories of extracellular vesicles according to the size and origin (based on Evans-Osses et al., 2015).

Exsomal formation is common for majority of the cell types. The first stage is the appearance of the small punctate structures in the cytoplasm that can be colocalized with early endosomal marker (e.g. EEA-1 in vascular smooth muscle cells). The next step is the MVB formation which occurs when invagination of the early endosome takes place. The inward budding of the endosome membrane generates the aggregation of small nanovesicles (30 – 150 nm in diameter) inside of the late endosome subset of MVB (Huotari and Helenius, 2011). Endosomal sorting complexes required for transport (ESCRT) are crucial for invagination of endosomal membrane (Hurley and Hanson, 2010). It is important to mention that MVB mostly fuses with lysosome, which leads to MVB's cargo degradation. In the rest of the cases, the process continues and MVB fuses with plasma membrane releasing the exosomes (Denzer et al., 2000). The endocytic network represents alternation to established classic secretory pathway (Van Niel et al., 2006; Schorey and Bhatnagar 2008).

The other two categories of the extracellular vesicles are especially relevant for parasites, however, have not been studied so far. The vesicles released from the cell surface represent the final step of the process of capping surface ligands. These vesicles often occurred in the host cells such as lymphocytes in higher eukaryote, and parasites such as *Entamoeba histolytica* (Trissl et al., 1977) and *Trypanosoma cruzi* (Schmunis et al., 1980). The vesicles require receptor-ligand binding and mobility. Exosome-like structures derived

from extracellular tubule-like structures are well known in parasite *Trypanosoma brucei*. First seen in blood of mouse infected with the parasite (Ellis et al., 1976), the exosome-like structures derived from tubule-like structures are now considered as a new category for its difference in formation from exosomes and ectosomes. However, the final step includes the subsequent release of typical EVs (Szempruch et al., 2016). These vesicles are able to fuse with lipid bilayers and the flagellar pockets and even with erythrocytes transferring their lipids and proteins. Proteomic analysis revealed presence of flagellar proteins on the top of virulent factors in the vesicles (Geiger et al., 2010).

2.3.5. Extracellular vesicles and cellular communication

Production and shedding of extracellular vesicles is often considered being the universal way of communication between cells and serves as a process of material and information passing, and behavioral modification, (Deolindo et al., 2013). The vesicles are composed of a single lipid bilayer with content of biomolecules and are released mandatory *in vitro* and *in vivo* as a response to agonist activation, physical stress or chemical stress (Silverman and Reiner, 2011).

When it comes to parasitic protists, vesicles can carry receptors, proteins, mRNA and miRNA molecules that deliver information to the recipient cells. The parasite-host interactions mediated by extracellular vesicles cause large scale of responses than can have modifying effects on the host cells. Increasing knowledge about this type of cell communication can reformulate concepts in parasitism (Evans-Osses et al., 2015).

It has been shown that after exosomes are released to extracellular matrix, there are several possibilities how they interact with the target cell. For example, the cargo can be released to the extracellular space, EVs can bind to the cell surface, which can lead to the membrane fusion and uptake by endocytrosis (Fig. 4). For EV engagement in cell signaling, EVs can directly bind to the receptors associated with the plasma membrane or vice versa. This type of recognition may also serve as a delivery mechanism to the certain cell type (Costa-Silva et al., 2015; Hoshino et al., 2015). To deliver cargo (bioactive biomolecules, RNAs), the initial binding to the target cell is followed by releasing of the cargo to the recipient cell. The release takes place straightly after the plasma membrane-EV fusion or after endosomal membrane-EV fusion after the endocytosis (Maas and Cao., 2018).

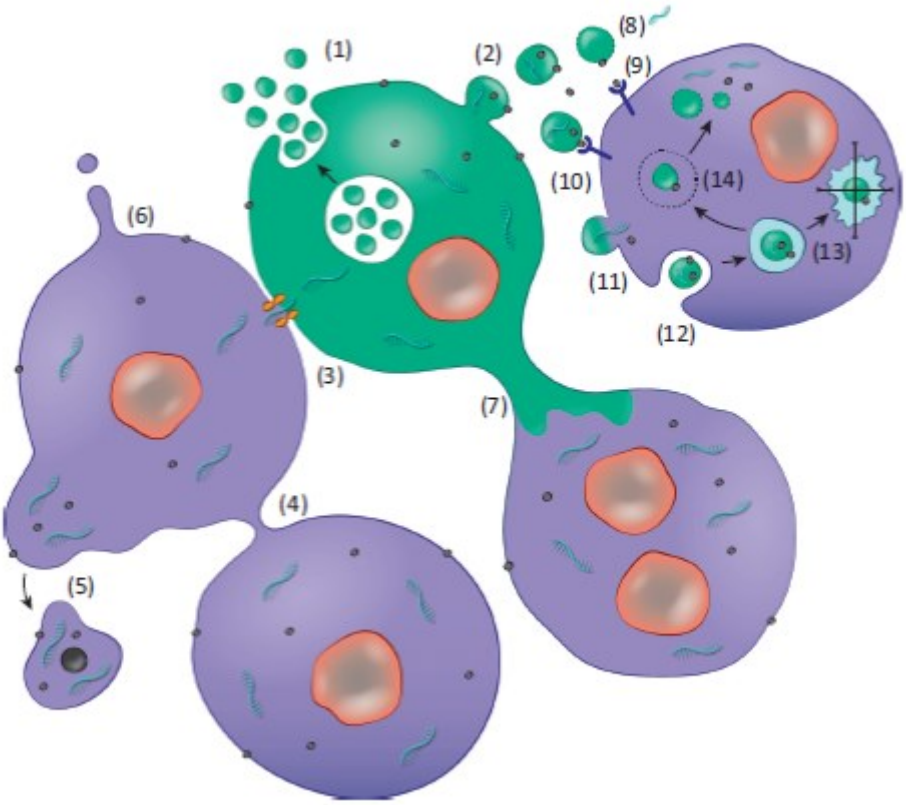

Fig. 4 Scheme of macromolecular information flow between the cells (based on Maas et al., 2015)

1 – MVB formation and release after its fusion with plasma membrane, 2 – formation of microvesicles (ectosomes), 3 – gap junction, 4 – nanotube cell connection, 5 – large vesicles separation (e.g. oncosomes), 6 – membrane protrusions with apical release of vesicles, 7 – microtubular cell connection, 8 – extracellular cargo release, 9 – ligand-receptor connection, 10 – vesicle-cell binding via ligand-receptor connection, 11 – vesicle-plasma membrane fusion, 12, 13 – lysosomal degradative pathway, 14 – functional cargo release in the cytoplasm.

It has been also considered that exosomal trafficking shares mechanisms similar to viral uptake. This possibility represents a new type of cellular communication in addition to the well-known types such as gap junctions and synapses (de Souza and Barias, 2020).

2.3.6. *T. vaginalis* exosomes vs ectosomes

Exosomes

The first study about *T. vaginalis* exosomes was performed by Twu et al. (2013). They found presence of three proteins from tetraspanin protein (Tsp) family that are known to be constitutive components of several types of exosomes (Schorey and Bhatnagar, 2008). *T.*

vaginalis Tetraspanin 1 (TSP1) protein appeared as a suitable marker of exosomes. Localization of hemagglutinin-tagged TSP1 revealed its presence on membrane of possibly MVB. They isolated vesicles with diameter in range from 50 to 100 nm from the conditioned medium of *T. vaginalis* cultures and the vesicles were analyzed by mass spectrometry. Proteomic analysis showed the total of 215 proteins. Of these, 73% and 40% were found to be orthologs of mammalian and *Leishmania donovani* exosomes, respectively, including protein families such as Alix, Rab, cytoskeletal proteins, surface proteins, HSP70, and proteases that may be involved in pathogenesis of *T. vaginalis*. To investigate exosome-host cell interactions, BODIPY-PC labeled exosomes were incubated with ectocervical cell *in vitro* that revealed formation of labeled structures inside of the ectocervical cells. As a control, labeled hydrogenosomes were not observed to label the ectocervical cells. Further an immunomodulatory effect of exosomes was investigated. Exosomes induced production of IL-6 in the acceptor cells incubated in the presence of parasites. There was induced also production of interleukin, IL-8, but to the lower degree. Possible role of exosomes in trichomnonas adherence to the host cells *in vitro* was also analyzed. Two *T. vaginalis* strains were used: 1) TV B7RC2 and TV G3, where strain TV B7RC2 is about 20 times more adherent than TV G3. Results showed that culture of TV G3 pre-incubated with exosomes from TV B7RC2 strain was around 2 times more adherent to ectocervical cells. In addition, the ectocervical cells pre-incubated with exosomes from TV B7RC2 resulted to 3 times higher attachment of TV G3 to these cells. The same experiment performed with other highly adherent strains showed the same results, concluding that the exosomes from highly adherent strains increase attachment of less adherent cells.

Ectosomes

The complex study on shedding vesicles by Nievas et al. (2017) focused on *T. vaginalis* ectosomes (microvesicles - MVs). Group around Nievas used filtration-based approach to enrich this population and to separate ectosomes (100-1000 nm) from smaller exosome-like vesicles (50-150 nm). To evaluate formation of MVs under regular conditions, two strains (TV B7CR2 and TV Jt) were analyzed using scanning electron microscopy (SEM). Results revealed that 1% of examined cells had vesicles 100-1000 nm in diameter, different in shape associated with the surface. To ensure that EVs were released ty *T. vaginalis*, authors used modified protocol for exosomal isolation. By double filtration through membrane with nominal diameter of 800 nm, followed by filtration through membrane with nominal diameter of 200 nm, they avoid cellular and exosomal contamination in the samples.

Comparing fraction enriched with MVs, where mean diameter was 380 nm, fraction enriched with exosomes had particles with mean diameter of 63 nm. Further examination of MVs revealed irregularities in shape of the membrane and differences in size, similar to the MVs released by another cell types (Shifrin et al., 2013). To identify the proteins in MVs enriched fractions, they used mass spectrometry. Results revealed total of 592 protein, out of them 82% were predicted to possess known domains and remaining 16% were hypothetical proteins. Further analysis showed that 39% of MVs proteins were found also in exosome proteome and remaining 61% was unique for MVs with possible specific functions. Comparing *T. vaginalis* proteome of MVs and human EVs proteome, approximately 56% of proteins were homologs. Some of the homologous proteins were found in different studies, thus can be considered as conserved among EVs of different origin, including cytoskeletal proteins (actin, tubulin, villin and plastin), metabolic enzymes (enolase, phosphoglycerate kinase, pyruvate kinase, and lactate dehydrogenase), various ribosomal proteins, heat shock proteins and Tsp proteins. Importantly, the proteome included ADP-ribosylation factor (ARF) proteins that are important for the process of shedding (Muralidharan-Chari et al., 2009) and cargo selection to MVs (D'Souza-Schorey and Chavrier, 2006). Interestingly, the same two BspA-like proteins were found in the proteome of MVs as well as in exosomes. Immunofluorescence analysis of hemagglutinin-tagged TvTSP8 was performed. This protein accumulated in structures smaller than 1000 nm, but also vesicles larger than 1000 nm in the parasites. Any vesicle larger than 1000 nm is considered as apoptotic body, however these large vesicles (LV) were excreted from growing parasites. Isolated *T. vaginalis* LVs and MVs were shown to interact with the parasite cells suggesting that they may mediate communication between trichomonads. They also interact with the host cells to modulate their properties.

3. Materials and methods

3.1. Cultivation of organisms

3.1.1. Cultivation of *T. vaginalis*

T. vaginalis strains: TV 17-2MI was isolated from patient in Prague, Czech Republic (not published 2017), TV 10-02, TV 17-48, TV 79-49, and TV 85-08 were isolated from patients in Prague, Czech republic (Kulda, 1973). The cells were cultivated at 37°C in tryptone-yeast extract-maltose (TYM) medium with 10% horse heat inactivated serum (Thermo Fisher Scientific, Waltham, Massachusetts, USA). Trichomonads were subcultured every day or every second day as needed. Transfected T1 cells were grown in the TYM medium with 100 µg/ml geneticin.

3.1.2. Cultivation of *Escherichia coli*

In all experiments with *E. coli*, strain TOP 10 was used. The cells were cultivated in Luria-Bertani broth (LB) medium (Bertani, 1951) on the shaker (220 rpm) at 37°C. Transfected *E. coli* cells were grown using LB plates with ampicillin (100 µl/ml) for selection. Transformed *E. coli* TOP 10 were stored in LB medium with 20% glycerol in freezer at -80°C.

3.2. Cultivation media

TYM medium (Diamond, 1957)

Distilled H_2O	900 ml
K_2HPO_4 (Sigma-Aldrich, Saint-Louis, Missouri, USA)	0,8 g
KH_2PO_4 (Sigma-Aldrich, Saint-Louis, Missouri, USA)	0,8 g
Ascorbic acid (Sigma-Aldrich, Saint-Louis, Missouri, USA)	0,2 g
L-cystein (Sigma-Aldrich, Saint-Louis, Missouri, USA)	1 g
Maltose (Sigma-Aldrich, Saint-Louis, Missouri, USA)	5 g
Yeast extract (Sigma-Aldrich, Saint-Louis, Missouri, USA)	10 g
Tryptone (Sigma-Aldrich, Saint-Louis, Missouri, USA)	20 g
Ferric ammonium citrate	1 ml

Agar (Sigma-Aldrich, Saint-Louis, Missouri, USA)	0,5 g

All components were dissolved in smaller amount of distilled H2O, agar was added directly to the bottle for medium. pH was then adjusted with 1M HCl to 6,2. The final volume was adjusted to 900 ml and medium was autoclaved in glass bottle. Medium with agar was mixed after sterilization. After cooling down (the next day), 100 ml of horse serum was added and mixed.

LB medium

LB medium (Sigma-Aldrich, Saint-Louis, Missouri, USA)	20 g
Distilled H_2O	final volume 500 ml

Sterilized by autoclaving at 120°C for 20 minutes.

LB agar plates

LB agar (Sigma-Aldrich, Saint-Louis, Missouri, USA)	17 g
Distilled H_2O	final volume 500 ml

LB agar was sterilized by autoclaving at 120°C for 20 minutes and distributed to sterile Petri dishes (VWR International).

Super Optimal broth with Catabolite repression (SOC) medium

Tryptone (Sigma-Aldrich, Saint-Louis, Missouri, USA)	2 g
Yeast extract (Sigma-Aldrich, Saint-Louis, Missouri, USA)	0,5 g
NaCl (Sigma-Aldrich, Saint-Louis, Missouri, USA)	0,058 g
250 mM KCl (Sigma-Aldrich, Saint-Louis, Missouri, USA)	1 ml
Distilled H_2O	final volume 100 ml

All the components were dissolved in distilled H_2O and sterilized by autoclaving in a glass bottle. After sterilization, 20% of filter sterilized glucose and 2M sterile $MgCl_2$ was added. SOC medium was then aliquoted and stored at -20°C.

3.3. Buffers and solutions for the cell manipulation

Phosphate-Buffered Saline (PBS)

	Concentration (g/L)
NaCl	8.0
KCl	0.2
Na_2HPO_4	1.44
KH_2PO_4	0.24

All the components were dissolved in 1l of distilled H_2O and pH was set to 7.2.

3.4. Antibiotics stock solutions

Penicillin (100.000 I.U./ml, Sigma-Aldrich, Saint-Louis, Missouri, USA)

Amikacin (25 mg/ml, Sigma-Aldrich, Saint-Louis, Missouri, USA)

Geneticin (100 mg/ml, Sigma-Aldrich, Saint-Louis, Missouri, USA)

3.5. Agarose gel electrophoresis

DNA samples were analyzed using 1% agarose gel electrophoresis.

1) To prepare 40 ml of gel add 0,4 g of agarose (Sigma-Aldrich, Saint-Louis, Missouri, USA) to 40 ml of Tris-Acetate-EDTA (TAE) buffer.
2) Heat the mixture in the microwave and mix gently every 30s. Don't let the mixture to boil.
3) Once the agarose is dissolved, carefully cool the mixture to approximately 50°C and add the gel dye (SYBR stain – use 20 µl of dye per 50 ml of gel). Mix well so the dye is distributed evenly.
4) Pour the gel into the try and insert the comb.
5) Let it cool for at least 20 minutes, remove the comb and insert the gel to the electrophoresis instrument, multiSUB Mini, Mini Horizontal Electrophoresis System (Cleaver Scientific, Rugby, England, GB)
6) Make sure the gel is fully immersed in TAE buffer.

7) Load the samples into the gel. Use GeneRuler^{TM} DNA Ladder Mix (Thermo Fisher Scientific, Waltham, Massachusetts, USA) as a standard.
8) Run the gel for 40 minutes on 90V (check every 15 minutes) and visualize under the UV transluminator.

Required solutions:

TAE (Tris-acetate-EDTA) electrophoresis buffer (40 mM Tris, 20 mM acetic acid, 1 mM EDTA) 1x diluted with distilled water from 50x TAE Buffer (Thermo Fisher Scientific, Waltham, Massachusetts, USA).

Agarose gel staining dye

SYBR Safe DNA Gel Stain (20 µl dye/ 50 ml of gel, Thermo Fisher Scientific, Waltham, Massachusetts, USA)

3.6. Sodium dodecyl sulfate polyacrylamide gel electrophoresis (SDS-PAGE)

Protein samples were analyzed using Mini-PROTEAN Tetra Cell (Bio-Rad, Hercules, California, USA) instrument. For a single 12% running gel with 0.75mm spacer add:

1.6 ml of 30% acrylamide solution
2ml of C solution,
0.32 ml of dH_2O,
5 µl of TEMED and
40 µl of G solution.

Vortex and pour the mixture in assembled glass form leaving cca 3 cm on the top for stacking gel. Fill water on the top of the mixture until the gel solidifies.

For stacking gel add:
0.24 ml of acrylamide,
0.75 ml of D solution,
0.47 ml of water,
5 µl of TEMED and
20 µl of G solution.

Remove the water and pipette the stacking gel on top of the running gel. Insert the comb and let it solidify. Once the gel is solidified, remove the comb and put the glass form with the gel to the electrophoresis device. Pour the running buffer in the upper and lower chamber before loading the samples onto the gel.

Load the standard (protein ladder) and samples onto the gel and let the electrophoresis run for 20 minutes at 90V. Once it passes the stacking gel let it run at 180V. Check frequently.

Required solutions:

Tris-Glycerin-SDS (TGS)

1x concentrated Tris-Glycerin-SDS (TGS) running buffer diluted with distilled water from 10x TGS buffer premixed electrophoresis buffer (contains 25 mM Tris, 192 mM glycine, 0.1% SDS, pH 8.3; Bio-rad, Hercules, California, USA).

Solution C

9.1 g of Trizma base (Tris) dissolve in 50 ml of distilled water, adjust the pH to 8.8. Then add 0.2 g of SDS. Adjust the volume to 100 ml. Store in the fridge at 4°C.

Solution D

3 g of Trizma base (Tris) dissolve in 50 ml of distilled water, adjust the pH to 6.8. Then add 0.2 g of SDS. Adjust the volume to 100 ml. Store in the fridge at 4°C.

Solution G

1 g of ammonium persulfate dissolve in 10 ml in distilled water. Store in the freezer at -20°C.

Tetramethylethylenediamine = TEMED (Thermo Fisher Scientific, Waltham, Massachusetts, USA)

SDS-PAGE gel visualization solutions

Coomasie gel dye (Coomasie Briliant Blue Solution; CBB)

Coomasie Brilliant Blue	200 mg
Denatured ethanol	225 ml
Distilled water	225 ml
Acetic acid	50 ml

Destain Solution

Denatured ethanol	250 ml
Acetic acid	100 ml
Distilled H_2O	650 ml

3.7. Western blotting

1) Soak 2 pieces of filter paper, nitrocellulose membrane and the gel in the blotting buffer for few minutes.
2) On the blotting device (Semi Dry Blotter; Cleaver Scientific, Rugby, England, GB / Trans-Blot Turbo Transfer System, Bio-rad, Hercules, California, USA) assemble filter papers, cellulose membrane, gel and other two filter paper.
3) Transfer the proteins from the gel to the nitrocellulose membrane for 60 minutes at 1.5 mA per 1 cm^2 of membrane using Semi Dry Blotter (Cleaver Scientific, Rugby, England, GB) or use the Tubro program on Trans-Blot Turbo Transfer System (Bio-rad, Hercules, California, USA) to have the blot ready in 7 minutes
4) Stop the procedure and remove the membrane. To check the protein transfer pour Ponceau dye over the membrane. Let it stain for 2 minutes and stop the reaction with distilled water
5) Block the membrane in 5% milk with 0,1% Tween 20 (Sigma-Aldrich, Saint-Louis, Missouri, USA) overnight in the fridge
6) Remove the milk and incubate the membrane with primary antibody (1:400 in in blocking solution for 1 hour on the orbital shaker to distribute the antibody evenly.
7) Wash 3 times in blocking solution for 10 minutes
8) Incubate with secondary antibody in blocking solution for 1 hour on the orbital shaker
9) Wash twice with 0,1% Tween 20 for 10 minutes and twice with PBS to wash the milk residue
10) Pour the substrate onto the membrane to visualize expected protein.

Blotting buffer

10x concentrated SDS buffer	100 ml
Methanol	200 ml

Distilled water	700 ml

Blocking solution

Low fat dried milk	5 g (total concentration of 5%)
Tween 20	100 µl (total concentration of 0,1%)

Ponceau S membrane dye solution

Ponceau S	0,5%
Acetic acid	1%

Substrate for alkaline phosphatase

Sigma Fast BCIP/NBT (tablet form)	1 piece (Sigma-Aldrich, Saint-Louis, Missouri, USA)
Distilled water	10 ml

3.8. Antibodies

Primary antibodies

Mouse monoclonal anti-haemaglutinin (HA) antibody (IgG, mouse)(Exbio, Vestec, Czech Republic), dilution 1:400

Secondary antibodies

Anti-mouse IgG conjugated with alkaline phosphatase (původ?) used in dilution 1:1000

3.9. Immunoflourescence microscopy

3.9.1. Preparation of slides using methanol/acetone method

1) Drip a small drop of well grown cell culture on slide glass.
2) Check under the microscope and let it dry completely.
3) Fix the cells for 5 minutes in methanol in freezer (-20°C).
4) Remove, let dry for couple of minutes and put to the acetone for 5 minutes in the freezer (-20°C).
5) Remove and let dry well.

6) Drip a small drop of Fluoroshield mounting medium with DAPI and carefully put cover glass on the top. Seal the cover glass with nail polish.

3.9.2. Preparation of slides using formaldehyde

1) Fix 5 ml of well grown cells in medium by adding 312 µl of 32% formaldehyde (final concentration 2% formaldehyde. Incubate for 30 minutes at 37°C
2) Spin the cells at 900 x g for 5 minutes
3) Resuspend the pellet in 5 ml of 1x PEM
4) Spin the cells at 900 x g for 5 minutes
5) Add 10 µl of polylysine solution between 2 clean cover glasses. Rub against each other till the friction appears. Put in the sterile 6 well plate and let dry for 15 minutes.
6) Resuspend the pellet in 150 µl of 1x PEM with Pasteur pipette
7) Add a small drop of cell suspension on polylysine cover glass and carefully spread evenly
8) Let dry for 5 minutes
9) Drip 0.1% Triton solution (10 µl of 10% Triton X-100 in 1 ml of 1x PEM) over the cover glass and let incubate for 15 minutes
10) Remove Triton solution and wash 3 times with 1x PEM for 20 seconds
11) Drip PEMBALG over the cover glass and incubate for 30 minutes
12) Remove the PEMBALG and incubate with the primary antibodies (1:1000 in PEMBALG) for 1 hour
13) Wash 3 times with 1x PEM for 7 minutes
14) Incubate with the secondary antibodies (1:1000 in PEMBALG) for 1 hour in the dark
15) Wash 3 times with 1x PEM for 7 minutes in dark
16) Drip a small drop of VECTASHIELD Antifade Mounting Medium with DAPI (Vector Laboratories, Burlingame, USA)
17) Carefully put the cover glass on the top and seal with nail polish

18) Observe with fluorescence microscope Leica SP8 LIGHTNING confocal microscope (Leica Microsystems, Wetzlar, Germany)

Required solutions:

2x PEM buffer (pH 6,9) (Mooberry et al., 1999)

PIPES	30,2 g
0,5 mM EDTA	2 ml
1M MgSO4	100 µl

The components were first solubilized in smaller amount of distilled water. NaOH was added till the color of buffer was transparent. pH was than adjusted to 6,9 and volume was adjusted to 500 ml. Buffer was sterilized using autoclave. 1x PEM diluted with ultra pure water was used for slide preparation.

PEMBALG

1x PEM buffer	100 ml
BSA	1 g
Lysin	1,8 g
Cold water fish skin gelatin	0,5 g

Triton X-100 (10%) – used diluted with PEM to final concentration of 0,1%

3.10. Nucleic acid isolation

3.10.1. RNA isolation using TRIzol™ Reagent (Thermo Fisher Scientific, Waltham, Massachusetts, USA)

1) Spin 5-10 ml of well grown cell culture (5-10 * 10^6 cells) for 10 minutes at 1000g
2) Remove supernatant carefully without disturbing the pellet
3) Add 1 ml TRIzol reagent
4) Incubate for 5 minutes at room temperature for higher efficiency
5) For 1 ml TRIzol add 200 µl of chloroform
6) Shake vigorously (do not vortex)

7) Incubate for 3 minutes at room temperature
8) Spin for 10 minutes at 13000 RPM at 4°C
9) Remove the top aqueous phase with RNA without disturbing the interphase and move it to the new tube. Remaining interphase and bottom phase can be used to isolate the DNA and protein. Use them immediately or freeze at -80°C.
10) For 1 ml TRIzol add 500 µl of isopropanol
11) Precipitate the sample for 10 minutes at room temperature
12) Spin for 10 minutes at 13000 RPM at 4 °C
13) Remove the supernatant without disturbing the RNA pellet
14) Wash with ethanol. For 1 ml TRIzol use 1 ml of 70% ethanol
15) Spin for 5 minutes at 8000 RPM at 4°C
16) Remove the ethanol as much as you can without disturbing the pellet
17) Dry the pellet to the point where it's gel-like consistency
18) Elute in nuclease-free water for 5 minutes at 55°C
19) Use immediately for further analysis or freeze at -80°C.

Required solutions:

TRIzol reagent (ready to use)

PBS (sterile, only for RNA isolation)

Chloroform (RNAse free)

Isopropanol (sterile, only for RNA isolation)

75% ethanol (sterile, only for RNA isolation)

PCR water (sterile, only for RNA isolation)

3.10.2. DNase I treatment

The RNA concentration in sample was measured using NanoDrop™ 2000 (Thermo Fisher Scientific, Waltham, Massachusetts, USA).

1) To 200 µl PCR tube add: 1 µg of RNA, 1 µl od DNase I, 1 µl of reaction buffer and nuclease-free water to total reaction volume of 10 µl
2) Incubate in cycler for at least 30 minutes at 37°C
3) Add 1 µl of EDTA to stop the reaction

4) Incubate for 10 minutes at 65°C
5) Use immediately for cDNA synthesis or store in freezer at -20°C.

3.10.3. cDNA synthesis using SuperScriptIII

1) To 11 µl reaction from DNase treatment add: 1 µl dNTPs, 1 µl oligo dT primers
2) Incubate for 5 minutes at 65°C to anneal the primers
3) Leave the sample on ice for at least 1 minute to inhibit the reaction
4) Add: 4 µl 5xFS buffer, 1 µl dTT (1M), 0,5 µl RNase OUT, 0,5 MgCl2, 1 µl SuperScriptIII reverse transcriptase
5) Incubate for 60 minutes at 42°C
6) Inhibit the reaction for 15 minutes at 70°C
7) Use directly for PCR reaction of store in freezer at -80°C.

3.10.4. Genomic DNA isolation

Genomic DNA was isolated using Wizard® Genomic DNA Purification Kit (Promega). To isolate a high quality gDNA, the protocol from the kit was followed. (https://worldwide.promega.com/resources/protocols/technical-manuals/0/wizard-genomic-dna-purification-kit-protocol/).

3.10.5. PCR amplifications

1) For total volume of 25 µl reaction mixture, pipette to the sterile 200 µl PCR tubes:
   12.5 µl of Emerald MasterMix (Thermo Fisher Scientific, Waltham, Massachusetts, USA)
   1 µl of forward DNA primer
   1 µl of reverse DNA primer
   2 µl of synthetized cDNA
   8.5 µl of ultra pure PCR water

2) For the virulence testing, two programs were used:

A. Gradient PCR for detection of viral DNA in samples

5 minutes at 95°C

30 seconds at 95°C	
30 seconds at 65°C	20 cycles (- 0.5°C with each cycle)
80 seconds at 72°C	
30 seconds at 95°C	15 cycles
30 seconds at 45°C	
∞ at 4°C	

B. PCR program for *M. hominis* detection in samples

2 minutes at 94°C	
30 seconds at 94°C	
30 seconds at 55°C	39 cycles
30 seconds at 72°C	
∞ at 4°C	

Primer name	**Sequence (5'→3')**
TVV1F2875 (TVV1 - forward)	ATTAGCGGTGTTTGTGATGCA
TVV1R3443 (TVV1 - reverse)	CTATCTTGCCATCCTGACTC
TVV2F2461 (TVV2 - forward)	GCTTGAGCACTGCTCGCG
TVV2 (TVV2 - reverse)	TCTCTTTTGGCATCGCTT
TVV3F61 (TVV3 - forward)	AAATTAATCAACACCCTCC
TVV3R482 (TVV3 - reverse)	CAGATCACTTTGTGTGTC
TVV4F1338 (TVV4 - forward)	ATGCCAGTTGCTTTCCG
TVV4R1834 (TVV4 - reverse)	TTCCCCAATAGTTATCAG

Tab. 1 Primers used for TVV amplifications (based on Goodman et a., 2011)

3.11. Purification of exosomes: protocol I.

1) 1000 ml of cell culture in logarithmic grown phase spin at 1000 x g for 10 minutes at 4°C
2) Wash the pellet 3 times in 50 ml TYM medium without horse serum. Each time, resuspend the pellet well and spin at 1000 x g for 10 minutes at 4°C
3) Resuspend the pellet in 100 ml of TYM medium without horse serum and divide into the two 50 ml falcon tubes.
4) Incubate one tube at 4°C for 4 hours and the other one at 37°C for 4 hours
5) Spin the cells at 1000 x g for 10 minutes at 4°C.
6) Pass the supernatant through the 0.22 μm filter to remove cell debris and larger extracellular vesicles.
7) Spin at 100 000 x g for 75 minutes at 4°C
8) Remove the supernatant to the clean falcon tube
9) Resuspend the pellet of microvesicles in 70 μl of I sample buffer to obtain the sample for SDS-PAGE.
10) Precipitate the proteins in supernatant with acetone. To 10 ml of supernatant add 40 ml of cold acetone. Incubate in freezer (-20°C) overnight. On the next day, spin at 14 000g for 10 minutes at 4°C and remove the supernatant. Let the acetone evaporate as much as you can. Take 10 μl of the pellet and resuspend in I sample buffer. Incubate for 5 minutes at 95°C in dry bath
11) Compare the protein content in samples using SDS-PAGE and Western blot as described previously.

3.12. Purification of exosomes: protocol II.

3.12.1. Exosomal production and excretion

1) Spin 1000 ml of cell culture with density of around 1 milion cells/ml at 2000 x g for 15 minutes at 20°C
2) Wash the cells 3 times in TYM medium without agar and without horse serum (TYM -ag, -HS)
3) Resuspend the pellet in 1000 ml TYM -ag, -HS and incubate for 3 hours at 37°C
4) Spin at 2000 x g for 15 minutes at 4°C
5) On ice, filter the supernatant over 0.22 μm filter

6) Concentrate the supernatant containing exosomes using Tangential flow filtration (TFF) using Vivaflow 50 system (Sartorius).

3.12.2. Sucrose gradient (10 – 70% sucrose)

1) Start with making the two solutions: 250 mM sucrose with HEPES pH 7.2 (light)
   3 M sucrose with HEPES pH 7.2 (heavy)
2) On Gradient master 108 (Biocomp Instruments) set the long gradient program in SW41 tubes
3) Balance the deck using the level and draw two lines according to the template
4) Pour the light solution first 2-3 mm over the first line without making any bubbles
5) Sublayer the light solution with the heavy solution exactly to the second line
6) Close the tube and run the program to make the gradient
7) Open the tube and load no more than 700 µl of the sample down the wall onto the gradient
8) Spin at 100 000 x g at 4°C overnight
9) The next day, carefully take apart the gradient in 1 ml volumes starting from the bottom
10) Place each sample to the 50 Beckmann tubes and adjust the volumes with the 250 mM sucrose solution so they match
11) Spin at 100 000 x g for 75 minutes at 4°C
12) Discard the supernatants and resuspend each pellet in 50 µl of 1x I sample buffer
13) Proceed with the SDS-PAGE and Western blot analysis

Required solutions:

TCA protein precipitation

100% trichloroacetic acid

VIVAFLOW washing solution	**total volume 250 ml**
NaClO (0,5 mM)	1,98 ml
NaOH	5 g

The components were dissolved in distilled water.

3.13. Testing of TV 17-2MI clones

3.13.1. Preparation of TV 17-2MI clones based on limited dilution method

1) Count the cells in logarithmic phase of growth using Bürker chamber.
2) Gradually dilute the cells to 5 cells in 25 ml of TYM with 10% medium volume of Penicillin-Streptomycin (Sigma-Aldrich, Saint-Louis, Missouri, USA)
3) Using the multichannel pipette, add 250 µl of the cell suspension to each well of
4) 96 well sterile microtitration plate. Check each well under the microscope and mark those containing a single cell
5) Incubate the cells under anaerobic conditions at 37°C for 5-7 days. Check cells every day.
6) Once there is apparent cell growth, transfer most of well volume to the cultivation tube (5 ml).
7) Grow the culture for few passages and cryopreserve at liquid nitrogen using 5% dimethyl sulfoxide (DMSO).

3.13.2. Mouse intraperitoneal virulence test

1) Count the cells in logarithmic phase of growth using Bürker chamber. It should be aproximatelly $2x10^6$ cells in 1 ml.
2) Inject $1x10^6$ cells in 500 µl in each mouse intraperitoneally. Use duplicates or triplicates for each tested clone.
3) Check the mice at least once a day and keep the notes about the overall health of each subject.
4) Once the mouse died, immediately perform the autopsy, isolate trichomonads from peritoneal cavity and infected tissues for further analysis.
5) Alternatively, sacarify infected mouse 5 days after infection for isolation of trichomonads from peritoneal cavity and for isolation of tissue samples.

3.13.3. Histology sample preparation

1) Dissect the mouse abdomen and observe carefully every organ.
2) Dissect abscesses with adjacent tissue.
3) Fix the samples in 10% formaldehyde in PBS solution for 24 hours in fridge.

4) Next transfer the samples to 70% ethanol solution and store in fridge until further processing.

Required solutions:

Fixing solution	**total volume 100 ml**
Formaldehyde 32% (ml)	32 ml
PBS (sterile)	68 ml

Two components were mixed together thoroughly to form 10% formaldehyde in PBS solution.

Storage solution	**total volume 100 ml**
Ethanol 96%	70 ml
Distilled water	30 ml

Components were mixed together.

In the Histopathology unit (Biocev), the tissue samples were embedded in paraffin and sectioned in 5 μm thick sections, while only each 4th was taken. All the slides were stained with standard hematoxylin-eosin solution. We were provided with 4-5 slides from each tissue sample. The slides were then analyzed using Nikon Eclipse Ti2 microscope with wide-field color camera system (Nikon corporation, Minato City, Tokyo, Japan).

3.13.4. Detection of *T. vaginalis* in mouse peritoneum samples

1) After the dissection of skin on abdomen, inject the 1-2 ml of sterile PBS into the abdominal cavity without damaging the peritoneum.
2) Remove the PBS solution and place it into the sterile 1.5 ml tube.
3) Isolate the RNA using TRIzol reagent as described previously.
4) Proceed the sample with DNase I treatment and synthetize the cDNA as described previously.
5) For PCR, primers for mouse glyceraldehyde-3-phosphate (GAPDH), TV DNA topoisomerase II, TV 40S rRNA 23S protein and TV 6S rRNA L10a protein were used. PCR reaction was provided using Emerald MasterMix as previously described.
6) PCR program for the detection

   3 minutes at 95°C

20 seconds at 95 °C

30 seconds at 67°C (- 0.5°C with each cycle) 35 cycles

30 seconds at 72°C

---

5 minutes at 72°C

∞ at 4°C

7) The PCR product was visualized using 1% agarose gel electrophoresis.

Mouse GAPDH (5'-3')	
forward primer	AGGTCGGTGTGAACGGATTTG
reverse primer	TGTAGACCATGTAGTTGAGGTCA
TV DNA topoisomerase II (5'-3')	
forward primer	ATCGGTGTCGGTTGGTCAAG
reverse primer	TGGCTGTTTGACACCGTCTTT
TV 40S rRNA 23S protein (5'-3')	
forward primer	TGCTCGTAAACTCCGTCTTG
reverse primer	GAGAAACCAGCGACCTTGATA
TV 6S rRNA L10a protein (5'-3')	
forward primer	ACTGCGAAGAAGCTCAGAAG
reverse primer	CATGTTGACGTTGCCGATTG

Tab. 2 Primers used for *T. vaginalis* detection and control mouse GADPH

3.14. Expression of HA-tagged proteins in *T. vaginalis*

Three genes were selected for cloning and expression in *T. vaginalis*: tetraspanin (TSP) 1 gene (TVAG_01980), SNARE gene (TVAG_249080) and gene for multivesicular body protein gene (TVAG_396070).

3.14.1. Gene amplification by PCR

As a template DNA, the DNA isolated from T1 strain was used. Genes for tetraspanin 1 (TSP1), SNARE protein and multivesicular body protein (MBP) were amplified using PCR. Primers were designed using Geneious® software (Biomatters).

TSP 1, restriction sites **NdeI, BamH1**	
forward primer	5'-CATA**CATATG**ACCTGCTGTTCATGCATG-3'
reverse primer	5'-TACT**GGATCC**AACGTATGTGATGCCTTCCTTCT
Snare, restriction sites **NdeI, BamH1**	
forward primer	5'-TACT**CATATG**TCTTTTGTCTACGCTTTAGTTGC
reverse primer	5'-CATA**GGATCC**AGCGGTCTTATCCTTCTTAGTGC
MBP, restriction sites **NdeI, BamH1**	
forward primer	5'-TACT**CATATG**AAGCGCTTATTCGGAAAGA
reverse primer	5'-TATT**GGATCC**CCAGGCTTCCTTCTGAGGTG

Tab. 3 Primers used for gene amplification

3.14.2. PCR reaction

1) Total volume of the reaction mixture was 25 µl in the sterile 200 µl PCR tubes:

   5 µl of 5x Q5 reaction buffer (NEB)

   5 µl of 5x Q5 High GC enhancer (NEB)

   0.5 µl of dNTPs (10 mM)

   1 µl of gDNA (150 ng/ µl)

   1.25 µl of forward primer (10µM)

   1.25 µl of reverse primer (10µM)

   0.25 µl of Q5® High-fidelity DNA polymerase (NEB)

   10.75 µl of ultra pure PCR water

2) PCR program for the amplification

   30 seconds at 98°C

   ---

   10 seconds at 98°C

   25 seconds at 72°C (-1°C with every cycle) 25 cycles

   30 seconds at 72°C

   ---

   2 minutes at 72°C

   ∞ at 4°C

3.14.3. DNA isolation from the gel using Gel/PCR DNA Fragments Kit (Geneaid BIOTECH LTD, Taiwan)

1) Separate PCR product by electrophoresis, cut off the desired band precisely and put it to the sterile 1.5 ml tube.
2) Add 500 µl of DF Buffer to the sample and vortex.
3) Incubate for 15 minutes at 60°C until the gel slice if completely dissolved.
4) Place the DF Column into the 2 ml Collection Tube.
5) Transfer maximum of 800 µl of the sample to the DF Column (if there's more than 800 µl of the sample, repeat the steps 5-7).
6) Spin at 16 000g for 30 seconds, discard the flow-through and place the DF Column back to the Collection Tube.
7) Add 400 µl of W1 Buffer into the DF Column.
8) Spin at 16 000g for 30 seconds, discard the flow-through and place the DF Column back to the Collection Tube.
9) Add 600 µl of Wash Buffer into the DF Column.
10) Let stand for 1 minute at room temperature.
11) Spin at 16 000g for 30 seconds, discard the flow-through and place the DF Column back to the Collection Tube.
12) Spin at 16 000g for 3 minutes to dry the column matrix.
13) Transfer the DF Column into the new 1.5 ml tube.
14) Add 30 µl of Elution Buffer to the center of the DF Column.
15) Let stand for 2 minutes at room temperature.
16) Spin at 16 000g for 2 minutes to elute the DNA.

3.14.4. Ligation into the pJET vector (blunt vector)

Amplified genes were first subcloned into the pJET vector with ampicillin resistance.

1) Ligation reaction mixture contains:
   5 µl 2x ligation buffer (Sigma-Aldrich, Saint-Louis, Missouri, USA)
   0.5 µl T4 DNA ligase (Sigma-Aldrich, Saint-Louis, Missouri, USA)
   0.5 µl pJET1.2 (Thermo Fisher Scientific, Waltham, Massachusetts, USA)
   4 µl gene DNA
   Proceed ligation at 15°C overnight.

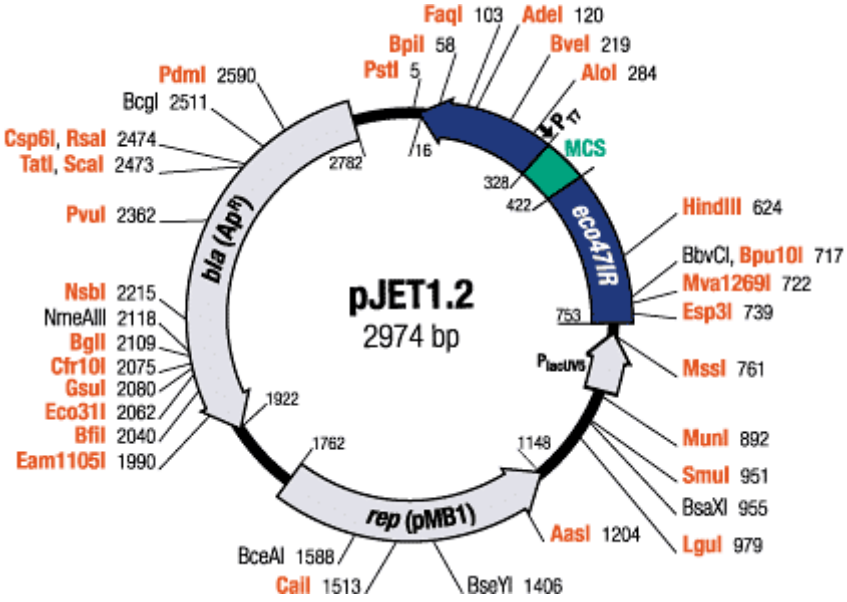

Fig. 5 Map of pJET1.2 vector (Thermo Fisher Scientific, Waltham, Massachusetts, USA)

3.14.5. Transformation of TOP10 competent *E.coli* cells

TOP10 competent *E.coli* cells were used for the plasmid propagation.

1) Remove the TOP10 competent cells from -80°C and let them dissolve for 10-20 minutes on ice.
2) Carefully add 5 µl of plasmid on the surface.
3) Incubate for 20 minutes on ice.
4) Immerse the tube in water bath (42°C) for 30 seconds so bacteria will incorporate the plasmid under the heat shock.
5) Incubate for 2 minutes on ice,
6) Add 250 µl of SOC medium.
7) Incubate for 60 minutes at 37°C on shaker.
8) Take the LB plates from the fridge and distribute 50 µl of ampicillin evenly all over the plate.
9) Add 30 µl of transformed TOP10 cell mixture onto the LB plate and evenly distribute.
10) Incubate at 37°C overnight.
11) Use the next day or store at 4°C.

3.14.6. Isolation of pJET with inserted gene using Hybrid-Q Plasmid Rapidprep (GeneAll®, Lisbon, Portugal)

1) Transfer a single colonies from the plate to the tube with LB medium and ampicillin (5 µl of ampicillin stock solution to 5 ml of LB medium)
2) Incubate at 37°C for 16 hours on the shaker.
3) Spin the bacterial culture at 10 000 x g for 5 minutes, discharge the supernatant.
4) Resuspend the pellet of the cells in 170 µl of S1 buffer.
5) Add 170 µl of S2 buffer and mix the components via inverting the tube 4-5 times.
6) Add 250 µl of G3 buffer and mix again via inverting the tube 4-5 times.
7) Transfer the lysate to EzClear filter column by decanting.
8) Spin at 13 000 x g for 1 minute.
9) Discard the upper column unit, remove the collecting tube and discard the flow-through.
10) Reinsert the bottom part of EzClear filter column to the collecting tube.
11) Add 500 µl in the column and spin at 13 000 x g for 30 seconds.
12) Discard the pass-through, reinsert the column to the collecting tube and spin for extra 1 minute to remove the residue from wash buffer.
13) Add 50 µl of EB to the column and let stand for 1 minute on the desk.
14) Spin at 13 000 x g for 1 minute to elute the plasmid DNA.

3.14.7. Re-cloning of the gene into TagVag vector

The gene in pJET1.2 was recloned to TagVag plasmid with geneticin (G418) resistance and hemagglutinin (HA) tag Hrdý et al., 2004 (Fig. 6), that allows protein expression with C-terminal HA tag in *T. vaginalis* and selection of transformants under geneticin (G418) antibiotic in concentration of 10 µl/ml.

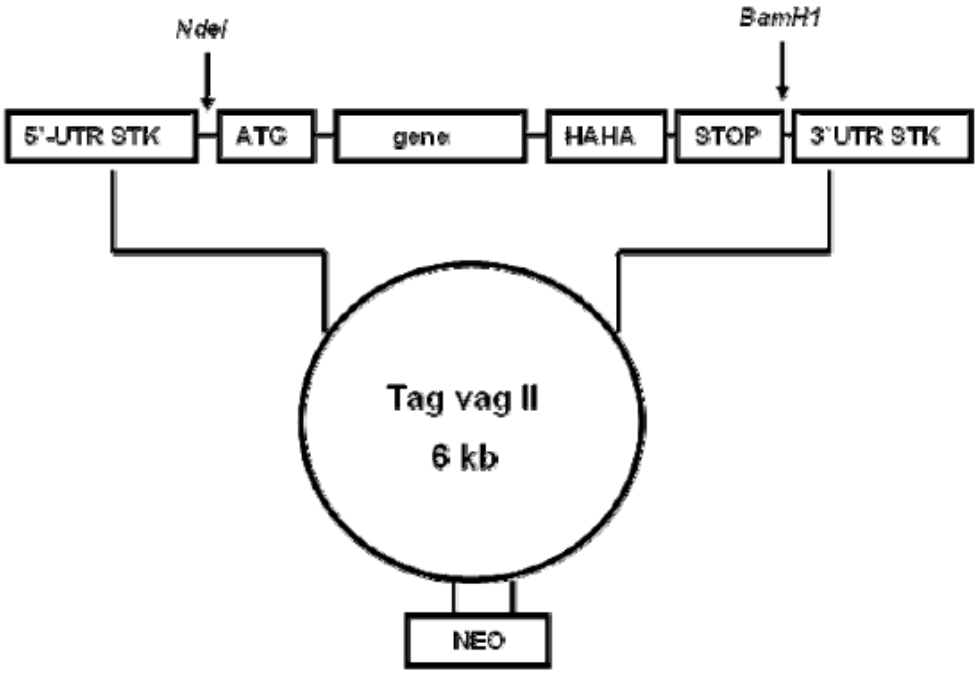

Fig. 6 Expression vector for *T. vaginalis* transfection (adapted from diploma thesis by E. Nývltová, 2008). The final plasmid has strong succinate thiokinase (**STK) promotor**, **HAHA tag** and the gene for neomycine resistance (**NEO)**.

For restriction add:

1) 26 µl of insert gene (for TagVag: 5 µl of TagVag and 21 µl of water),
2) 3 µl of Fast Digest buffer,
3) 0.5 µl od NdeI and 0.5 µl od BamH1
4) Incubate for 40 minutes at 37°C
5) Analyze the samples using 1% agarose gel electrophoresis

The DNA from the gel was then isolated using Gel/PCR DNA Fragments Kit (Geneaid BIOTECH LTD, Taiwan) as described previously.

The DNA was then ligated to the TagVag using the ligation protocol as described previously.

TOP10 competent cells were then transformed as described previously.

The plasmid DNA was isolated from the cells and correct sequence of inserted gene was verified by DNA sequencing.

3.14.8. Midiprep isolation of TagVag using Wizard *Plus* Midipreps DNA Purification System (Promega, Madison, Wisconsin, USA)

If the sequencing results were positive (the gene was cloned to the vector correctly), a larger volume of transformed cell cultures (100 ml) was prepared for the vector isolation.

1) Spin the bacteria cells at 8000g for 10 minutes at 4°C
2) Resuspend in 3 ml of Cell Resuspension Solution
3) Add 3 ml of Cell Lysis Solution and mix gently
4) Add 3 ml of Neutralization Solution and mix gently
5) Spin at 8000g for 15 minutes at 4°C
6) Add 10 ml of resin to the DNA and resuspend
7) Connect the midi column to the vacuum
8) Decant the DNA with resin to the midi column and let the liquid flow through the vacuum. Resin will form a little balls with the DNA attached to it.
9) Wash twice with 15 ml of Column Wash Solution
10) After the second wash, let the vacuum run for extra 30 seconds
11) Turn the vacuum off and disconnect the column and reservoir. Put column to the 1.5 ml tube and spin at 10 000g for 2 minutes
12) Put the column to the new sterile1.5 ml tube and add 300 µl of ultra pure preheated water
13) Let it stand for 1 minute and spin at 10 000g for 20 minutes
14) Store in the freezer at -20°C ready for the transfection

3.14.9. Transfection of *T. vaginalis* using electroporation method

1) Harvest 1 l of T1 strain culture in logarithmic phase of growth
2) Spin the cells down in 50 ml falcon tubes at 1000 x g for 15 minutes at 4°C
3) Weigh the final pellet and add 0,5 ml of TYM medium with horse serum per 1 g of cells
4) Gently resuspend with Pasteur pipette and pass through 23G needle twice
5) Place Gene Pulser cuvette 0,4 cm on ice and add 300 µl of cell suspension and 50 µg of plasmid in ≤ 30 µl Mix gently and incubate on ice for 10 minutes
6) Electroporate the cells using Gene Pulser Bio-rad electroporator (Bio-rad, Hercules, California, USA) set on 350 V and 975 µF

7) Immediately transfer the cells into 50 ml sterile falcon tube with TYM and 1000 U/ml of penicillin and 250 µg/ml of amikacin and incubate at 37°C
8) Add 50 µl of geneticin) after 4-6 hours of incubation
9) Check cell growth daily.

4. Results

4.1. Detection of *T. vaginalis* endosymbionts

To investigate the virulence of *T. vaginalis* strains we first had to determine the presence of cellular endosymbionts that may affect *T. vaginalis* properties – dsRNA TVV1-4 and *Mycoplasma hominis*. For this testing, RNA was isolated from strains using TRIzol reagent, treated with the DNase I to remove any DNA contamination and then cDNA was synthesized using SSIII reverse transcriptase. For RT-PCR, a sets of primers specific for TVV1-4 species were used according to Goodman et al., 2011. Four strains, TV17-2MI, TV 85-08, TV 79-49 and TV10-02 were selected for the test. TV17-2MI was a fresh isolate, in which presence of endosymbionts was not tested, TV85-08 and TV79-49, and TV10-02 were shown to be positive for TVV (Hampl et al., 2001), however, species of the virus was not known. TV10-02 serves also as a positive control for M. hominis.

RT-PCR test revealed that strains TV 85-08 and TV 17-2MI were free of TVV species (Fig. 10, Fig. 8). The strain TV 10-02 was infected with TVV2 (Fig. 7) and the strain TV 79-49 harbored three species TVV1, TVV2 and TVV3 (Fig. 9).

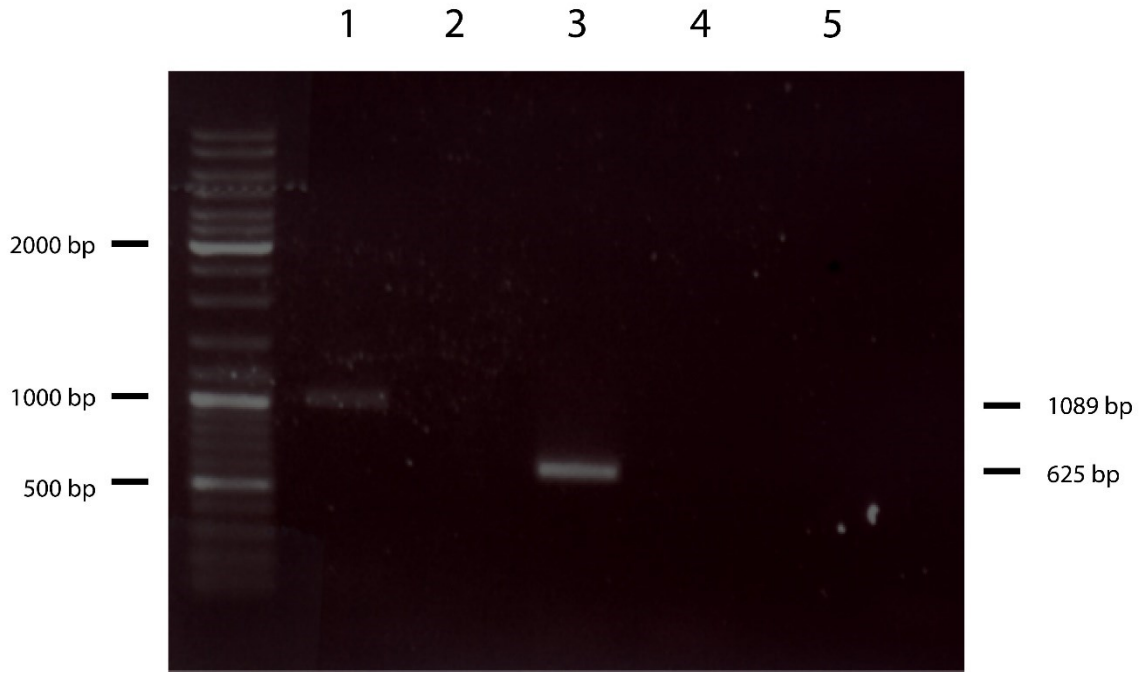

Fig. 7 Detection of trichomonasvirus species TVV in TV 10-02 strain using RT-PCR. 1 – Control of RNA isolation (SPDI primers), 2 –TVV1 primers, 3 –TVV2 primers, 4 –TVV3 primers, 5 –TVV4 primers.

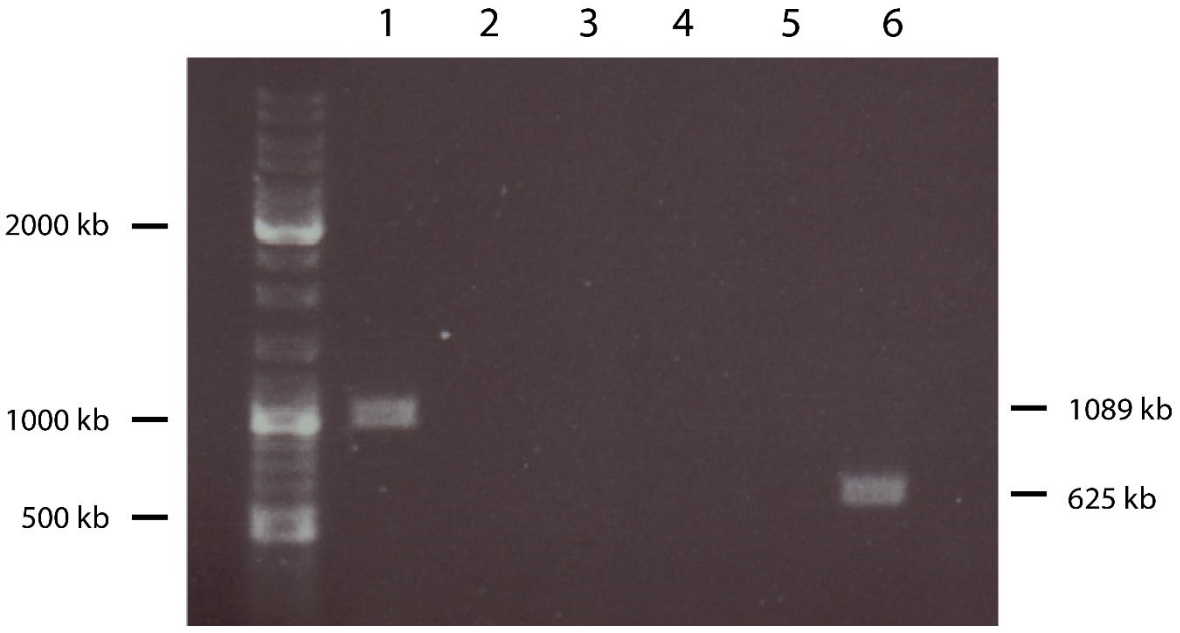

Fig. 8 RT-PCR detection of TVV species in TV 17-2MI strain. 1 –control for RNA preparation (SPDI primers), 2 –TVV1 primers, 3 –TVV2 primers, 4 –TVV3 primers, 5 –TVV4 primers, 6 – TV 10-02 with TVV2 primers.

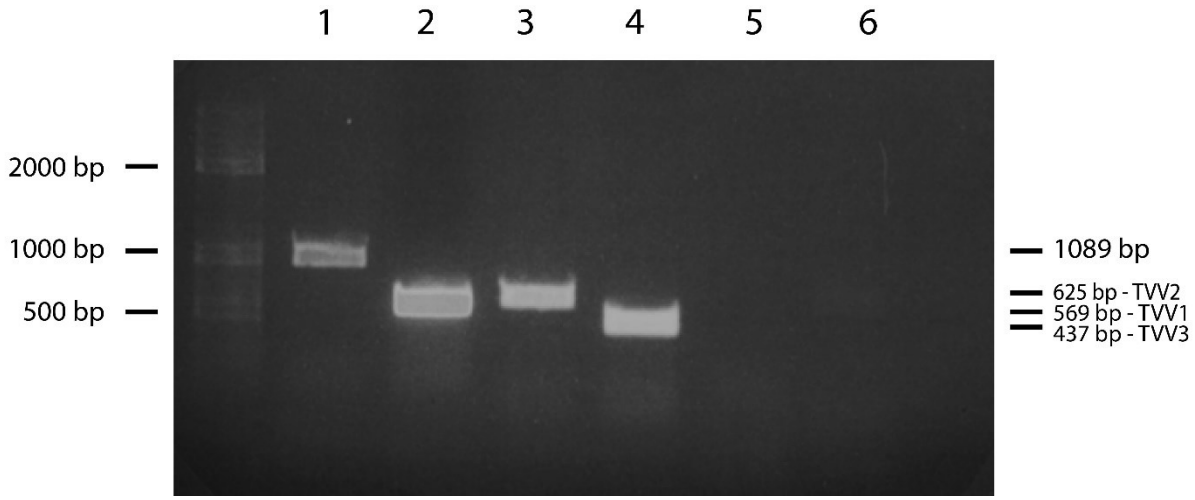

Fig. 9 RT-PCR detection of TVV species in TV 79-49 strain. 1 – control for RNA preparation (SPDI primers, 1089); 2-5, TV79-49; 2 –TVV1 (569 bp); 3 TVV2 (625 bp); – 4 –TVV3 (437 bp) ; 5 –TVV4 (514 bp), 6 – TV 10-02 positive control with TVV2 (625 bp)

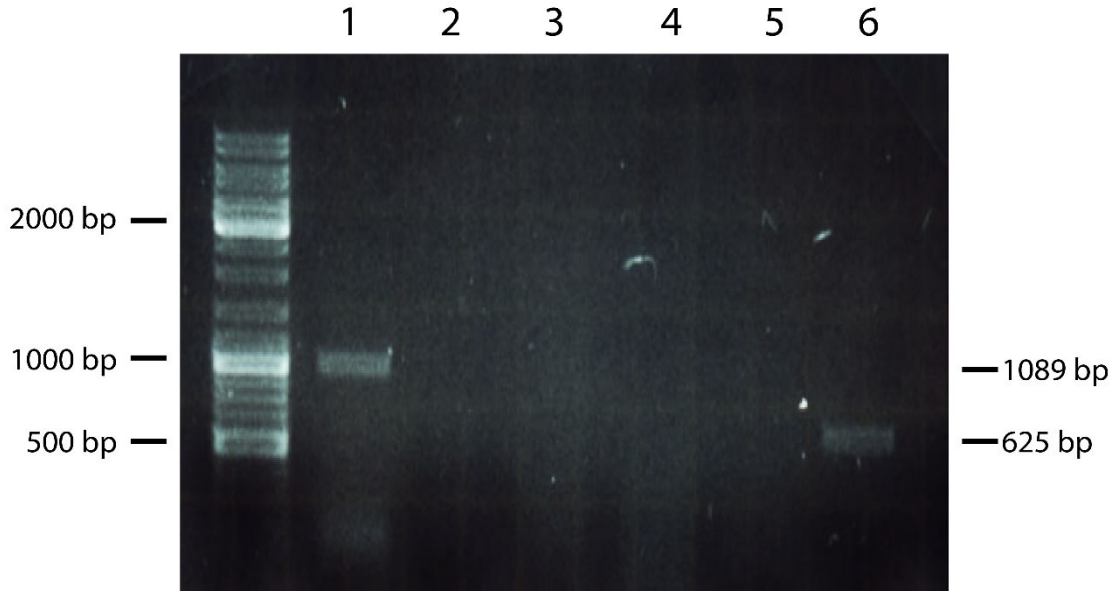

Fig. 10 RT-PCR detection of TVV species in TV 85-08 strain. 1 – positive control (TV 85-08 cDNA template and SPDI primers), 2 – TV 85-08 cDNA template with TVV1 primers, 3 – TV 85-08 template with TVV2 primers, 4 – TV 85-08 template with TVV3 primers, 5 – TV 85-08 template with TVV4 primers, 6 – TV 10-02 with TVV2 primers.

These strains were further tested for presence of *M. hominis*. First, we used staining of nucleic acids with DAPI and fluorescence microscopy to analyze fixed cells. DAPI clearly labeled pear-shaped nucleus in cells of all strains (Fig. 11, Fig. 12, Fig. 13, Fig. 14). *M. hominis* was visible only in the control strain – TV 10-02 (Fig. 13) as dots spread in the cytoplasm. It is difficult to determine the exact number of the *M. hominis* in each cell, because

the strong infestation makes it impossible to tell apart single *M. hominis* cells. To confirm the results from fluorescence microscopy, we run the PCR with primers that amplified 16S rRNA of *M. hominis*. Results confirmed presence of *M. hominis* in TV 10-02 (Fig. 15). Moreover, it detected M. hominis also in the strain TV 85-08 even though there was no evidence of *M. hominis* infection in strain TV 85-08 using fluorescence microscopy (Fig. 14).

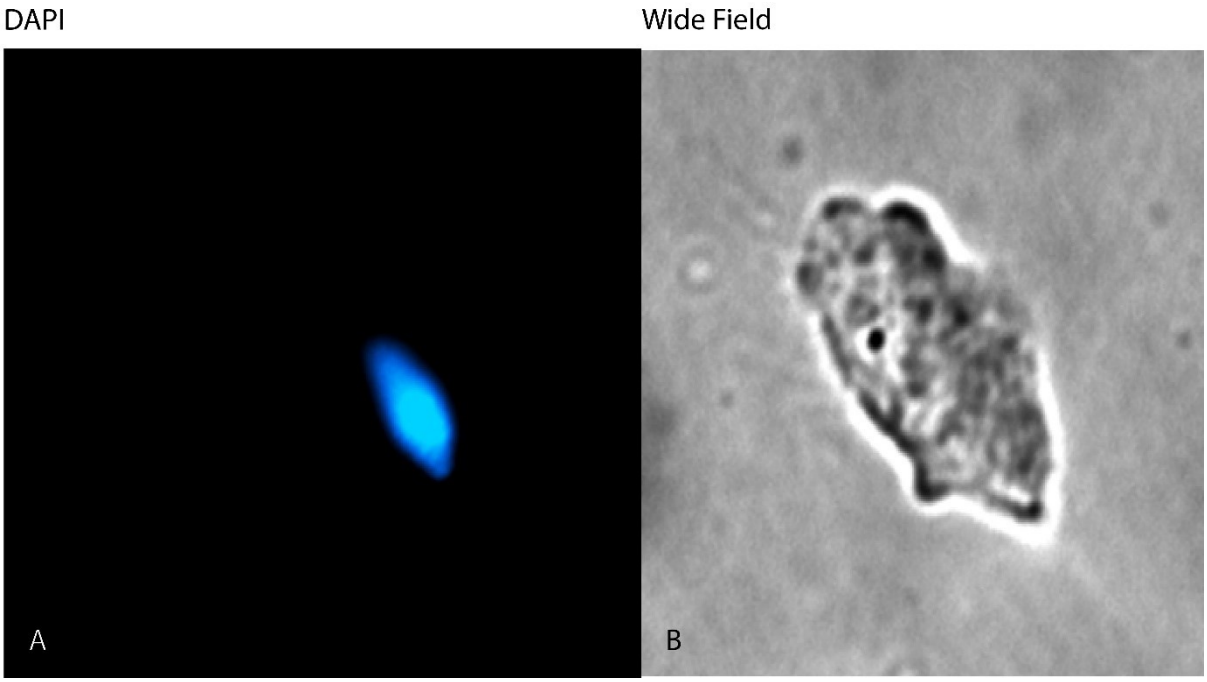

Fig. 11 Fluorescence microscopy of TV 17-2MI using DAPI for nucleic acid staining. No *M. hominis* is visible.

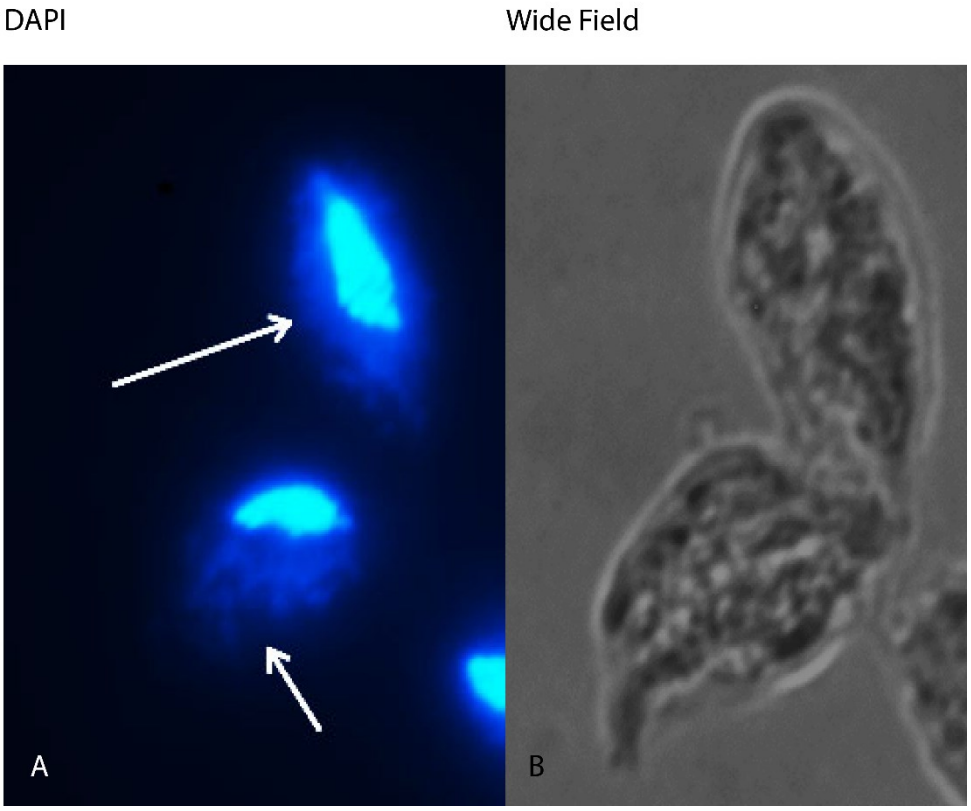

Fig. 12 Fluorescence microscopy of TV 10-02 using DAPI for nucleic acid staining. Arrows point to *M. hominis.*

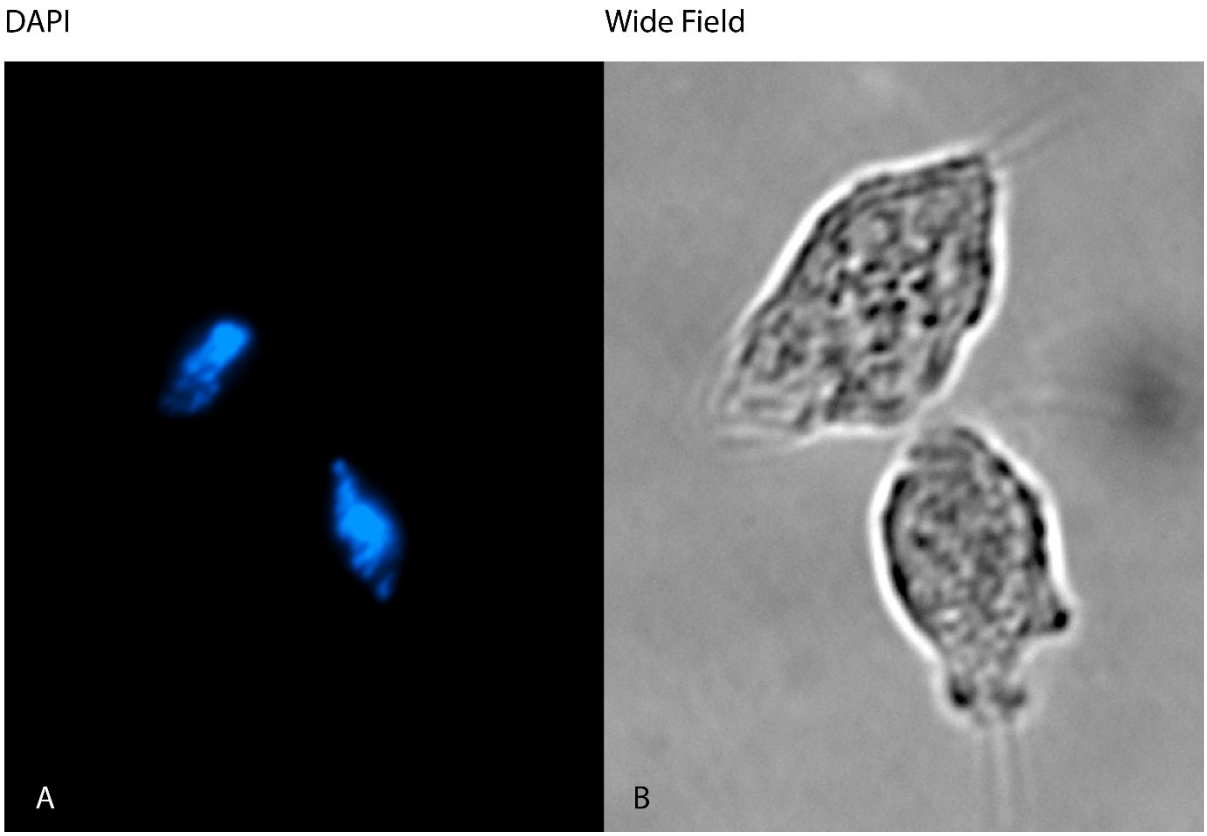

Fig. 13 Fluorescence microscopy of TV 70-49 using DAPI for nucleic acid staining.

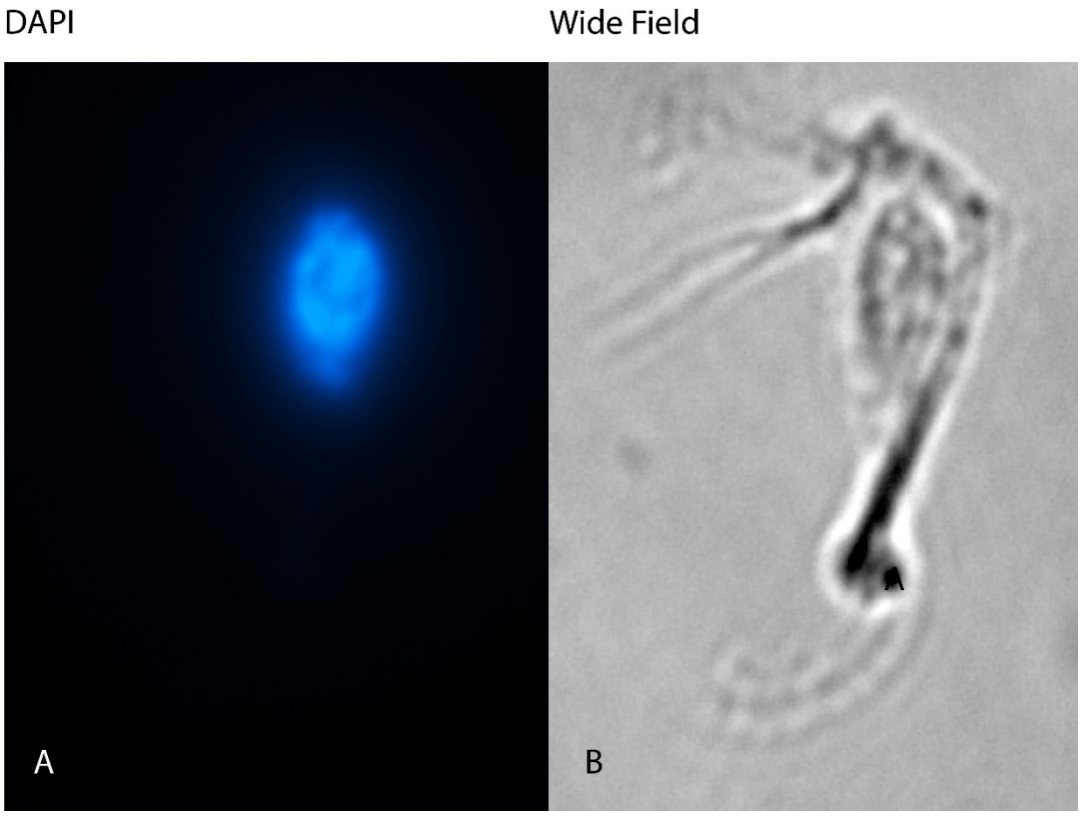

Fig. 14 Fluorescence microscopy of TV 85-08 using DAPI for nucleic acid staining. No *M. hominis* is visible.

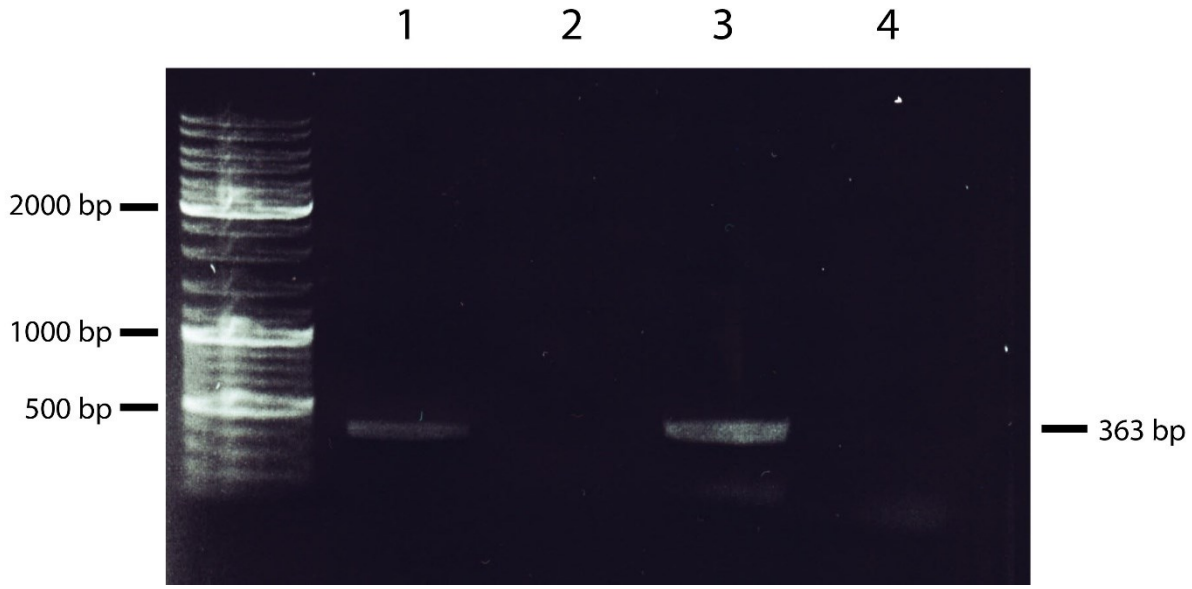

Fig. 15 Detection of *M. hominis* in strains of *T. vaginalis* using primers for amplification of 16SrRNA gene fragment (363 bp). 1 –TV 10-02, 2 – TV 17-2MI, 3 – TV 85-08, 4 – TV 79-49.

The presence or absence of TVV species and *M. hominis* in *T. vaginalis* strains are summarized in table below (Tab. 4). Based on these results, strain TV 17-2MI was chosen for mouse intraperitoneal experiment because there is presence of neither the TVV nor *M. hominis*.

Strain	**TVV1**	**TVV2**	**TVV3**	**TVV4**	***M. hominis***
TV10-02	-	+	-	-	+
TV 17-2MI	-	-	-	-	-
TV 79-49	+	+	+	-	-
TV 85-08	-	-	-	-	+

Tab. 4 Summary of the symbiont detection in various TV strains.

4.2. Testing the virulence in clones of TV 17-2MI using mouse peritoneal test

The strain TV 17-2MI had been isolated from the patient in Prague, and axenized. First, we wanted to know if this strain represents a homogenous population concerning its virulence or if the population is heterogenous and various clones behave differently.

Stage I

In the first stage we derived 6 clones from TV 17-2MI strain using limited dilution method. These clones were cultivated for about two weeks and cryopreserved. Virulence of clones was tested by mouse peritoneal virulence test using albino, lab-bred strain of BALB/c. We divided the mice to 7 groups with 2 mice in each group, 6 groups for clones and the 7^{th} for the parent strain). All the mice were infected with 1 mil of cells intraperitoneally. Experiment proceeded as depicted in scheme below (Fig. 16).

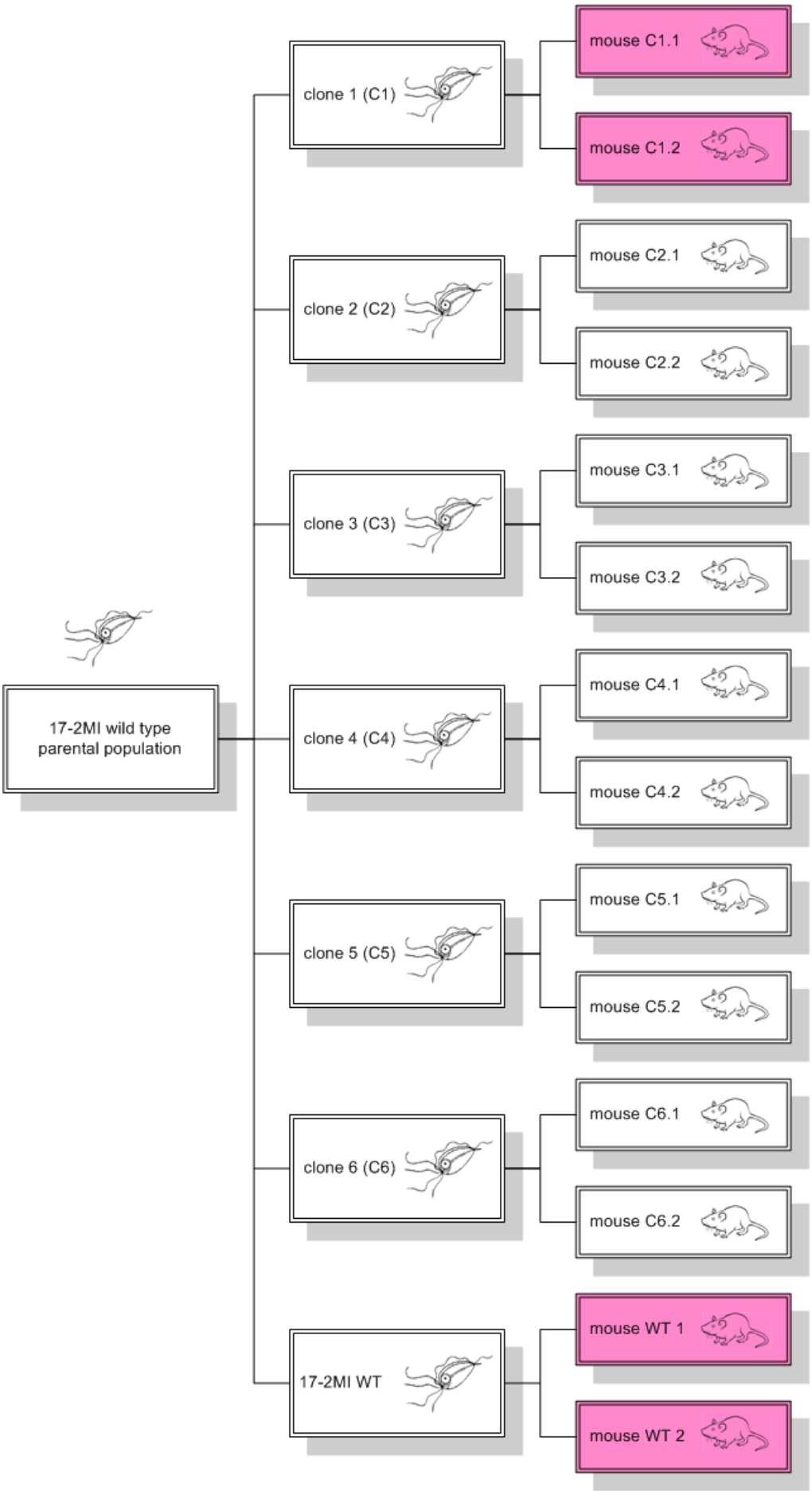
17-2MI wild type
parental population
clone 1 (C1)
clone 2 (C2)
clone 3 (C3)
clone 4 (C4)
clone 5 (C5)
clone 6 (C6)
17-2MI WT
mouse C1.1
mouse C1.2
mouse C2.1
mouse C2.2
mouse C3.1
mouse C3.2
mouse C4.1
mouse C4.2
mouse C5.1
mouse C5.2
mouse C6.1
mouse C6.2
mouse WT 1
mouse WT 2

Fig. 16 Scheme of the first stage of the virulence test. The 6 clones (C1-C6) and the parental TV 17-MI-2 strain were inoculated intraperitoneally to mice in duplicates. Mice infected with the parent strain and the clone C1 died four and five days after infection, respectively (in red).

The mice were checked daily to ensure that none of the possible changes in health was missed. Mice infected with the parent strain TV 17-2MI (group 7) and C1 clone (group1) showed decreased fitness, limited movement, and hair bristled up. Both mice of group 7 died 4 days after the infection. The next day, both mice of group 1 also died. No signs of infection were observed in mice of groups 2-6 during following month of observation. Thus, only one out of 6 clones caused a lethal infection and was considered as a virulent clone.

To reisolate trichomonads from the mice of group 1, we rinsed the abdominal cavity using sterile PBS solution with penicillin and amikacin and inoculated samples to TYM medium for cultivation. Reisolated trichomonads (C1-M) were stabilized in liquid nitrogen for further experiments. Opened abdominal cavities of C1-M infected mice revealed abscesses on the liver, spleen and intestines. Dissection of the abscesses revealed the presence of the *T. vaginalis* cells that were checked by native microscopy.

Stage II

In this stage we wanted to investigate whether reisolated C1-M clone has a stable phenotype and all clones derived from C1-M are virulent.

We performed limited dilution method for recloning of the C1-M. Five cloned were derived from the C1-M culture that were named C1-M/A to C1-M/E and maintained for about 2 weeks to stabilize the culture. To test virulence of these reclones, we injected peritoneally each reclone to two mice and we used parent 17-2MI strain as a control group). We proceeded the experiment as described in the scheme below (Fig. 17).

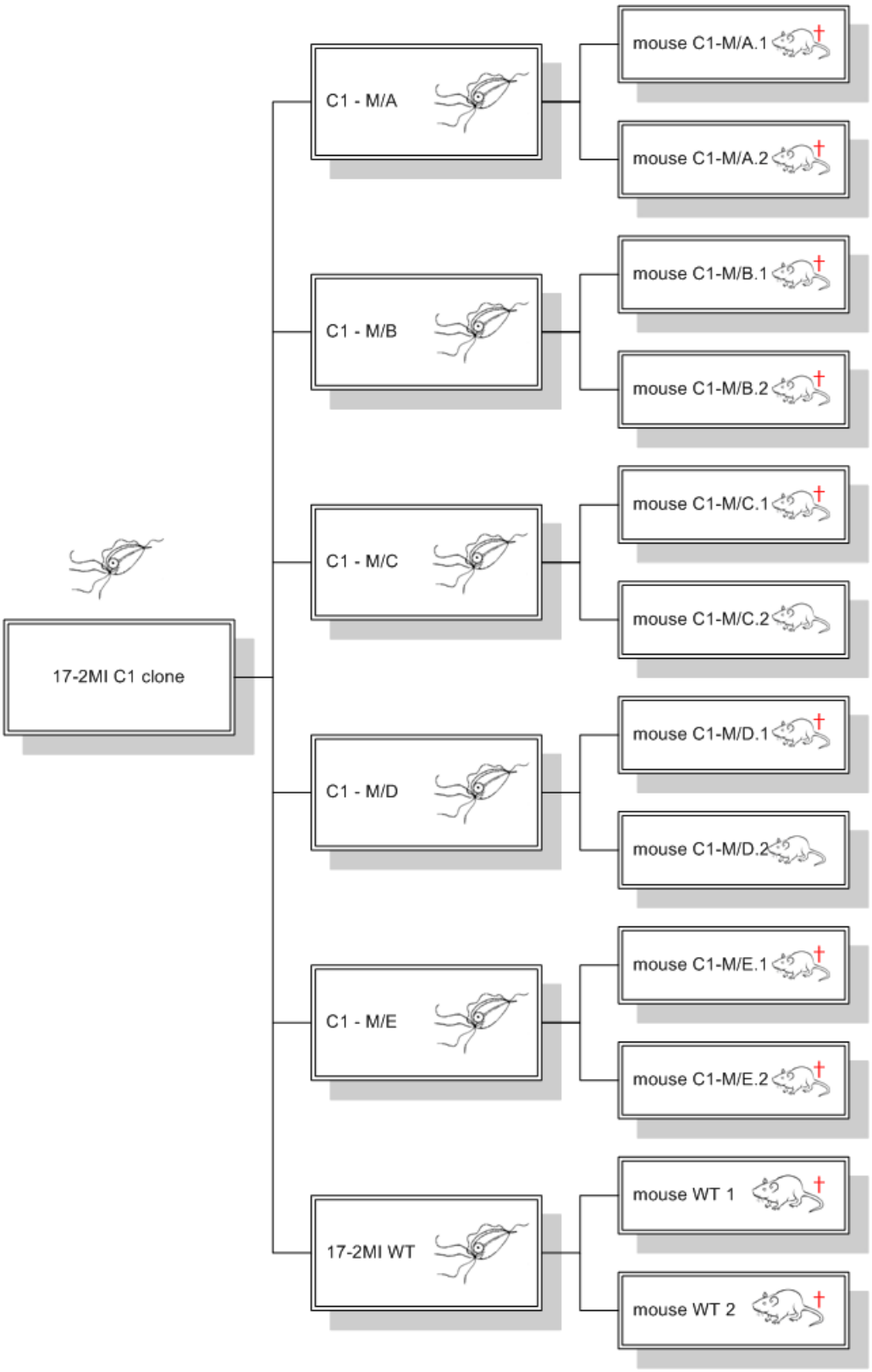

Fig. 17 Scheme of the second stage of the virulence test. The mice marked with the red cross died within the week after infection.

The infected mice were checked daily. They started to die at day 4 after infection to day 7 after intraperitoneal inoculation of trichomonads (Tab. 5).

TV 17-2MI	mouse 1	mouse 2
C1/A	† 22/4/2019 (day 4)	† 24/2/2019 (day 6)
C1/B	† 23/4/2019 (day 5)	† 25/2/2019 (day 7)
C1/C	† 22/4/2019 (day 4)	-
C1/D	† 22/4/2019 (day 4)	-
C1/E	† 24/42019 (day 6)	† 24/4/2019 (day 6)
WT	† 23/4/2019 (day 5)	† 25/4/2019 (day 7)

Tab. 5 Dynamics of the lethal peritoneal infection of mice with *T. vaginalis* virulent reclones and the parent strain TV 17MI-2.

Dissection of mice with fatal infection revealed the typical hypertrophy of the spleen and liver as well as the calcified abscess on the liver, spleen and on the intestines. In two cases, reclones C1-M/B and C1-M/C, only a single out of two mice died.

Stage III

Final stage of the virulence experiments was focused to confirm the differences between selected virulent and non-virulent clones and to collect samples for histopathological analysis. We used C1-M/A as a virulent and C2/B as a non-virulent clone. C2/B was re-cloned from the non-virulent clone TV 17-2MI C2 from stage I to ensure that it is derived from a single cell. We used 2 groups of 3 mice in each group for inoculation of the virulent and non-virulent clones as described in scheme below (Fig. 18).

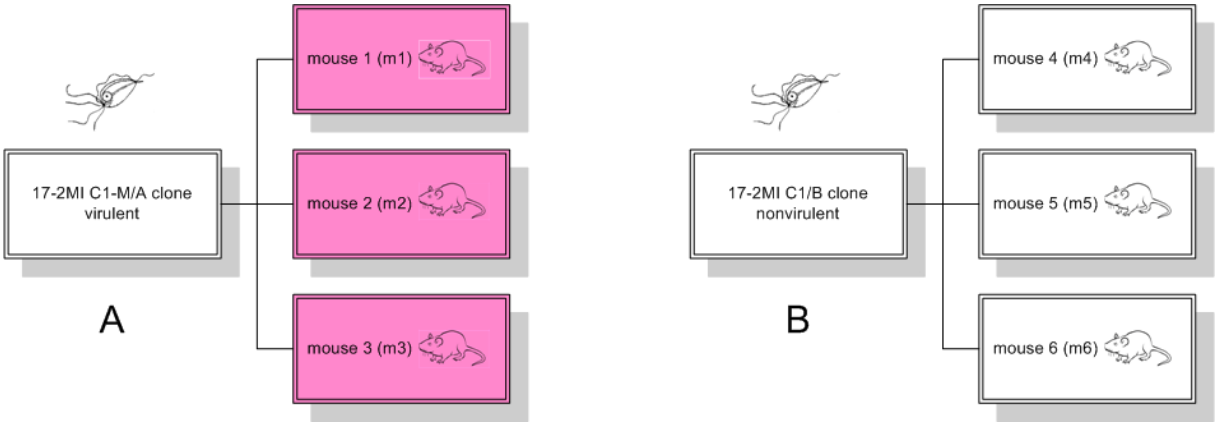

Fig. 18 Scheme of the stage III. virulence test. The mice were divided to the groups of 3 for peritoneal infection with the virulent clone C1-M/A (A), and non-virulent C2/B (B).

The mice were checked daily. Five days after infection, the mice of the virulent group were visibly fatigue with hair bristled up. We decided to terminate all mice next day. On the day 6 two mice from the virulent group dies, all others were terminated the same day.

4.2.1. Pathology and morphology of mice peritoneal cavity

From the first overall look of the mice, there was a marked difference between those infected with virulent strain and those infected with non-virulent strain. The mice infected with virulent strain had unhealthy cachectic appearance with bristled fur and enlarged abdomen. The mice infected with non-virulent strain showed no signs of the infection. Their appearance was normal, undistinguishable from non-infected mice (Fig. 19).

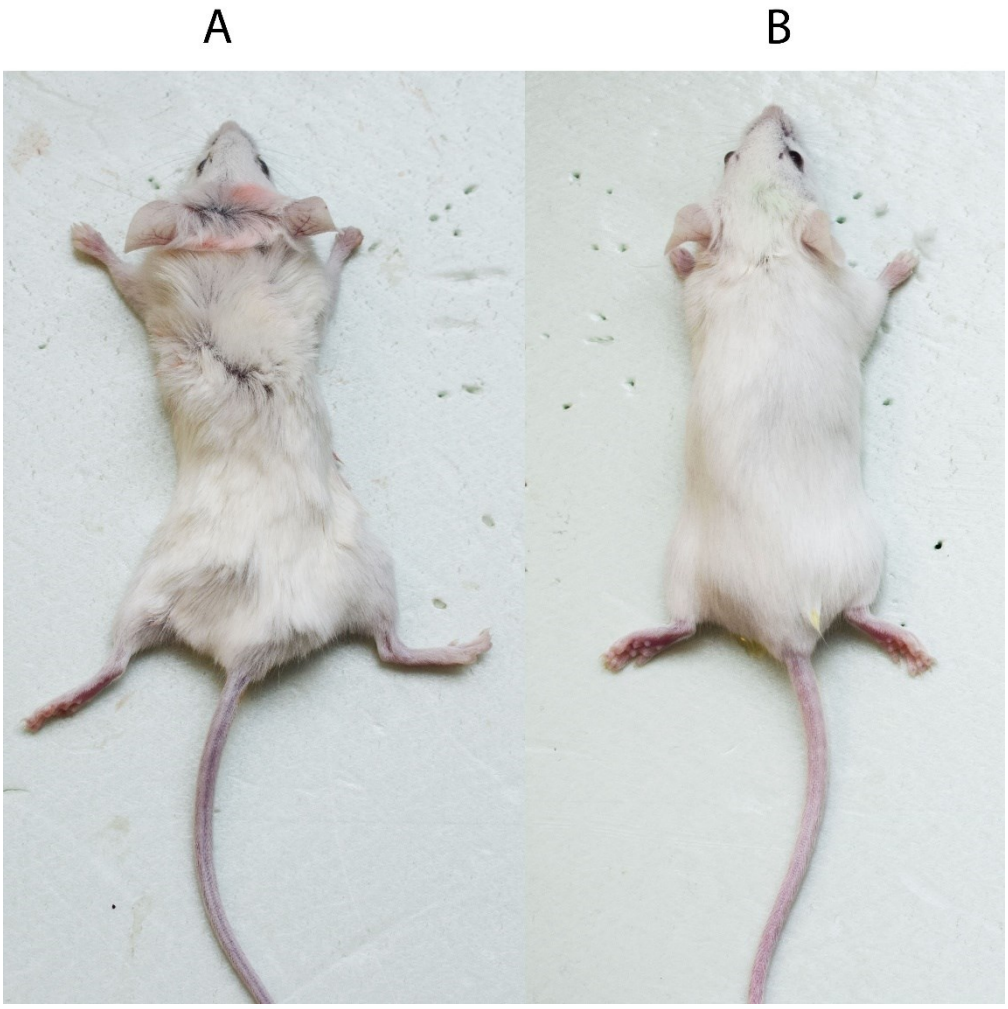

Fig. 19 Overall appearance of mice after 6 days of intraperitoneal infection with the non-virulent C2/B (A) and virulent C1-M/A (B) *T. vaginalis* clones.

When we carefully separated skin from peritoneal membrane, we observed clear difference between mice infected with the virulent clone C1-M/A and non-virulent clone C2/B. The mice infected with the virulent clone revealed marked hypertrophy of liver, intestines and spleen and ascitic fluid formation (Fig. 20).

A B

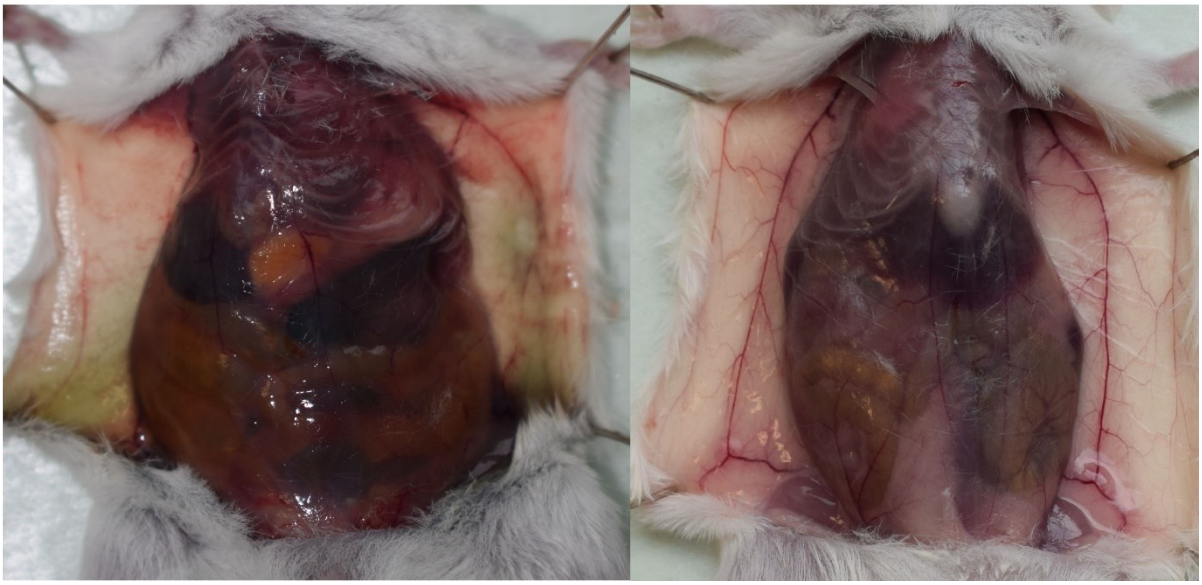

Fig. 20 Comparison of mice intraperitoneally infected with the virulent clone C1-M/A (A) and non-virulent clone C2/B (B). There is visible organ enlargement and presence of liver abscess, due to aggressive infection of *T. vaginalis*.

To collect trichomonads, we injected 1.5 ml of sterile PBS solution to wash the peritoneal cavity, slightly rub the abdomen and then aspirated from the cavity. Small aliquots of aspirated PBS were used to count a number of trichomonads using Bürker counting chamber. The number of trichomonads aspirated from mouse that we infected with the virulent clone ranged from 0.97 to 2,04x10^6/ml (Tab. 6).

Sample	***T. vaginalis* cell count**
mouse 1 (m1) virulent	2.04 *10^6 /ml
mouse 2 (m2) virulent	0.92 *10^6 /ml
mouse 3 (m3) virulent	1.13 *10^6 /ml
mouse 4 (m4) non-virulent	Not found in sample
mouse 5 (m5) non-virulent	Not found in sample
mouse 6 (m6) non-virulent	Not found in sample

Tab. 6 Number of trichomonads aspirated from abdominal cavity. The cells were found under microscope only in samples obtained from the mice that were intraperitoneally infected with the virulent clone C1-M/A.

The rest of samples was used to isolate RNA that was stored for later RT-PCR analysis and for analysis of transcriptome (not subject of this thesis).

Cutting through the transparent peritoneal membrane provided an access to organs. In mice infected with the virulent clone, hepatosplenomegaly was observed. We also saw visible abscesses and necrotic foci on various internal organs. Every subject from the virulent group had abscess on the liver, some of them had also abscesses on other internal organs such as spleen, lungs and intestines (Fig. 21 A). In comparison, the mice infected with non-virulent clone showed no signs of the organ or tissue changes. There was no organ hypertrophy or presence of abscesses in any of them (Fig. 21 B).

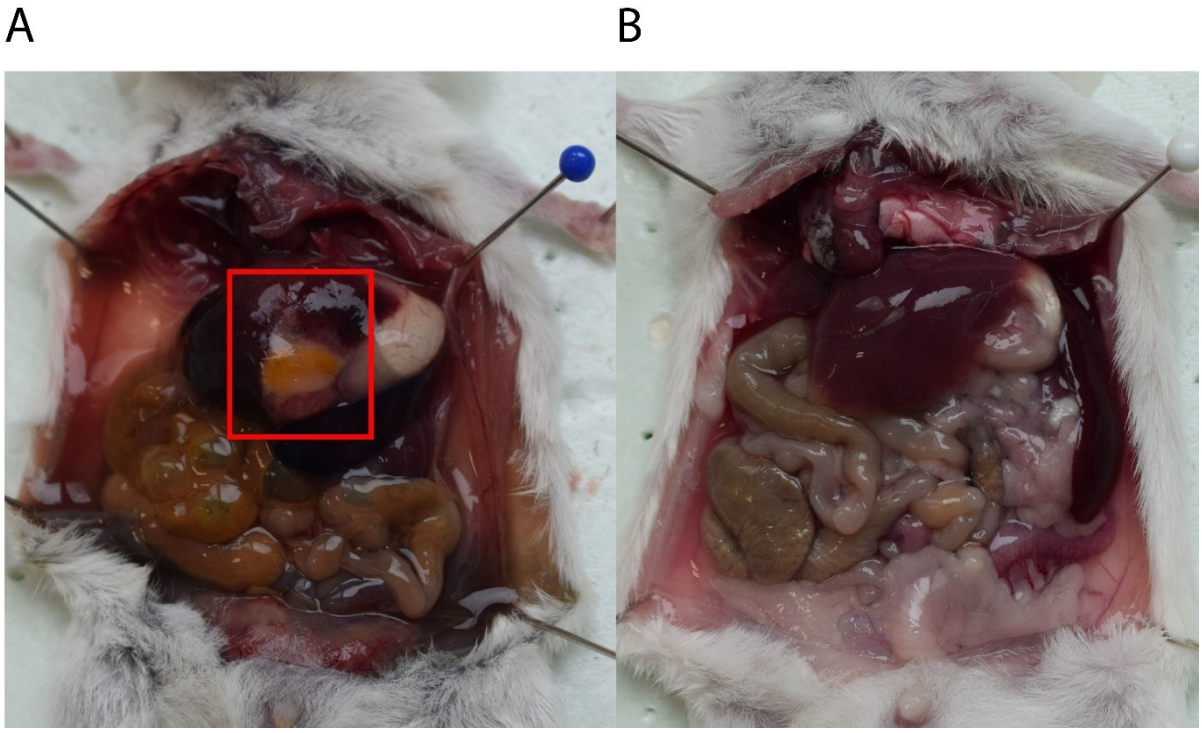

Fig. 21 Comparison of abdominal cavities in mice infected with *T. vaginalis* clones of different virulence. **A**. mouse that was intraperitoneally infected with virulent clone C1-M/A. Visible organ hypertrophy, especially prominent on the liver and intestines. Liver abscess is visible in a red box. **B** the mouse infected with the non-virulent clone C2/B. Normal anatomy without organ enlargement.

4.2.2. Histopathology of *T. vaginalis* infected mice

After overall examination of abdominal cavity, we proceeded with the autopsy of pathologies. We carefully dissected abscesses with the adjacent tissue, fixed them in 10% formaldehyde solution in PBS for 24 hours. Abscesses were held for 72 hours in 70% ethanol

solution and submitted to Histopathology unit in Biocev for further slide preparation. Slides were then analyzed under the wide-field microscope.

Examination of liver abscess showed a zone of perivascularly penetrating *T. vaginalis* cells, zone of leukocytes and the abscess (Fig. 22, Fig. 23). Structure of trichomonads including pear-shape nucleus, flagella and undulating membrane was apparent at higher magnification (Fig. 24, Fig. 25).

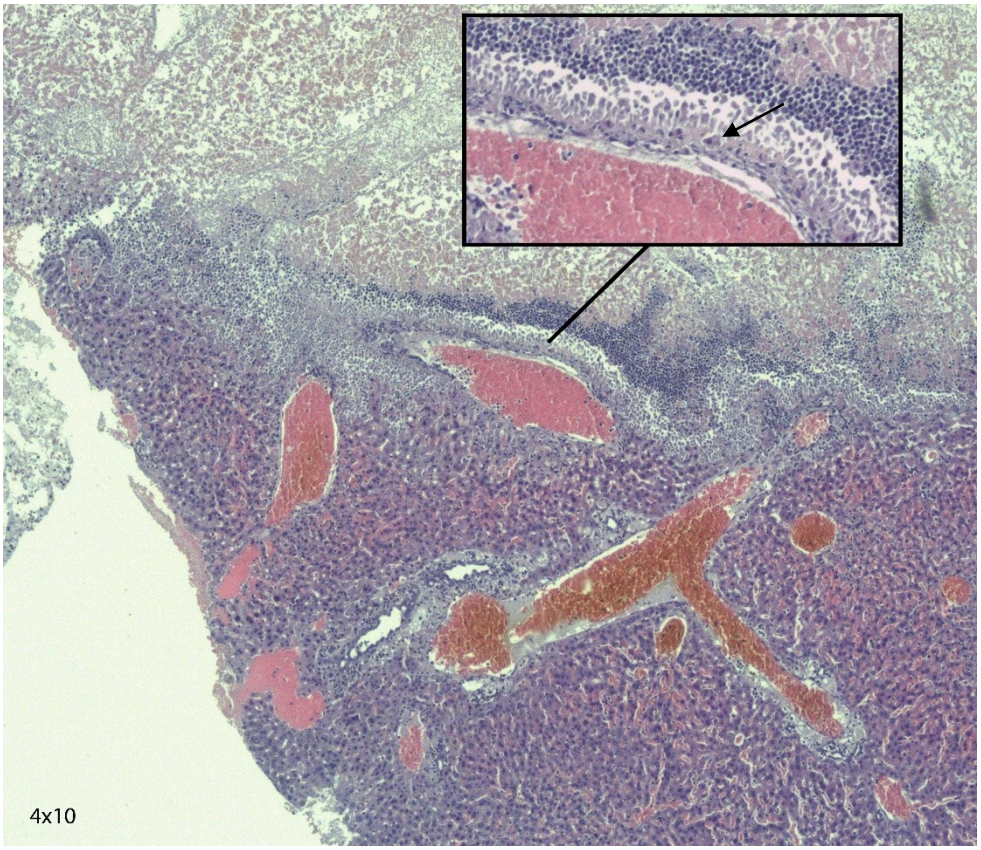

Fig. 22 Liver abscess from mouse infected with the virulent clone C1-M/A (magnification 4x10). The liver tissue is dense, whereas the less colored is necrotic tissue. The layer of trichomonads is visible in the box (magnification 10x10) and marked with an arrow.

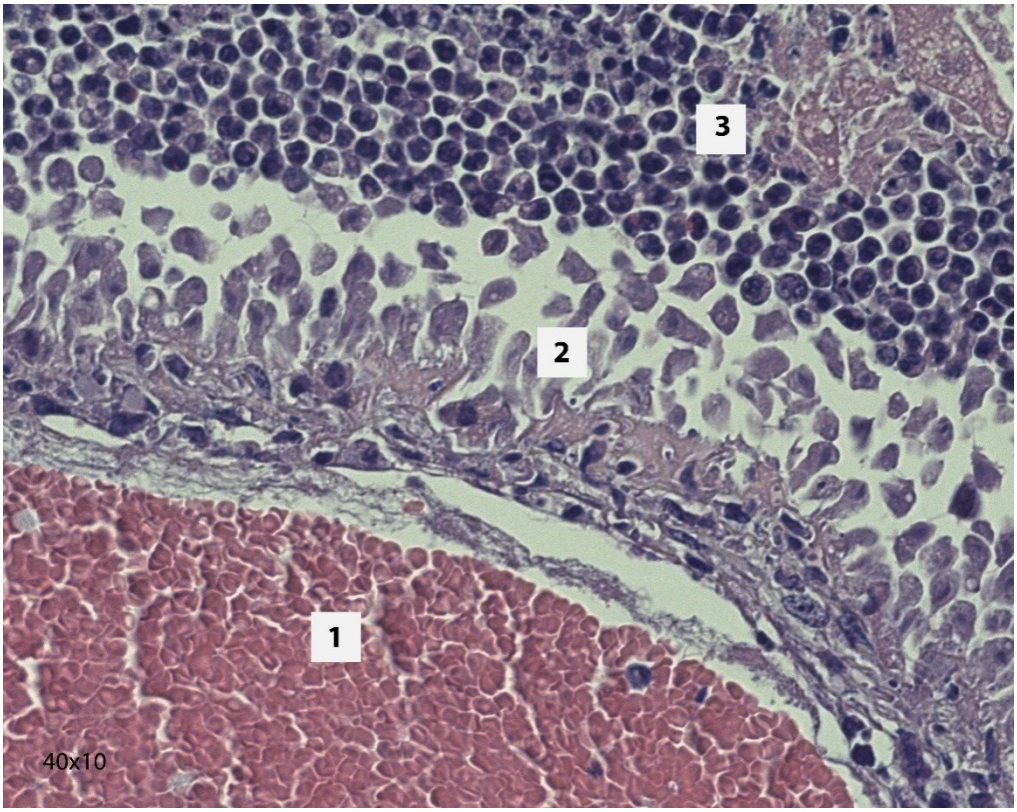

Fig. 23 Liver abscess from mouse infected with the virulent clone (magnification 40x10). 1 – central lobular vein, 2 – layer of trichomonads, 3 – layer of immune cells (leucocytes).

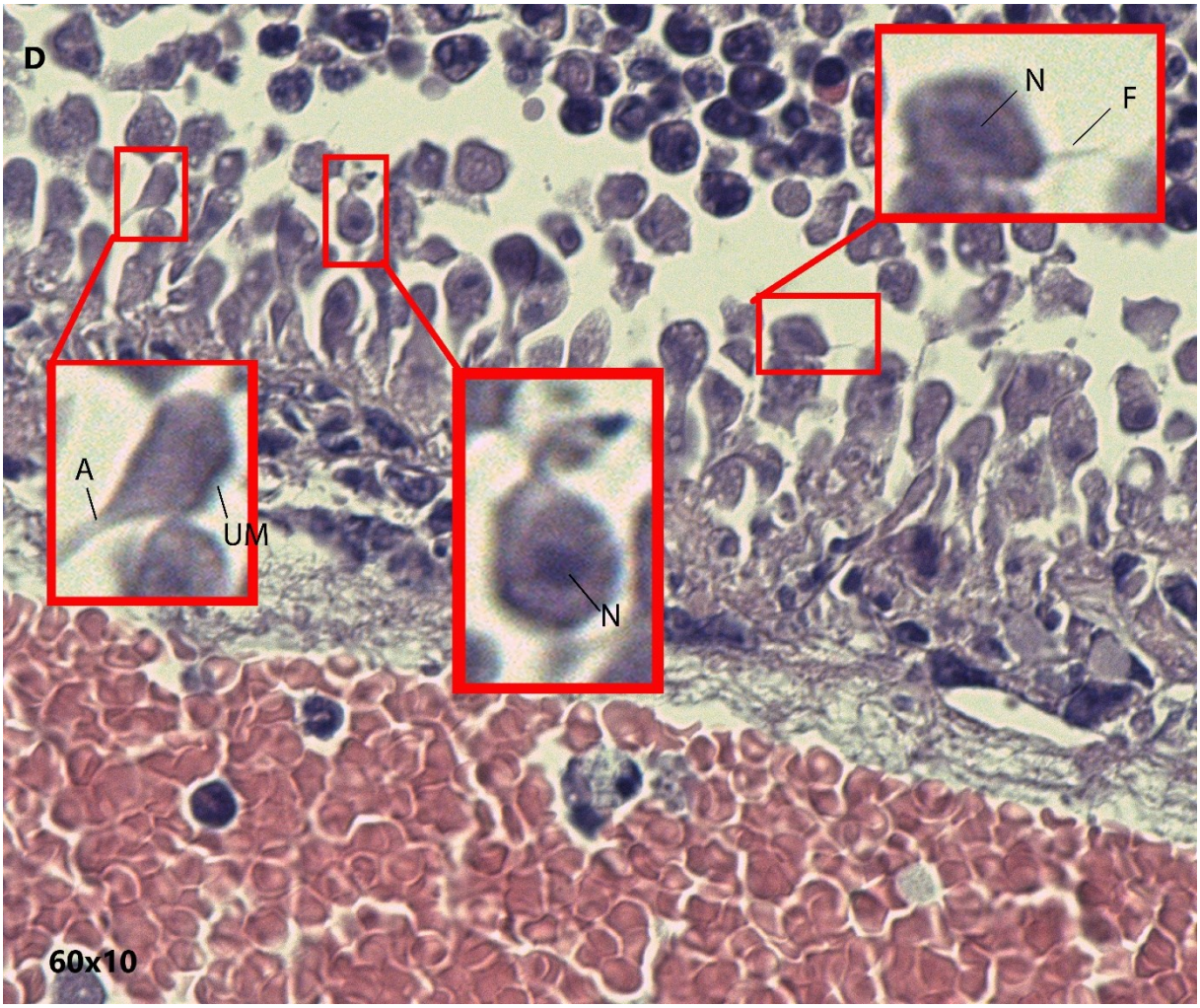

Fig. 24 Liver abscess from virulent clone infected mouse (magnification 60x10). Detail of the layer of trichomonads. The single cells (red boxes) were zoomed to show the detail structures of *T. vaginalis*; **A –** axostyle, **F** – flagellum, **N** – nucleus, **UM** – undulating membrane.

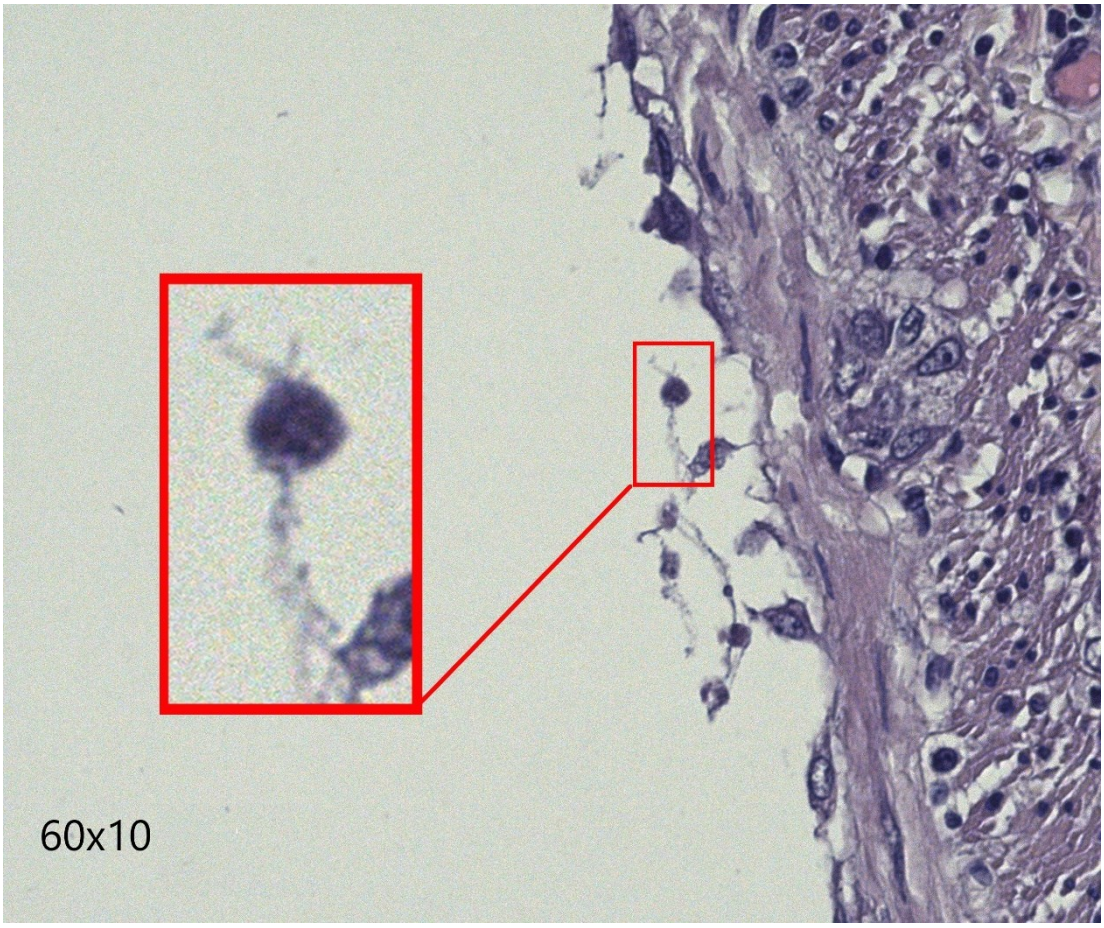

Fig. 25 *T. vaginalis* that adhere at the intestinal wall (magnification 60x10). In the red boxes showed zoomed *T. vaginalis* cell

The volume of fluid aspired from the abdominal cavity was further used to detect the presence of *T. vaginalis* genetic material. As a control of correct isolation and further manipulation with the sample, we used primers that amplified sequence for mouse GADPH gene. The *T. vaginalis* detection was performed using primers that amplified genes for TV 40S rRNA 23S protein and TV 60S rRNA L10a protein. As expected, all the samples with virulent clone were positive for *T. vaginalis* (Fig. 26, Fig. 27). However, we were able unable to detect trichomonads in samples from non-virulent *T. vaginalis* infections, only DNA fragments for mouse GADPH were amplified (Fig. 28). No evidence of *T. vaginalis* cells in samples from non-virulent clone infected mice indicates that the infection was successfully suppressed by mouse immune system rather than being present in latent form.

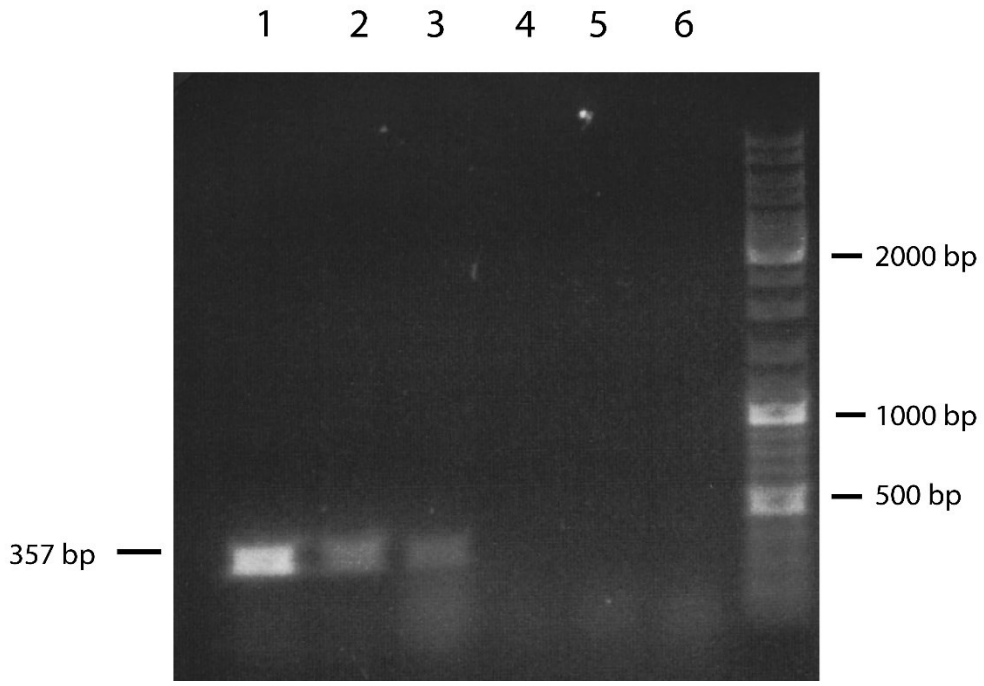

Fig. 26 Detection of *T. vaginalis* in samples isolated from mice (m1 – m6) peritoneum using primers for amplification of DNA fragment of TV 40S rRNA 23S protein. 1 – m1, 2 – m2, 3 – m3, 4 – m4, 5 – m5, 6 – m6. Samples 1-3 taken from mice infected with virulent clone showed the presence of *T. vaginalis*. Samples 4-6 collected from mice infected with non-virulent clone showed no evidence of *T. vaginalis*.

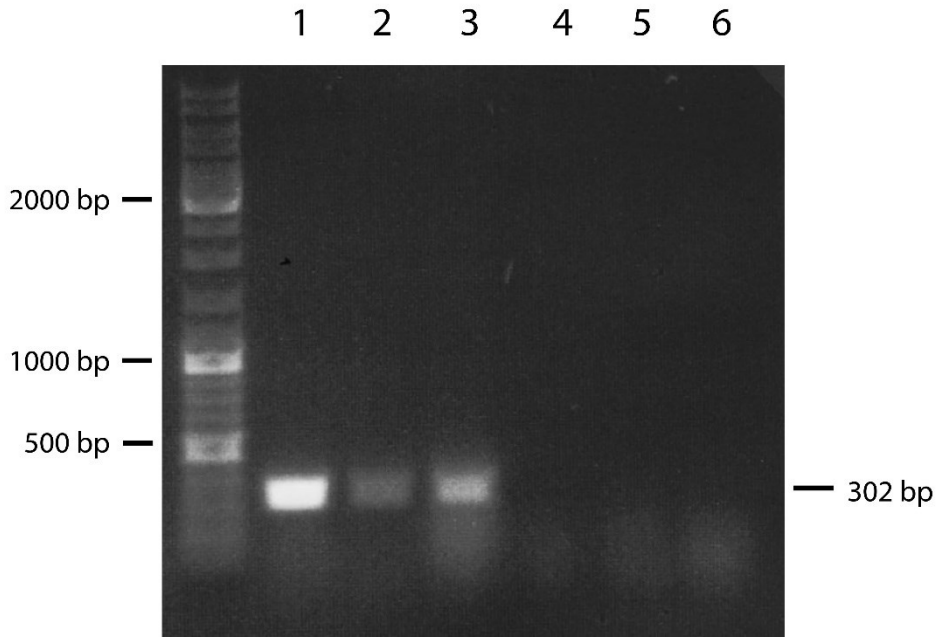

Fig. 27 Detection of *T. vaginalis* in samples isolated from mice peritoneum using primers for amplification of TV 60S L10a protein. 1 – m1, 2 – m2, 3 – m3, 4 – m4, 5 – m5, 6 – m6. Samples 1-3

taken from mice infected with virulent clone showed the presence of *T. vaginalis* genetic material. Samples 4-6 taken from mice infected with non-virulent clone showed no evidence of *T. vaginalis*.

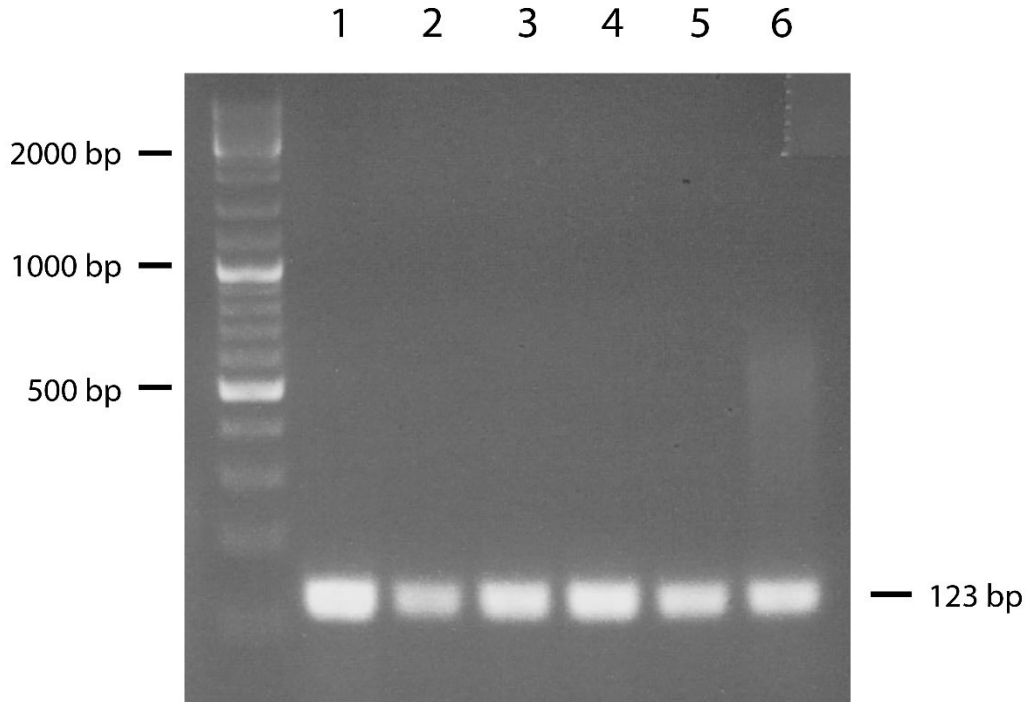

Fig. 28 Detection of DNA fragment for the mouse GADPH. 1 – m1, 2 – m2, 3 – m3, 4 – m4, 5 – m5, 6 – m6. Samples 1-3 were from the mice infected with virulent clone (C1-M/A) of *T. vaginalis* and samples 4-6 were from the mice infected with non-virulent clone (C2/B). m1-m6, mouse 1-6.

In conclusion, using the intraperitoneal test on mice, we could confidently say, that the *T. vaginalis* strain TV 17-2MI is a heterogenous culture, so while as a population appearing as virulent, it consists of virulent and non-virulent cells. By picking two model cultures grew from single cell colony, re-cloned from parental strain, C1/A (virulent) and C2/B (non-virulent), we determined the differences in process of infection. Comparing the two clone cultures we were also able to detect the pathological changes in the mice. Because the infection from non-virulent clone was so mild, if even present, we used those mice as a normal, "healthy" subjects.

To complete this test, we also investigated the remaining 6 mice from previous stages. All of them were terminated on the same day with no visible changes in appearance. There were 4 mice from stage I, infected with 3 types of TV 17-2MI clones for 6 months (Tab. 7). The examination of the intraperitoneal cavity showed small abscess on liver in one mouse. The abscess was dissected and processed to the Histopathology department in Biocev. We examined the tissue under the microscope, but there was no presence of *T. vaginalis* cells.

Abscess was not the cause of death, without presence of parasite was marked as irrelevant. None of the mice showed any presence of *T. vaginalis* cells after PBS wash of peritoneum, as well as no pathological internal organ changes.

TV 17-2MI clone in mouse	Duration of infection	Pathological changes
C2	6 months	-
C2	6 months	-
C3	6 months	+
C5	6 months	-
C1-M/C	5 months	-
C1-M/D	5 months	-

Tab. 7 Summary of the examination of remaining mice from previous stages of experiment.

4.3. Investigation of *T. vaginalis* exosomes

Clones C1-M/A and C2/B with different virulence were derived and characterized to serve for comparative studies of their exosomes. As *T. vaginalis* exosomes were shown to be involved in the parasite virulence, we can expect differences in exosomal cargo between virulent and non-virulent trichomonads. First, we attempt to identify suitable marker proteins for exosome and to establish protocol for exosome isolation.

4.3.1. Selection and testing of exosomal markers

As there are not suitable antibodies for detection of marker proteins for *T. vaginalis* exosomes, we first selected three exosomal proteins for antibody preparation.

To select the exosomal markers for *T. vaginalis* we used proteomics data, collected from strain TV T1 (Twu et al., 2013). We focused on the category of vacuolar membrane associated proteins and we selected two of them: multivesicular body protein (MVP) and SNARE protein. The third selected protein was tetraspanin 1 protein (TSP1) that was previously shown to be present in the exosomal membrane (Twu et al., 2013).

TSP1 (TVAG_019180) is conserved hypothetical protein with 4 transmembrane domains and a signal peptide. Its mammalian orthologs are components of exosomes and they are routinely used as markers for these vesicles (Rana and Zoller, 2011).

Putative SNARE protein (TVAG_249080) contains one transmembrane domain situated at the C-terminus of protein (186-209 AA). SNAREs membrane-bound proteins are essential for vesicular transport in the cell (Alberts et al., 2015)

MBP protein (TVAG_396070) supposes to associated with the surface of the multivesicular bodies. Unlike SNARE protein, MBP doesn't have transmembrane domain and signal peptide.

First, we investigate cell localization of selected markers. All proteins were cloned to TagVag vector that allow expression of protein with C-terminal HA tag in *T. vaginalis*. After transformation of *T. vaginalis* cells, the protein expression was tested using Immunoblot with specific antibodies against HA tag (Fig. 29).

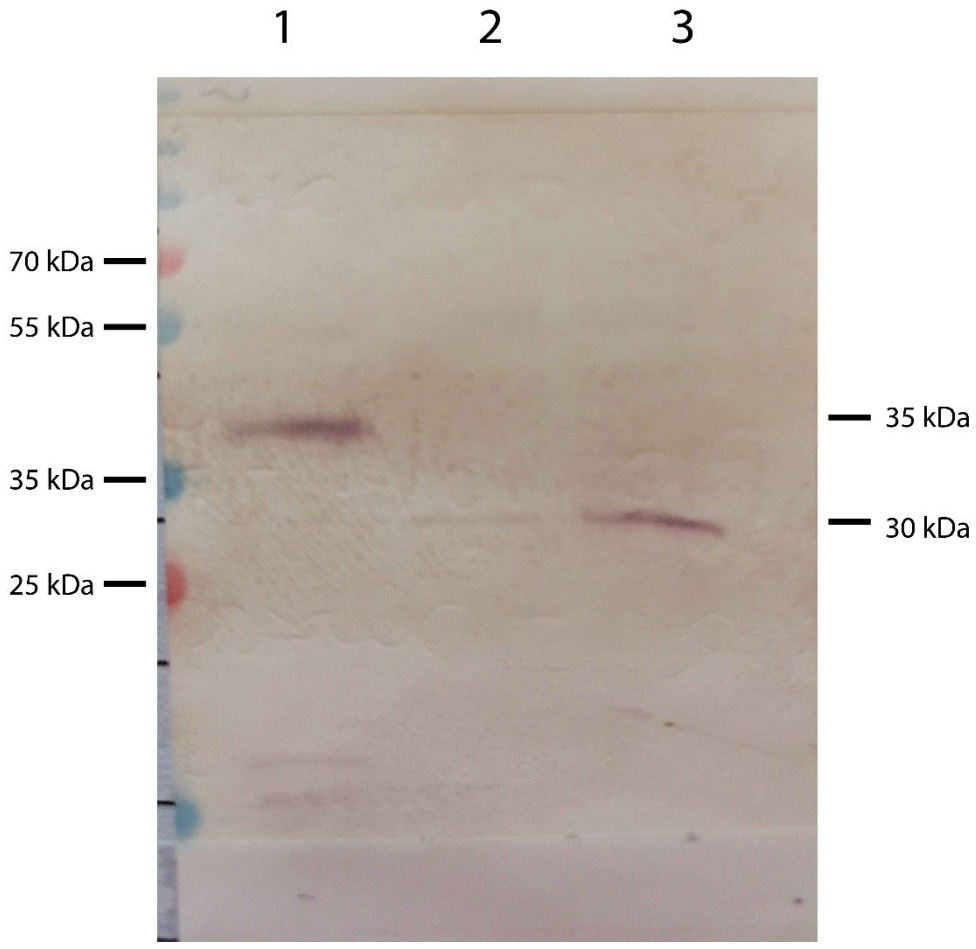

Fig. 29 Expression of HA tagged TSP1, SNARE and MBP proteins in TV T1 transfected cultures. Line 1, HA tagged TSP1 (~35 kDa); line 2 HA tagged SNARE (~30 kDa); line 3. HA tagged MBP (~30 kDa).

We can see expressed proteins on the blot, first is HA tagged TSP1 with expected size ~35 kDa, second one is HA tagged SNARE protein with expected size ~30 kDa and the last

one is HA tagged MBP protein with expected size ~30 kDa. The expression of HA tagged SNARE protein is rather weak compared to other proteins.

After we confirmed the protein expression, we proceeded with the localization in the cell by immunofluorescence microscopy. Tagged proteins were detected using rabbit monoclonal anti HA-tagged antibody and anti-mouse ALEXA Fluor 488 antibody (green), cytoskeleton was visualized using mouse monoclonal ani-acetylated tubulin and mouse ALEXA flour 594 antibody (red), nucleus was labeled using DAPI (blue) in the Vectashield mounting medium.

The pattern of tagged protein distribution in the cell looks rather random in the slide with visualized SNARE protein (Fig. 31) as well as in the one with MBP protein (Fig. 32). SNARE protein appeared as a small dots scattered in the trichomonads cytosol. MBP labeled large dots of various sizes. However, tagged TSP1 protein was observed in large ring-like structures present all over the cell (Fig. 30). Usual exosome size in perimeter is 50-100 nm. Therefore, the labeled ring-like structures with size of 863 nm are most likely multivesicular bodies (MVB).

.

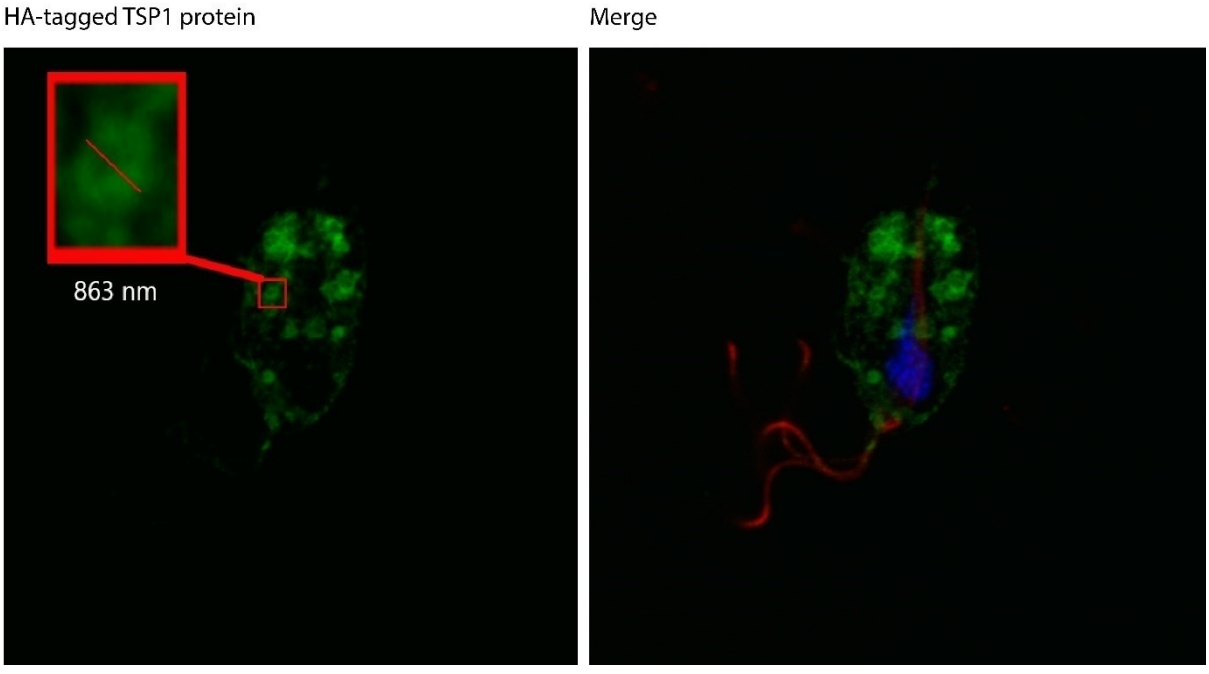

Fig. 30 Visualization of HA-tagged TSP1 protein in *T. vaginalis*

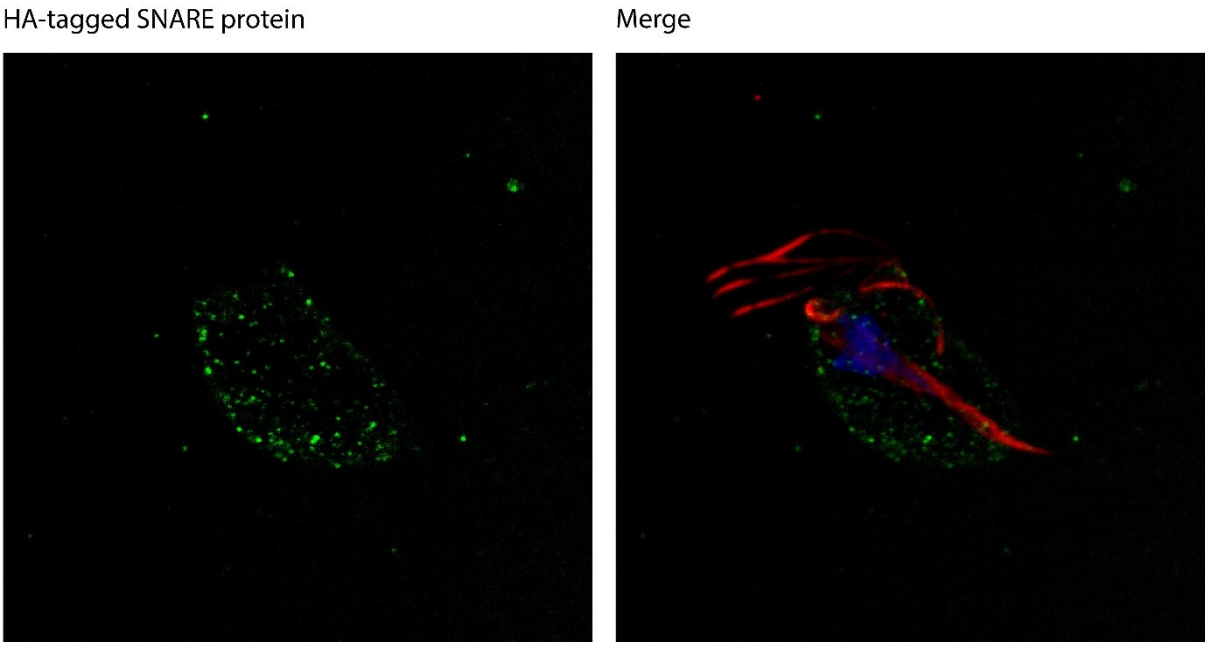

Fig. 31 Visualization of HA-tagged SNARE protein in *T. vaginalis*.

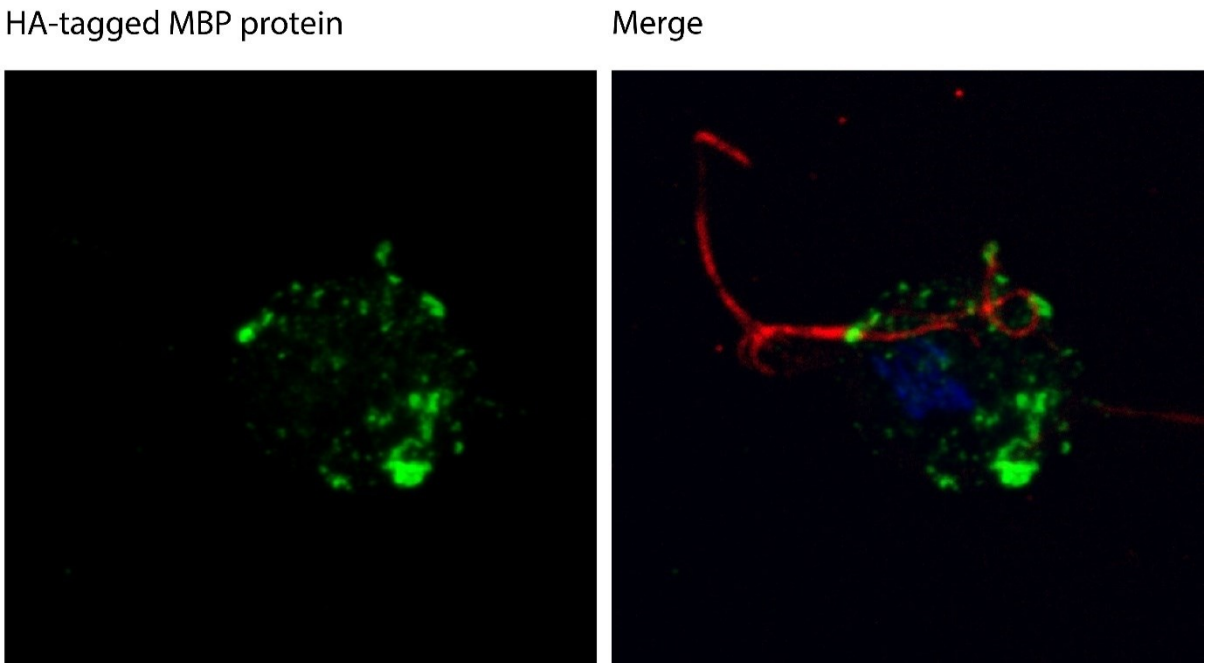

Fig. 32 Visualization of HA-tagged MBP protein in *T. vaginalis.*

According to the results of these experiments, we selected HA-tagged TSP1 protein for further analysis.

4.3.2. Isolation of exosomes

For exosomal isolation, we first performed the simple preliminary experiment to test temperature dependency of exosomal production. We simultaneously tested the possible marker (TSP1) expression in cell lysate, microvesicles and in secreted proteins. After that, we performed more sophisticated purification of exosomes using Vivaflow tangential filtration system and sucrose gradient followed by immunoblot and SDS-PAGE analysis.

In preliminary experiment we simply tested whether any microvesicles with TSP1 marker are produced and if the production is dependent on temperature. *T. vaginalis* culture (1 liter) in logarithmic phase of growth were harvested and washed with TYM medium without serum 3 times. Half of the cells was then incubated for 4 hours at 37°C, the other half was incubated at 4°C. Then the cells were spinned and stored for further analysis. The supernatant was passed through 0,22 μm filter to remove any impurities from the cellular fraction and the filtrate was spinned at 100 000 x g for 75 minutes at 4°C. Soluble secreted proteins in supernatant were precipitated with acetone. The immunoblotting of all samples revealed that the production of microvesicles by *T. vaginalis* is dependent on temperature and excreted out. The TSP1 protein is strictly membrane-bound protein and there was no sign of TSP1 present in soluble precipitated proteins.

Immunoblotting analysis showed that TSP1 was present in the cells incubated under both 37°C and 4°C (Fig. 33). However, extracellular TSP1 signal associated with microvesicles was observed only after incubation of cells at 37°C (Fig. 33). In the supernatant containing soluble secreted proteins, TSP1 was not present at any temperature (Fig. 33/5, 6). Next, we proceeded with the isolation of exosomes using tangential filtration (Vivaflow) and sucrose gradient.

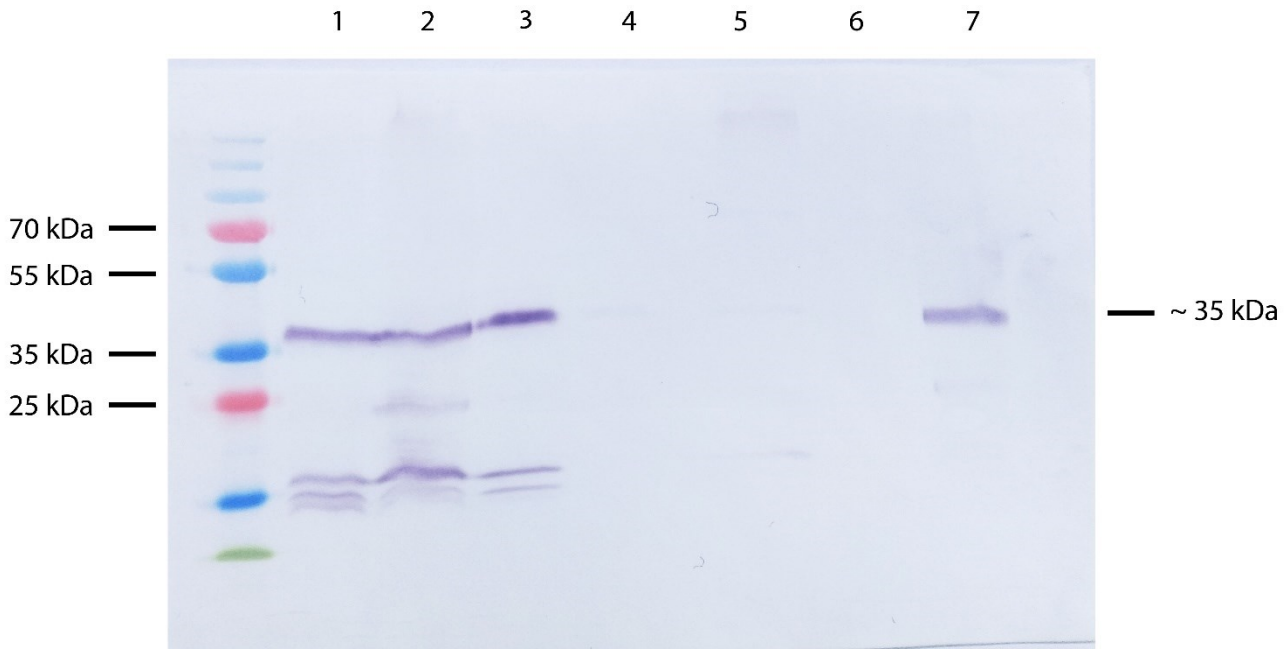

Fig. 33 Temperature-dependent release of HA-tagged TSP1 by *T. vaginalis*. 1 –lysate of cells incubated at 37°C/4 hrs, 2 lysate of cells incubated at 4°C/hrs, 3 – pellet of microvesicles released by cells incubated at 37°C/4hrs, 4 –pellet of microvesicles released by cells incubated at 4°C/4hrs, 5 – soluble proteins released at 37°C/4hrs, 6 – soluble proteins released at 4°C/4hrs, 7 – positive control (lysate of cells expressing HA- tagged TSP1 protein)

The next step was isolation of exosomes based on tangential flow filtration via Vivaflow system, followed with sucrose gradient separation. The presence of microvesicles in the gradient fractions were screened using anti TSP1 antibody (Fig. 35). Immunoblot analysis revealed that the most TSP1-enriched fraction was fraction 3 (middle of the protein cloud) (Fig. 34). We also included the SDS-PAGE with Coomassie gel strain (Fig. 36).

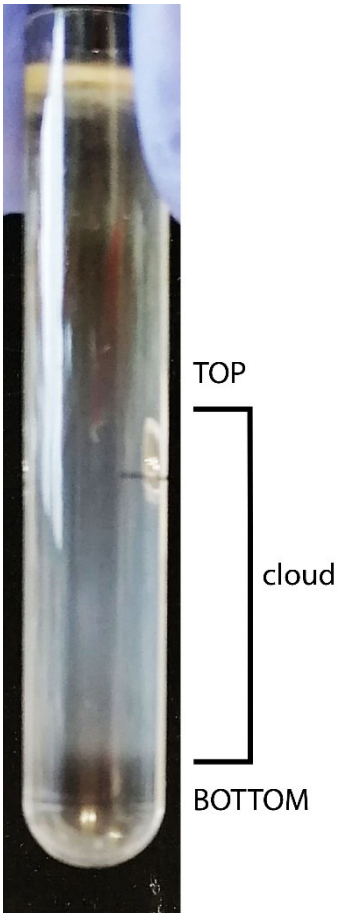

Fig. 34 Sucrose gradient (10-70% top to bottom) of microvesicular fractions. We collected 6 fractions of 0.5 ml starting at the bottom of the cloud (in the box) up to the top part of the cloud.

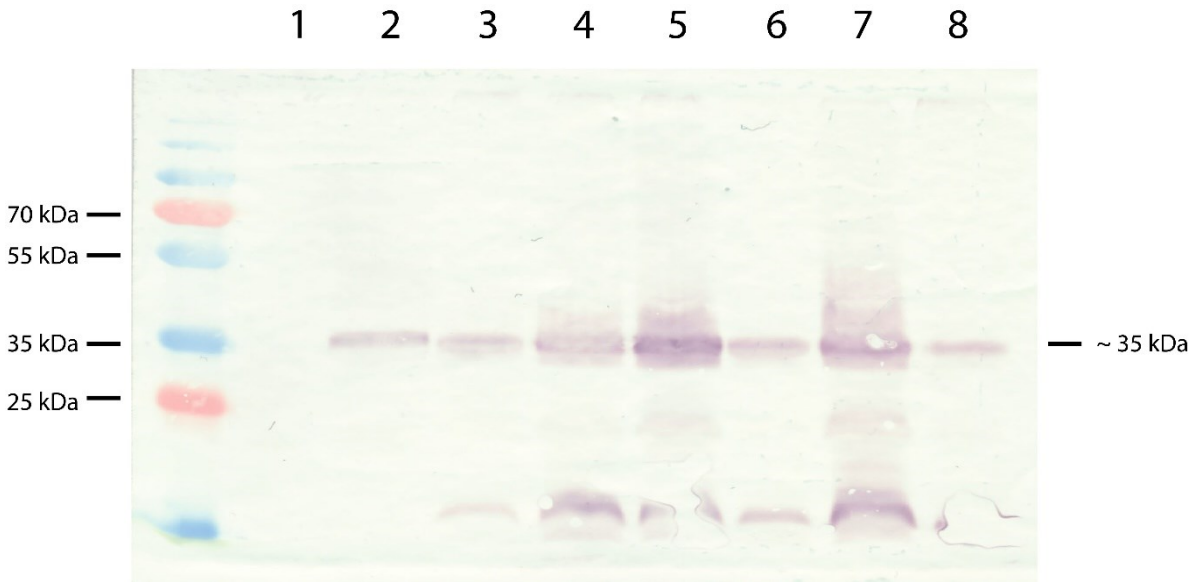

Fig. 35 Immunoblot analysis of microvesicular fractions isolated from cells overexpressing TSP1 protein using sucrose gradient. 1 – negative control (TV T1 wild type cells), 2 – positive control (TV T1

cells overexpressing TSP1 protein), 3 – F1; 4 – F2; 5 – F3, 6 – F4, 7 – F5, 8 – F6. F1-F6 fractions separated from sucrose gradient, from the bottom to the top.

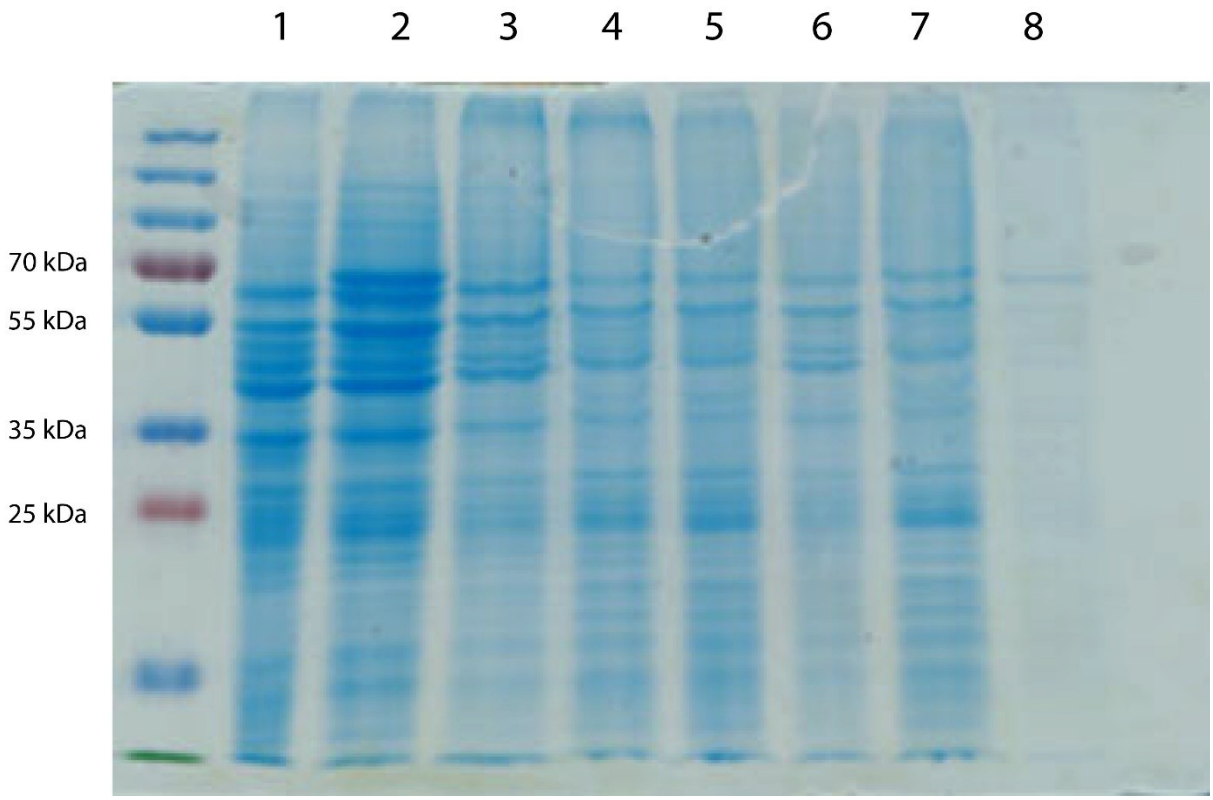

Fig. 36 SDS-PAGE analysis of miscovesicular fractions from cells expressing HA-tagged TSP1 protein that were isolated by sucrose gradient. 1 – negative control (TV T1 wild type cells), 2 – positive control (TV T1 cells overexpressing TSP1 protein), 3 – F1, 4 – F2, 5 – F3, 6 – F4, 7 – F5, 8 – F6. F1-F6 are fractions separated from sucrose gradient, bottom to the top (Fig. 32). Each section was 0.5 ml of the liquid from the gradient.

4.4. Proteomic analysis of exosomes

Proteomic analysis of isolated exosomes by mass spectrometry (MS) was the last planned experimental procedure. Unfortunately, because of the coronavirus outbreak, we were not able to finish the sample preparation for the final measurement, thus I analyzed data of two preliminary experiments that were performed by Petr Rada (Tab. 8, Tab. 9). Exosomes were isolated from two *T. vaginalis* strains TV T1 and TV 17-2MI. TV T1, the middle fraction from the sucrose gradient was precipitated with TCA. Precipitated proteins were then dissolved in SDS loading buffer and analyzed by MS. In the case of TV 17-2MI, the cells were incubated for 4 hours in TYM medium without serum and agar, the microvesicles were spinned by ultracentrifugation at 100 000 x g. The pellet was directly dissolved in the SDS

loading buffer and provided for MS analysis. In the next step, the data were annotated and compared with the previous analysis by Twu et al., (2013)

The proteome of exosomes isolated from TV T1 and TV 17-2MI strains includes 2305 and 1335 identified proteins, respectively. Two et al (2013) analyzed exosomes from TV T1 strain and obtain only 215 proteins. All three proteomes included expected marker proteins TSP1, MVB and SNARE. Because of large number of identified proteins in our samples, these proteomes included most of proteins identified by Twu et al. (2013). In our TV T1 proteome, only 9 proteins were missing in comparison to TV B7RC2 Twu proteome (Tab. 8). In out TV 17-2MI, there were 14 proteins missing compared to TV B7RC2 Twu proteome (Tab. 9). As shown in the table below, there are two similar proteins missing in both measurements, both from the same category.

	Protein category	**TrichDB ID #**	**Protein desciption**
1	Kinases/Phosphatases	TVAG_218820	histidine acid phosphatase
2	Kinases/Phosphatases	TVAG_218800	histidine acid phosphatase
3	Hypothetical proteins	TVAG_218790	conserved hypothetical protein
4	Hypothetical proteins	TVAG_239650	conserved hypothetical protein
5	Hypothetical proteins	TVAG_099730	conserved hypothetical protein
6	Others	TVAG_178140	phosphoenolpyruvate-protein phosphotransferase
7	Glycolytic enzymes	TVAG_043060	fructose-bisphosphate aldolase
8	Glycolytic enzymes	TVAG_043070	fructose-bisphosphate aldolase
9	Protein Folding	TVAG_171670	heat shock protein

Tab. 8 Proteins that are missing from out proteomics of TV T1 compared to Twu et al.,2013,

	Protein category	**TrichDB ID #**	**Protein desciption**
1	Hypothetical proteins	TVAG_454160	conserved hypothetical protein
2	Hypothetical proteins	TVAG_239650	conserved hypothetical protein
3	Hypothetical proteins	TVAG_099730	conserved hypothetical protein
4	Others	TVAG_470120	protein tolA
5	Others	TVAG_418970	thioredoxin m(mitochondrial)-type
6	Others	TVAG_576970	lipid binding protein (Giardia)
7	Others	TVAG_151830	dihydroorotate dehydrogenase
8	Others	TVAG_338230	dihydroorotate dehydrogenase
9	Others	TVAG_468240	dihydropyrimidine dehydrogenase

10	Translation	TVAG_197820	translation initiation inhibitor
11	Glycolytic enzymes	TVAG_347410	glyceraldehyde 3-phosphate dehydrogenase
12	Glycolytic enzymes	TVAG_165340	succinate thiokinase a subunit
13	Protein Folding	TVAG_163000	heat shock protein
14	Protein Folding	TVAG_184320	heat shock protein

Tab. 9 Proteins that are missing from our proteomics of TV 17-2MI compared to Twu et al.,2013.

Full dataset is included in supplementary data on the CD attached to the thesis.

5. Discussion

In this work we performed initial steps to evaluate a role of exosomes in virulence of *T. vaginalis*. For the study we selected *T. vaginalis* strains (TV 17-2MI) that lacked endosymbionts (*M. hominis,* and *TVV*) as presence of endosymbionts may affect *T. vaginalis* properties. To have isogenic lines of *T. vaginalis*, we derived several clones from this strain. Surprisingly, when we tested virulence of these clones, we discovered that only a single clone out of 10 was highly virulent while the other clones were mildly virulent or non-virulent using mouse intraperitoneal test. Next, we established and optimized method for isolation of exosomes from the virulent and non-virulent clones with aim to compare their protein cargo and we performed pilot experiments for future detail studies.

5.1. Selection of *T. vaginalis* strain without endosymbionts.

Four strains of *T. vaginalis* were tested for presence of endosymbionts (*M. hominis* and TVV) with aim to identify endosymbiont-free strain. The endosymbionts are known to modulate the symptoms of *T. vaginalis* infection, immune response of host and contribute to the development of serious comorbidities such as infertility, miscarriages and malignant transformations in urogenital tract (Margarita et al.,2016; Fichorova et al., 2012). Endosymbionts also may affect content of exosomes. For example, tumor cells infected with *M. hominis* can affect the immune cells due to modifications of exosomal cargo. The study by Yang et al. (2012) showed that exosomes released from tumor cells infected by *M. hominis* had B cell stimulatory and cytokine induction ability that were not observed in tumor cells without *M. hominis* infection. Moreover, the B cells stimulated by these exosomes were able to inhibit the T cell response. The effects were specifically associated with the *M. hominis* presence in the cell and disappeared when infected cells were treated with mycoplasma-

removal agent (Yang et al., 2012). Modification of exosomal cargo, especially RNA components, was also observed upon presence of virus in the cell (Chahar et al., 2017). Infection of airway epithelial cells (A549 cell line) with Respiratory Syncytial Virus (RSV) resulted in presence of the viral proteins, viral RNA and different host RNA fragments of mRNA, and rRNA, as well as differences in small non-coding RNAs (miRNAs, piRNAs, tRNAs) in exosomes in comparison with virus-free cells. It has been also found that exosomes isolated from RSV-A549 cells are capable to initiate the immune response by releasing specific proinflammatory mediators. (Chahar et al., 2017). Therefore, it is critical to select *T. vaginalis* strain without endosymbionts to investigate whether and how *T. vaginalis* exosomes are involved in virulence of this parasite.

After testing of several *T. vaginalis* strains, we found one strain (TV 10-02) that was infected by a single TVV species (TVV 2) and a strain (TV 79-49) infected with three TVVs (TVV1, 2 and 3). When we compared our results with the study by Hampl et al. (2001), we did not identify any virus in TV 85-08 strain, while Hampl et al (2001) reported presence of virus in this strain. This contradiction might be causeed by different methodology. In our study we used highly sensitive RT-PCR analysis, while in the former study, horizontal electrophoresis of total RNA isolated from *T. vaginalis* strains was used to detect a putative viral RNA as a specific band.

We also tested *T. vaginalis* strains for *M. hominis* presence. In a simple fluorescence analysis using DAPI DNA stain we found one strain infected with mycoplasma (TV 10-02). We than performed RT-PCR analysis with specific primers that amplified 16S rRNA of *M. hominis*. This test confirmed mycoplasma infection in TV 10-02. Surprisingly, the results shown presence of *M. hominis* in another strain (TV 85-08) that appeared negative under the microscope. This result was in contradiction with the previous study (Hampl et al., 2001) that reported absence of mycoplasma in TV85-08. The difference could be explained by difference in selected primers for PCR amplification. Hampl et al. (2001) used the primers for 16S rRNA specific to all members of class *Mollicutes*, while we used the primers specific for amplification of 16S rRNA of *M. hominis* only, which could ensure maximal sensitivity for detection. Importantly, our results showed that strain TV17-2MI did not harbor any endosymbiont and thus is suitable for further experiments.

5.2. Testing of virulence

Next, we were interested in virulence of the selected TV17-2MI strain. To test virulence of *T. vaginalis* is rather challenging as there are various *in vivo* tests providing results with various reliability. From commonly used model organisms we selected mouse, specifically laboratory breed Balb/c for testing *T. vaginalis* virulence. There are several mouse tests that differ in the site of the parasite inoculation such as intraperitoneal, subcutaneous, intramuscular and intravaginal test (Schnitzer et al., 1950). The last one requires pre-treatment of an animal with estrogen to establish the sexual cycle (Maestrone and Semar, 1967). For our experiments we selected intraperitoneal mouse test according to Kulda (Honigberg et al., 1990) that was simple to perform and was shown to provide valid data. In our experiments, the intraperitoneally inoculated strain TV17-2MI was able to kill the mice in 5-7 days using $1x10^6$ cells per mouse peritoneum in 0.5 ml. This dose results in an infection rate close to 100% for majority of *T. vaginalis* strains and allows to observe the difference between various pathogenic isolates (Honigberg et al., 1990).

Reardon et al. (1961), showed that two strains of *T. vaginalis*, one derived from severe case of vaginitis (C-1) and the other from a mild case (R), revealed clear difference in virulence using mouse intraperitoneal test. While virulent strain C-1 caused 143 fatal outcomes out of 148 inoculated mice, infection with strain R never produced fatalities with minimal lesion formation at most observed mice. In 15 separate experiments, various sizes of C-1 strain inoculum were tested: $1*10^7$, $1*10^6$ and $1*10^5$. This test revealed extension in survival time from median of 15.5 days with $1*10^7$ up to 21 days with inoculum of $1*10^6$ parasites. Inoculum of $1*10^5$ C-1 *T. vaginalis* strain failed to kill the mice. In our experiments, the survival time with $1*10^6$ trichomonads was significantly shorter.

The differences between the studies could be the result of using the different breed of the animal model. Reardon et al. (1961) was using different types of mouse breeds, such as A/LN, C57BL, A/HeN (inbred strains), C3H/p, CFW (brother-sister matings) and GP (general purpose random matings). She performed a comparative analysis where A/LN mice inoculated with TV C-1 strain was used as a standard. After infection of the rest of the mouse breeds with the same *T. vaginalis* strain, the results shown not significant difference between these breeds. Landolfo et al. (1979) points out on differences in susceptibility of various inbred stains of mice to *T. vaginalis*, viewing the strain Balb/c as the most susceptible, which was also used in our study.

Intraperitoneal inoculation of *T. vaginalis* causes peritonitis with abscesses and necrotic foci in abdominal organs and production of ascitic fluid. The severity of the infection reflects the virulence of the inoculated strain, considering possible variations in the response of each animal. A pattern of pathological changes and mortality rate of infected mice are generally reproducible under standard experimental conditions. However, the correlation of a strain's virulence for mice with the severity of disease in human patients is not always ideal (Honigberg, 1987).

Honigberg (1961) compared the development of abdominal lesions in mice at different time after inoculation using four *T. vaginalis* strains: TV 1, TV 3, TVC and TVC_1. TV 1 and TV 3 have history of prolong cultivation *in vitro* after isolation and the history of patient symptoms was not known. TVC and TVC_1 were both isolated from patients with severe vaginitis, and thus considered as highly virulent. In highly virulent strains (TVC and TVC_1), there was early formation (after 6 days) of intraperitoneal lesions filled with trichomonads, including hepatic abscesses. TV 1 and TV 3 appeared as milder virulent strains with later lesion formation (after 14 days), with the same characteristic features. Thus, an early lesion formation may be the sign of higher virulence of *T. vaginalis* strain.

All previous studies correlated the virulence of *T. vaginalis* strains as they were isolated from patients. However, we asked a question, how homogenous is a population of trichomonads in a single strain concerning their virulence. Surprisingly, our results showed significant differences between clones derived from a single strain. The differences ranged from absence of any abscess formation (non-virulent clones) to formation of large numerous intraperitoneal abscesses (virulent clone) that were comparable with infection using the parent TV 17-2MI strain. This is possibly the most important result of this study.

While no study compared properties of *T. vaginalis* clones derived from a single strain so far, there were few studies testing virulence of genetically related cells of *E. histolytica* (Meyer et al., 2016; Biller et al., 2009). Biller et al. (2009) compared different pathogenic properties between cell lines A and B, derived from the *E. histolytica* strain HM-1:IMSS. They studied an ability of these cell lines to form liver abscesses, other phenotypic aspects (larger trophozoites, higher growth rate, higher cysteine peptidase activity and higher resistance to nitric oxide stress in pathogenic cell line) and compared their proteomic differences (for example regulation of antioxidants). Line A was nearly incapable to form liver abscess, compared to line B that produced large liver abscesses. In recent study by Meyer et al. (2016), 12 clones from cell line HM-1:IMSS-A (non-pathogenic) and 12 clones

from cell line HM-1:IMSS-B (pathogenic) were isolated. Derived clones were inoculated to the gerbil model and after 7 days, the amoebic liver abscess (ALA) formation was analyzed and compared between different clones. Results shown that HM-1:IMSS-A cell line is a homogenous population. Majority of animals infected with the clones derived from this cell line shown no ALA formation. On the other hand, analysis of clones derived from HM-1:IMSS-B cell line showed differences in virulence. Eight out of twelve clones shown the same pathogenicity phenotype as the original paternal cell line. The other four clones revealed reduced ability to form ALA in the model animal. This observation is similar to our findings of various virulence level observed in *T. vaginalis* clones.

5.3. Exosomal isolation from *T. vaginalis*

Another aim of this work was to establish protocol for reproducible isolation of exosomes. The first challenge was to find suitable exosomes marker and develop specific antibody against such a marker. We couldn't use available antibodies against known exosomal markers such as TSP, CD63, flotillin-1, alix, TSG101 etc., because of the diversity in protein sequence (TSP) or absence of conventional eukaryotic markers in *T. vaginalis* exosomes.

The necessity for a specific antibody against exosomal marker is given by equirement to trace exosomes in *T. vaginalis* cells by immunofluorescence microscopy, and particularly for western blot analysis of cellular fractions during exosome isolation. Previous proteomic analysis of trichomonad's surface showed that there is variety of proteins on the outer membrane. Interestingly, at least three TSPs were found on the surface (de Miguel et al., 2010). The proteins from TSP family are often used as exosomal markers (Rana and Zoller, 2011). For *T. vaginalis* exosomes, TSP1 was used in previous study (Twu et al., 2013). After thorough examination of published proteomics data (Twu et al., 2013), we decided to include TSP1 and two other proteins (MBP and SNARE protein) as a potential markers for our study. Genes coding potential exosomal markers (TSP1, MBP and SNARE) were expressed with HA tag in TV T1 strain. The size of HA-tagged TSP1 in our strain (~35kDa) was the same when compared with HA-tagged TSP1 reported by Twu et al (2013). Immunofluorescence microscopy showed the signal for TSP1 partially on the surface, and in vesicles. Similarly, in previous study, TSP1 was observed in plasma membrane and in vesicular structures, however the formation of labeled vesicles was observed after exposure of parasites to ectocervical

cells. In parallel, we investigated localization of HA-tagged MBP and SNARE protein using the immunofluorescence microscope, however, their localization within the cell was not conclusive. Therefore, TSP1 was chosen to be used as exosomal marker for exosome isolation.

Preliminary proteomics analysis revealed significant difference in quantity of detected exosomal proteins isolated from TV T1 (2305) and TV 17-2MI (1335). The difference likely resulted from different approach in each isolation. Sample of TV T1 exosomes was obtained after ultracentrifugation followed with fractionation on sucrose gradient. The middle fraction from the gradient was then precipitated with acetone and dissolved in SDS buffer. The sample of TV 17-2MI exosomes was prepared based on differential centrifugation without the gradient purification step.. Both samples were further analyzed following the same MS protocol.

In both experiments we obtained surprisingly high number of proteins in comparison to the proteome by Twu et al. (2013) that identified only 215 proteins. There are several possible reasons that might be responsible for observed difference in quantity of proteins in our experiments compared to published data. First, we used more sensitive Orbitrap Fusion™ Tribrid™ Mass Spectrometer while Twu at al. (2013) used older model LTQ Orbitrap XL™ ETD Hybrid Ion Trap-Orbitrap Mass Spectrometer. The Orbitrap Fusion mass spectrometer is about 10-fold more sensitive and quantify more accurately, which could lead to considerably higher number of proteins in our detections (Karel Harant, Proteomics Core Facilty BIOCEV, personal information). It is also possible that our preparation of exosomes was more contaminated with other cellular organelles or ectosomes. Indeed, we found in our dataset several hydrogenosomal proteins (e.g. thioredoxins, malic enzyme, pyruvate:ferredoxin oxidotreductase, ferredoxin1, peroxiredoxins, superoxide dismutases, NAD-dependent epimerases/dehydratases, succinate tiokinase) that may represent hydrogenosomal contaminantion. We also found proteins that can be contaminants from other organels (endoplasmic reticulum, Golgi complex etc.). All possible contaminants are listed in the table (Tab. S2) on the CD attached to the thesis. However, the hydrogenosomal protein succinate thiokinase α subunit was also found in exosomes by Twu et al. (2013). Although the number of proteins in our experiments is considerably higher than in the previous study, it is comparable with proteomes of exosome derived from other cells. For example, Liang et al. identified 2230 proteins in exosomes derived from ovarian cancer cell lines (OVCAR-3,

IGROV1) (Liang et al., 2013) and Wu with Liu identified total of 1062 proteins in sweat exosomes (Wu and Liu, 2018).

Not surprisingly, most proteins identified in the previous study was present in our proteome. However, there were 9 proteins missing in our TV T1 proteome and 14 in TV 17-2MI compared to strain TV B7RC2 (Twu et al., 2013). There were also two proteins missing from both our measurements, TVAG_239650 and TVAG_099730, both categorized as conserved hypothetical proteins. Exosomal marker proteins TSP1, MBP and SNARE appeared in all measurements.

Majority of the extra proteins compared to Twu (Twu et al., 2013) were hypothetical, conserved hypothetical or ribosomal proteins. In both samples were also found heat shock proteins, tRNA synthetases, ATPases, GTPases, cytoskeletal proteins, vacuolar membrane proteins, chaperons, proteins associated with calcium channels, drug resistance pumps and different types of enzymes (kinases, peptidases, transferases, hydrolases etc.). Further studies are required to more optimized exosome isolation and confirm exosomal localization of selected proteins and study their function.

6. Conclusion

This thesis focused on extracellular vesicles of parasitic protist *T. vaginalis* and its connection to the virulence. In the first part, we tested four *T. vaginalis* isolates and we selected TV 17-2MI that is free-of endosymbionts for further studies. To test whether TV 17-2MI cells are homogenous in virulence, we derived and tested six clones. Surprisingly, we found that these clones displayed significant difference in virulence using mice intraperitoneal test. Only a single clone was highly virulent causing abscesses on the organs and early death of tested animals.

The second part focused on selection of exosomal markers and proteomic analysis of exosomes. We selected three potential exosomal markers (TSP1, SNARE, MBP), expressed them in the cells, and localized them using immunofluorescence microscopy. Based on the localization studies, we considered TSP1 as the most suitable marker. The proteomic analysis of two samples of exosomes isolated from *T. vaginalis* revealed considerably higher quantity of detected proteins compared to the initial study performed by Twu et al. (2013).

Thus, in this thesis we derived and characterized clones of different virulence that could be used as a suitable model. We also obtained the first results on exosome isolation and their

proteomic analysis. These results will serve for future studies of their role in *T. vaginalis* virulence.

7. Literature

Afzan, M. Y., Suresh, K. 2012. Pseudocyst forms of *Trichomonas vaginalis* from cervical neoplasia. Parasitology Research, 111(1), 371-381.

Alberts, B., Bray, D., Lewis, J., Raff, M., Roberts, K., Watson, J. D. 1994. Molecular Biology of the Cell. Garland Publishing, Inc. New York. ISBN 0-8240-7282-7282-0

Bastida-Corcuera, F.D., Okumura, C.Y., Colocoussi, A., Johnson, P.J. 2005 *Trichomonas vaginalis* lipophosphoglycan mutants have reduced adherence and cytotoxicity to human ectocervical cells. Eukaryotic Cell 4: 1951–1958

Benchimol, M., de Souza, W. 1995. Carbohydrate involvement in the association of a prokaryotic cell with *Trichomonas vaginalis* and *Tritrichomonas foetus*. Parasitology Research, 81(6), 459-464.

Benchimol, M., Diniz, J. A. P., Ribeiro, K. 2000. The fine structure of the axostyle and its associations with organelles in Trichomonads. Tissue and Cell, 32(2), 178-187.

Benchimol, M., Chang, T. H., Alderete, J. F. 2002. *Trichomonas vaginalis*: observation of coexistence of multiple viruses in the same isolate. FEMS Microbiology Letters, 215(2), 197-201.

Benchimol, M., Ribeiro, K. C., Mariante, R. M., Alderete, J. F. 2001. Structure and division of the Golgi complex in *Trichomonas vaginalis* and *Tritrichomonas foetus*. European Journal of Cell Biology, 80(9), 593-607.

Bessarab, I. N., Liu, H. W., Ip, C. F., Tai, J. H. 2000. The complete cDNA sequence of a type II *Trichomonas vaginalis* virus. Virology, 267(2), 350-359.

Biller, L., Schmidt, H., Krause, E., Gelhaus, C., Matthiesen, J., Handal, G., Bruchhaus, I. 2009. Comparison of two genetically related *Entamoeba histolytica* cell lines derived from the same isolate with different pathogenic properties. Proteomics, 9(17), 4107-4120.

Brugerolle, G., Viscogliosi E. 1994. Organization and composition of the striated roots supporting the Golgi apparatus, the so-called parabasal apparatus, in parabasalid flagellates. Biology of the Cell, 81.3: 277-285.

Castro, C., Menna-Barreto, R. F. S., Fernandes, N. D. S., Vahia, L. S., Lopes, G. D., Britto, C., Jesus, J. B. D. 2016. Iron-modulated pseudocyst formation in *Tritrichomonas foetus*. Cambridge University Press. ISSN 0031-1820

Cepicka, I., Hampl, V., Kulda, J. 2010. Critical taxonomic revision of parabasalids with description of one new genus and three new species. Protist, 161(3), 400-433.

Cerkasov, J., Cerkasovova, A., Kulda, J., Vilhelmova, D. 1978. Respiration of hydrogenosomes of *Tritrichomonas foetus*. I. ADP-dependent oxidation of malate and pyruvate. Journal of Biological Chemistry, 253(4), 1207-1214.

Costa-Silva, B., Aiello, N. M., Ocean, A. J., Singh, S., Zhang, H., Thakur, B. K., Xiang, J. 2015. Pancreatic cancer exosomes initiate pre-metastatic niche formation in the liver. Nature Cell Biology, 17(6), 816-826.

da Costa Madeiro, R. F., Benchimol, M. 2004. The effect of drugs on cell structure of *Tritrichomonas foetus*. Parasitology Research, 92(2), 159-170.

De Jesus, J. B., Cuervo, P., Junqueira, M., Britto, C., Costa e Silva-Filho, F., Soares, M. J., Domont, G. B. 2007. A further proteomic study on the effect of iron in the human pathogen *Trichomonas vaginalis*. Proteomics, 7(12), 1961-1972.

de Miguel, N., Lustig, G., Twu, O., Chattopadhyay, A., Wohlschlegel, J. A., Johnson, P. J. 2010. Proteome analysis of the surface of *Trichomonas vaginalis* reveals novel proteins and strain-dependent differential expression. Molecular & Cellular Proteomics, 9(7), 1554-1566.

de Souza, W., Barrias, E. S. 2020. Membrane-bound extracellular vesicles secreted by parasitic protozoa: cellular structures involved in the communication between cells. Parasitology Research, 119, 2005–2023.

Denzer, K., Kleijmeer, M. J., Heijnen, H. F., Stoorvogel, W., Geuze, H. J. 2000. Exosome: from internal vesicle of the multivesicular body to intercellular signaling device. Journal of Cell Science, 113(19), 3365-3374.

Deolindo, P., Evans-Osses, I., Ramirez, M. I. 2013. Microvesicles and exosomes as vehicles between protozoan and host cell communication. Biochemical Society Transactions, 41 (1), 252–257.

Dessì, D., Rappelli, P., Diaz, N., Cappuccinelli, P., Fiori, P. L. 2006. Mycoplasma hominis and Trichomonas vaginalis: a unique case of symbiotic relationship between two obligate human parasites. Frontiers in Bioscience, 11, 2028-34.

Diamond, L. S. 1957. The establishment of various trichomonads of animals and man in axenic cultures. The Journal of Parasitology, 43(4), 488-490.

Dias-Lopes, G., Saboia-Vahia, L., Margotti, E. T., Fernandes, N. D. S., Castro, C. L. D. F., Oliveira Junior, F. O., Jesus, J. B. D. 2017. Morphologic study of the effect of iron on pseudocyst formation in *Trichomonas vaginalis* and its interaction with human epithelial cells. Memórias do Instituto Oswaldo Cruz, 112(10), 664-673.

Díaz, J. A. M., de Souza, W. 1998. Biochemical characterization of the Golgi-complex proteins of Tritrichomonas foetus. Parasitology research, 84(9), 760-762.

Douglas, D. J., Frank, A. J., Mao, D. 2005. Linear ion traps in mass spectrometry. Mass Spectrometry Reviews. 24 (1), 1–29.

D'Souza-Schorey, C., Chavrier, P. 2006. ARF proteins: roles in membrane traffic and beyond. Nature Reviews Molecular Cell Biology, 7(5), 347-358.

Ellis, D. S., Ormerod, W. E., Lumsden, W. H. 1976. Filaments of *Trypanosoma brucei*: some notes on differences in origin and structure in two strains of *Trypanosoma (Trypanozoon) brucei rhodesiense*. Acta Tropica, 33(2), 151-168.

Evans-Osses, I., Reichembach, L. H., & Ramirez, M. I. 2015. Exosomes or microvesicles? Two kinds of extracellular vesicles with different routes to modify protozoan-host cell interaction. Parasitology Research, 114(10), 3567-3575.

Fichorova, R. N., Lee, Y., Yamamoto, H. S., Takagi, Y., Hayes, G. R., Goodman, R. P., Beach, D. H. 2012. Endobiont viruses sensed by the human host–beyond conventional antiparasitic therapy. PloS One, 7(11), e48418.

Fichorova, R., Fraga, J., Rappelli, P., Fiori, P. L. 2017. *Trichomonas vaginalis* infection in symbiosis with *Trichomonasvirus* and *Mycoplasma.* Research in Microbiology, 168(9-10), 882-891.,

Fichorova, R.N., Trifonova, R.T., Gilbert, R.O., Costello, C.E., Hayes, G.R., Lucas, J.J., and Singh, B.N. 2006. *Trichomonas vaginalis* lipophosphoglycan triggers a selective upregulation of cytokines by human female reproductive tract epithelial cells. Infection and Immunity, 74: 5773–5779.

Fiori, P. L., Rappelli, P., Addis, M. F., & Carta, F. 1998. *Mycoplasma hominis* parasitism of *Trichomonas vaginalis*. The Lancet, 352(9136), 1286.

Flegr, J., Čerkasov, J., Kulda, J., Tachezy, J., Štokrová, J. 1987. The dsRNA of *Trichomonas vaginalis* is associated with virus-like particles and does not correlate with metornidazole resistance. Folia Microbiologica, 32(4), 345-348.

Flom, P. L., Friedman, S. R., Kottiri, B. J., Neaigus, A., Curtis, R., Des Jarlais, D. C., Zenilman, J. M. 2001. Stigmatized drug use, sexual partner concurrency, and other sex risk network and behavior characteristics of 18-to 24-year-old youth in a high-risk neighborhood. Sexually Transmitted Diseases, 28(10), 598-607.

Fraga, J., Rojas, L., Sariego, I., Fernández-Calienes, A. 2012. Genetic characterization of three Cuban *Trichomonas vaginalis* virus. Phylogeny of *Totiviridae* family. Infection, Genetics and Evolution, 12(1), 113-120.

Fraga, J., Rojas, L., Sariego, I., Fernández-Calienes, A., Nunez, F. A. 2007. Double-stranded RNA viral infection of *Trichomonas vaginalis* and association with clinical presentation. Acta Protozoologica, 46(2), 93.

Fraga, J., Rojas, L., Sariego, I., Fernández-Calienes, A., Nuñez, F. A. 2012. Species typing of Cuban *Trichomonas vaginalis* virus by RT-PCR, and association of TVV-2 with high parasite adhesion levels and high pathogenicity in patients. Archives of Virology, 157(9), 1789-1795.

Garcia, A. F., Alderete, J. F. 2007. Characterization of the *Trichomonas vaginalis* surface-associated AP65 and binding domain interacting with trichomonads and host cells. BMC Microbiology, 7(1), 1-10.

Garcia, A., Exposto, F., Prieto, E., Lopes, M., Duarte, A., Correia da Silva, R. 2004. Association of *Trichomonas vaginalis* with sociodemographic factors and other STDs among female inmates in Lisbon. International Journal of STD & AIDS, 15(9), 615-618.

Geiger, A., Hirtz, C., Bécue, T., Bellard, E., Centeno, D., Gargani, D., Peltier, J. B. 2010. Exocytosis and protein secretion in *Trypanosoma*. BMC Microbiology, 10(1), 20.

Ghabrial, S. T. Totiviruses *In* Desk Encyclopedia of Plant and Fungal Virology, **Mahy, B.W.J, Van Regenmortel, M.H.V (eds.)**, (Academic Press, **2008),** 565-576. ISBN 9780123751485.

Goodman, R. P., Freret, T. S., Kula, T., Geller, A. M., Talkington, M. W., Tang-Fernandez, V., Singh, B. N. 2011. Clinical isolates of *Trichomonas vaginalis* concurrently infected by strains of up to four *Trichomonasvirus* species (Family *Totiviridae*). Journal of Virology, 85(9), 4258-4270.

Granger, B. L., Warwood, S. J., Benchimol, M., & De Souza, W. (2000). Transient invagination of flagella by *Tritrichomonas foetus.* Parasitology Research, 86(9), 699-709.

Graves, K. J., Ghosh, A. P., Schmidt, N., Augostini, P., Secor, W. E., Schwebke, J. R., Muzny, C. A. 2019. *Trichomonas vaginalis* virus among women with trichomoniasis and associations with demographics, clinical outcomes, and metronidazole resistance. Clinical Infectious Diseases, 69(12), 2170-2176.

Hampl, V., Pavlícek, A., Flegr, J. 2001. Construction and bootstrap analysis of DNA fingerprinting-based phylogenetic trees with the freeware program FreeTree: application to trichomonad parasites. International Journal of Systematic and Evolutionary Microbiology, 51(3), 731-735.

He, D., Pengtao, G., Ju, Y., Jianhua, L., He, L., Guocai, Z., & Xichen, Z. 2017. Differential protein expressions in virus-infected and uninfected *Trichomonas vaginalis*. The Korean Journal of Parasitology, 55(2), 121.

Heath, I. B. 1980. Variant mitoses in lower eukaryotes: indicators of the evolution of mitosis? In International Review of Cytology, 64, 1-80.

Hirt, R. P. 2013. *Trichomonas vaginalis* virulence factors: an integrative overview. Sexually Transmitted Infections, 89(6), 439-443.

Hirt, R. P., de Miguel, N., Nakjang, S., Dessi, D., Liu, Y. C., Diaz, N., Mottram, J. C. 2011. *Trichomonas vaginalis* pathobiology: new insights from the genome sequence. Advances in Parasitology, 77, 87-140.

Hirt, R. P., Noel, C. J., Sicheritz-Pontén, T., Tachezy, J., Fiori, P. L. 2007. *Trichomonas vaginalis* surface proteins: a view from the genome. Trends in Parasitology, 23(11), 540-547.

Honigberg BM. 1987. Immunology of trichomonads, with emphasis on *Trichomonas vaginalis*. Acta Universitatis Carolinae – Biologica, 10, 321–336.

Honigberg, B. M.1961. Comparative pathogenicity of *Trichomonas vaginalis* and *Trichomonas gallinae* to mice. I. Gross pathology, quantitative evaluation of virulence, and some factors affecting pathogenicity. The Journal of Parasitology, 47(4), 545-571.

Honigberg, B. M. Trichomonads found outside the urogenital tract of humans In Trichomonads Parasitic in Humans. Honigberg, B. M (Springer, 1990), 342-393.

Honigberg, B. M., Mattern, C. F., Daniel, W. A. 1971. Fine structure of the mastigont system in *Tritrichomonas foetus* (Riedmüller). The Journal of Protozoology, 18(2), 183-198.

Hoshino, A., Costa-Silva, B., Shen, T. L., Rodrigues, G., Hashimoto, A., Mark, M. T., Singh, S. 2015. Tumour exosome integrins determine organotropic metastasis. Nature, 527(7578), 329-335.

Huotari, J., Helenius, A. 2011. Endosome maturation. The EMBO Journal, 30(17), 3481-3500.

Hurley, J. H., Hanson, P. I. 2010. Membrane budding and scission by the ESCRT machinery: it's all in the neck. Nature reviews Molecular Cell Biology, 11(8), 556-566.

Chahar, H. S., Corsello, T., Kudlicki, A. S., Komaravelli, N., Casola, A. 2018. Respiratory syncytial virus infection changes cargo composition of exosome released from airway epithelial cells. Scientific Reports, 8(1), 1-18.

Choi, D. S., Kim, D. K., Kim, Y. K., Gho, Y. S. 2015. Proteomics of extracellular vesicles: exosomes and ectosomes. Mass Spectrometry Reviews, 34(4), 474-490.

Johnston, V. J., Mabey, D. C. 2008. Global epidemiology and control of *Trichomonas vaginalis.* Current Opinion in Infectious Diseases, 21(1), 56-64.

Khoshnan, A., Alderete, J. F. 1994. *Trichomonas vaginalis* with a double-stranded RNA virus has upregulated levels of phenotypically variable immunogen mRNA. Journal of Virology, 68(6), 4035-4038.

Koch, A., Bilina, A., Teodorowicz, L., Stary, A. 1997. *Mycoplasma hominis* and *Ureaplasma urealyticum* in patients with sexually transmitted diseases. Wiener klinische Wochenschrift, 109(14-15), 584.

Kulda J. Employment of Experimental Animals in Studies of Trichomonas vaginals Infection. In Trichomonads Parasitic in Human**. Honigberg, B. M.** (Springer, **1990**), 112-154.

Kunratowska, A. 1964. Some cytochemical reactions in vaginal *Trichomonas* infection (*Trichomonas vaginalis* Donné). Wiadomosci Parazytologiczne, 10, 291-292.

Kurnatowska, A. 1966. Studies on *Trichomonas Vaginalis* Donné III.: Biometric Features of *T. vaginalis* from Different Clinical Forms of Trichomoniasis. Acta Protozoologica, 4:185–211.

Lal, K., Noel, C. J., Field, M. C., Goulding, D., Hirt, R. P. 2006. Dramatic reorganisation of *Trichomonas* endomembranes during amoebal transformation: a possible role for G-proteins. Molecular and Biochemical Parasitology, 148(1):99-102.

Landolfo, S., Marcucci, F., Giovarelli, M., Viano, I., Forni, G. 1979. Lymphokine production in mouse mixed lymphocyte reaction (MLR). Immunogenetics, 9(1), 245-253.

Liang, B., Peng, P., Chen, S., Li, L., Zhang, M., Cao, D., Shen, K. 2013. Characterization and proteomic analysis of ovarian cancer-derived exosomes. Journal of Proteomics, 80, 171-182.

Liang, B., Peng, P., Chen, S., Li, L., Zhang, M., Cao, D., Shen, K. 2013. Characterization and proteomic analysis of ovarian cancer-derived exosomes. Journal of Proteomics, 80, 171-182.

Lindmark, D. G., Müller, M. 1973. Hydrogenosome, a cytoplasmic organelle of the anaerobic flagellate *Tritrichomonas foetus*, and its role in pyruvate metabolism. Journal of Biological Chemistry, 248(22), 7724-7728.

Lipman, N. S., Lampen, N., Nguyen, H. T. 1999. Identification of pseudocysts of *Tritrichomonas muris* in Armenian hamsters and their transmission to mice. Comparative Medicine, 49(3), 313-315.

Maas, B. M., Cao, Y. 2018. A minimal physiologically based pharmacokinetic model to investigate FcRn-mediated monoclonal antibody salvage: effects of kon, koff, endosome trafficking, and animal species. Mabs. 10 (8), 1322-1331.

Maestrone, G., Semar, R. 1967. Experimental intravaginal infection with *Trichomonas foetus* in guinea pigs. Chemotherapy, 12(3), 137-145.

Margarita, V., Rappelli, P., Dessì, D., Pintus, G., Hirt, R. P., Fiori, P. L. 2016. Symbiotic association with *Mycoplasma hominis* can influence growth rate, ATP production, cytolysis and inflammatory response of *Trichomonas vaginalis.* Frontiers in Microbiology, 7, 953.

McClelland, R. S., Sangaré, L., Hassan, W. M., Lavreys, L., Mandaliya, K., Kiarie, J., Baeten, J. M. 2007. Infection with *Trichomonas vaginalis* increases the risk of HIV-1 acquisition. The Journal of Infectious Diseases, 195(5), 698-702.

Mercer, F., Diala, F. G. I., Chen, Y. P., Molgora, B. M., Ng, S. H., Johnson, P. J. 2016. Leukocyte lysis and cytokine induction by the human sexually transmitted parasite *Trichomonas vaginalis*. PLoS Neglected Tropical Diseases, 10(8), e0004913.

Meyer, M., Fehling, H., Matthiesen, J., Lorenzen, S., Schuldt, K., Bernin, H., Roeder, T. 2016. Overexpression of differentially expressed genes identified in non-pathogenic and pathogenic *Entamoeba histolytica* clones allow identification of new pathogenicity factors involved in amoebic liver abscess formation. PLoS Pathogens, 12(8), e1005853.

Meza-Cervantez, P., González-Robles, A., Cárdenas-Guerra, R. E., Ortega-López, J., Saavedra, E., Pineda, E., Arroyo, R. 2011. Pyruvate: ferredoxin oxidoreductase (PFO) is a surface-associated cell-binding protein in *Trichomonas vaginalis* and is involved in trichomonal adherence to host cells. Microbiology, 157(12), 3469-3482.

Mooberry, S. L., Tien, G., Hernández, A. H., Plubrukarn, A., Davidson, B. S. 1999. Laulimalide and isolaulimalide, new paclitaxel-like microtubule-stabilizing agents. Cancer Research, 59, 653–660.

Morada, M., Manzur, M., Lam, B., Tan, C., Tachezy, J., Rappelli, P., Yarlett, N. 2010. Arginine metabolism in *Trichomonas vaginalis* infected with *Mycoplasma hominis.* Microbiology, 156(12), 3734.

Morelli, A. E., Larregina, A. T., Shufesky, W. J., Sullivan, M. L., Stolz, D. B., Papworth, G. D., Falo, L. D. 2004. Endocytosis, intracellular sorting, and processing of exosomes by dendritic cells. Blood, 104(10), 3257-3266.

Müller, M., Lossick, J. G., Gorrell, T. E. 1988. In vitro susceptibility of *Trichomonas vaginalis* to metronidazole and treatment outcome in vaginal trichomoniasis. Sexually Transmitted Diseases, 15(1), 17-24.

Muralidharan-Chari, V., Clancy, J., Plou, C., Romao, M., Chavrier, P., Raposo, G., D'Souza-Schorey, C. 2009. ARF6-regulated shedding of tumor cell-derived plasma membrane microvesicles. Current Biology, 19(22), 1875-1885.

Namiki, K., Goodison, S., Porvasnik, S., Allan, R. W., Iczkowski, K. A., Urbanek, C., Rosser, C. J. 2009. Persistent exposure to *Mycoplasma* induces malignant transformation of human prostate cells. PloS One, 4(9), e6872.

Nielsen, M. H. 1975. The ultrastructure of *Trichomonas vaginalis* Donnè before and after transfer from vaginal secretion to diamonds medium. Acta Pathologica Microbiologica Scandinavica Section B Microbiology, 83(6), 581-589.

Nievas, Y. R., Coceres, V. M., Midlej, V., de Souza, W., Benchimol, M., Pereira-Neves, A., de Miguel, N. 2018. Membrane-shed vesicles from the parasite *Trichomonas vaginalis*: characterization and their association with cell interaction. Cellular and Molecular Life Sciences, 75(12), 2211-2226.

Noël, C. J., Diaz, N., Sicheritz-Ponten, T., Safarikova, L., Tachezy, J., Tang, P., Hirt, R. P. 2010. *Trichomonas vaginalis* vast BspA-like gene family: evidence for functional diversity from structural organisation and transcriptomics. BMC Genomics, 11(1), 99.

Nývltová, E. 2008. Charakterizace mitosomů u *Mastigamoeba balamuthi*.

Okumura, C. Y., Baum, L. G., Johnson, P. J. 2008. Galectin-1 on cervical epithelial cells is a receptor for the sexually transmitted human parasite *Trichomonas vaginalis*. Cellular Microbiology, 10(10), 2078-2090.

Pereira-Neves, A., Campero, C. M., Martínez, A., Benchimol, M. 2011. Identification of *Tritrichomonas foetus* pseudocysts in fresh preputial secretion samples from bulls. Veterinary Parasitology, 175(1-2), 1-8.

Pereira-Neves, A., Nascimento, L. F., Benchimol, M. 2012. Cytotoxic effects exerted by *Tritrichomonas foetus* pseudocysts. Protist, 163(4), 529-543.

Pereira-Neves, A., Ribeiro, K. C., Benchimol, M. 2003. Pseudocysts in trichomonads–new insights. Protist, 154(3-4), 313-329.

Pereyre, S., Sirand-Pugnet, P., Beven, L., Charron, A., Renaudin, H., Barré, A., de Daruvar, A. 2009. Life on arginine for *Mycoplasma hominis*: clues from its minimal genome and comparison with other human urogenital mycoplasmas. PLoS Genetics, 5(10), e1000677.

Petrin, D., Delgaty, K., Bhatt, R., Garber, G. 1998. Clinical and microbiological aspects of *Trichomonas vaginalis.* Clinical Microbiology Reviews, 11(2), 300-317.

Rada, P., Kellerová, P., Verner, Z., Tachezy, J. 2019. Investigation of the Secretory Pathway in *Trichomonas vaginalis*. Argues against a Moonlighting Function of Hydrogenosomal Enzymes. Journal of Eukaryotic Microbiology, 66(6), 899-910.

Rana, S., Zöller, M. 2011. Exosome target cell selection and the importance of exosomal tetraspanins: a hypothesis. Biochemical Society Transactions, 39(2), 559-62.

Rappelli, P., Are, R., Casu, G., Fiori, P. L., Cappuccinelli, P., Aceti, A. 1998. Development of a Nested PCR for Detection of *Cryptococcus neoformans* in Cerebrospinal Fluid. Journal of Clinical Microbiology, 36(11), 3438-3440.

Rappelli, P., Carta, F., Delogu, G., Addis, M. F., Dessì, D., Cappuccinelli, P., Fiori, P. L. 2001. *Mycoplasma hominis* and *Trichomonas vaginalis* symbiosis: multiplicity of infection and transmissibility of *M. hominis* to human cells. Archives of Microbiology, 175(1), 70-74.

Reardon, L. V., Ashburn, L. L., Jacobs, L., Davis, V. E. 1961. Differences in strains of *Trichomonas vaginalis* as revealed by intraperitoneal injections into mice. The Journal of Parasitology, 47(4), 527-532.

Ribeiro, K. C., Monteiro-Leal, L. H., Benchimol, M. (2000). Contributions of the axostyle and flagella to closed mitosis in the protists *Tritrichomonas foetus* and *Trichomonas vaginalis.* Journal of Eukaryotic Microbiology, 47(5), 481-492.

Ribeiro, K. C., Santos, C., Benchimol, M. 2015. Is *Trichomonas tenax* a parasite or a commensal?. Protist, 166(2), 196-210.

Ryan, C. M., de Miguel, N. D., Johnson, P. J. 2011. *Trichomonas vaginalis*: current understanding of host–parasite interactions. Essays in biochemistry, 51, 161-175.

Sadallah, S., Eken, C., Martin, P. J., Schifferli, J. A. 2011. Microparticles (ectosomes) shed by stored human platelets downregulate macrophages and modify the development of dendritic cells. The Journal of Immunology, 186(11), 6543-6552.

Shifrin Jr, D. A., Beckler, M. D., Coffey, R. J., Tyska, M. J. 2013. Extracellular vesicles: communication, coercion, and conditioning. Molecular Biology of the Cell, 24(9), 1253-1259.

Shuter, J., Bell, D., Graham, D., Holbrook, K. A., Bellin, E. Y. 1998. Rates of and risk factors for trichomoniasis among pregnant inmates in New York City. Sexually Transmitted Diseases, 25(6), 303-307.

Schara, K., Janša, V., Šuštar, V., Dolinar, D., Pavlič, J. I., Lokar, M., ... & Iglič, A. (2009). Mechanisms for the formation of membranous nanostructures in cell-to-cell communication. Cellular & Molecular Biology Letters, 14(4), 636-656.

Schmuñis, G. A., Szarfman, A., De Souza, W., Langembach, T. 1980. *Trypanosoma cruzi:* Antibody-induced mobility of surface antigens. Experimental Parasitology, 50(1), 90-102.

Schnitzer, R. J., Kelly, D. R., Leiwant, B. (1950). Experimental studies on trichomoniasis: 1. The pathogenicity of trichomonad species for mice. The Journal of Parasitology, 36(4), 343-349.

Scholtyseck, E., Teras, J., Kasakova, I., Sethi, K. K. 1985. Electron microscope observations on the interaction of *Mycoplasma fermentans* with *Trichomonas vaginalis.* Zeitschrift für Parasitenkunde, 71(4), 435-442.

Schorey, J. S., Bhatnagar, S. 2008. Exosome function: from tumor immunology to pathogen biology. Traffic, 9(6), 871-881.

Silverman, J. M., Reiner, N. E. 2011. Exosomes and other microvesicles in infection biology: organelles with unanticipated phenotypes. Cellular Microbiology, 13(1), 1-9.

Singh, B. N., Hayes, G. R., Lucas, J. J., Sommer, U., Viseux, N., Mirgorodskaya, E., Fichorova, R. N. 2009. Structural details and composition of *Trichomonas vaginalis* lipophosphoglycan in relevance to the epithelial immune function. Glycoconjugate Journal, 26(1), 3.

Stark, J. R., Judson, G., Alderete, J. F., Mundodi, V., Kucknoor, A. S., Giovannucci, E. L., Ma, J. 2009. Prospective study of *Trichomonas vaginalis* infection and prostate cancer incidence and mortality: Physicians' Health Study. JNCI: Journal of the National Cancer Institute, 101(20), 1406-1411.

Stein, J. M., Luzio, J. P. 1991. Ectocytosis caused by sublytic autologous complement attack on human neutrophils. The sorting of endogenous plasma-membrane proteins and lipids into shed vesicles. Biochemical Journal, 274(2), 381-386.

Szempruch, A. J., Sykes, S. E., Kieft, R., Dennison, L., Becker, A. C., Gartrell, A., Harrington, J. M. 2016. Extracellular vesicles from *Trypanosoma brucei* mediate virulence factor transfer and cause host anemia. Cell, 164(1-2), 246-257.

Štáfková, J., Rada, P., Meloni, D., Žárský, V., Smutná, T., Zimmann, N., Tachezy, J. 2018. Dynamic secretome of *Trichomonas vaginalis*: Case study of β-amylases. Molecular & Cellular Proteomics, 17(2), 304-320.

Tachezy, J. 1999. More on iron acquisition by parasitic protozoa. Parasitology Today, 15(5), 207.

Tai, J. H., Su, H. M., Tsai, J., Shaio, M. F., Wang, C. C. 1993. The divergence of *Trichomonas vaginalis* virus RNAs among various isolates of *Trichomonas vaginalis*. Experimental Parasitology, 76(3), 278-286.

Tetta, C., Ghigo, E., Silengo, L., Deregibus, M. C., Camussi, G. 2013. Extracellular vesicles as an emerging mechanism of cell-to-cell communication. Endocrine, 44(1), 11-19.

Théry, C., Witwer, K. W., Aikawa, E., Alcaraz, M. J., Anderson, J. D., Andriantsitohaina, R., Ayre, D. C. 2018. Minimal information for studies of extracellular vesicles 2018 (MISEV2018): a position statement of the International

Society for Extracellular Vesicles and update of the MISEV2014 guidelines. Journal of Extracellular Vesicles, 7(1), 12-22.

Trissl, D., Martinez-Palomo, A., Argüello, C., De la Torre, M., De la Hoz, R. 1977. Surface properties related to concanavalin A-induced agglutination. A comparative study of several *Entamoeba* strains. The Journal of Experimental Medicine, 145(3), 652-665.

Twu, O., de Miguel, N., Lustig, G., Stevens, G. C., Vashisht, A. A., Wohlschlegel, J. A., Johnson, P. J. 2013. *Trichomonas vaginalis* exosomes deliver cargo to host cells and mediate host: parasite interactions. PLoS Pathogen, 9(7), e1003482.

Tyndall, M. W., Patrick, D., Spittal, P., Li, K., O'Shaughnessy, M. V., Schechter, M. T. 2002. Risky sexual behaviours among injection drugs users with high HIV prevalence: implications for STD control. Sexually Transmitted Infections, 78(1), 170-175.

van Belkum, A., van der Schee, C., van der Meijden, W. I., Verbrugh, H. A., & Sluiters, H. J. 2001. A clinical study on the association of *Trichomonas vaginalis and Mycoplasma hominis* infections in women attending a sexually transmitted disease (STD) outpatient clinic. FEMS Immunology & Medical Microbiology, 32(1), 27-32.

Van Niel, G., Porto-Carreiro, I., Simoes, S., Raposo, G. 2006. Exosomes: a common pathway for a specialized function. Journal of biochemistry, 140(1), 13-21.

Vidakovics, M. L. A. P., Jendholm, J., Mörgelin, M., Månsson, A., Larsson, C., Cardell, L. O., Riesbeck, K. 2010. B cell activation by outer membrane vesicles—a novel virulence mechanism. PLoS Pathogen, 6(1), e1000724.

Wang, A. L., Wang, C. C. 1986. The double-stranded RNA in *Trichomonas vaginalis* may originate from virus-like particles. Proceedings of the National Academy of Sciences, 83(20), 7956-7960.

Ward, H., Day, S., Green, A., Cooper, K., Weber, J. 2004. Declining prevalence of STI in the London sex industry, 1985 to 2002. Sexually Transmitted Infections, 80(5), 374-376.

Ward, H., Pallecaros, A., Green, A., Day, S. 2000. Health issues associated with increasing use of “crack” cocaine among female sex workers in London. Sexually Transmitted Infections, 76(4), 292-293.

Wenrich, D. H., Emmerson, M. A. 1933. Studies on the morphology of T*ritrichomonas foetus* (Riedmüller) (protozoa, flagellata) from American cows. Journal of Morphology, 55(1), 193–205.

Witwer, K. W., Théry, C. 2019. Extracellular vesicles or exosomes? On primacy, precision, and popularity influencing a choice of nomenclature. Journal of Extracellular Vesicles. 2019; 8(1): 1648167.

World Health Organization. 2001. Global prevalence and incidence of selected curable sexually transmitted infections: overview and estimates (No. WHO/CDS/CSR/EDC/2001.10). World Health Organization.

World Health Organization. 2012. Global incidence and prevalence of selected curable sexually transmitted infections-2008.

SWYGARD, H., et al. 2004. *Trichomoniasis*: clinical manifestations, diagnosis and management. Sexually Transmitted Infections, 80.2: 91-95.

Wu, C. X., Liu, Z. F. 2018. Proteomic profiling of sweat exosome suggests its involvement in skin immunity. Journal of Investigative Dermatology, 138(1), 89-97.

Yang, C., Chalasani, G., Ng, Y. H., Robbins, P. D. 2012. Exosomes released from *Mycoplasma* infected tumor cells activate inhibitory B cells. PloS One, 7(4), e36138.

Yarlett, N., Martinez, M. P., Moharrami, M. A., Tachezy, J. 1996. The contribution of the arginine dihydrolase pathway to energy metabolism by *Trichomonas vaginalis*. Molecular and Biochemical Parasitology, 78(1-2), 117-125.

Zhang, Z. F., Begg, C. B. 1994. Is *Trichomonas vaginalis* a cause of cervical neoplasia? Results from a combined analysis of 24 studies. International Journal of Epidemiology, 23(4), 682-690.

Zuo, Y., Riley, D. E., Krieger, J. N. 1999. Flagellar duplication and migration during the Trichomonas vaginalis cell cycle. The Journal of Parasitology, 85, 203-207.